

İSTANBUL TECHNICAL UNIVERSITY ★ INSTITUTE OF SCIENCE AND TECHNOLOGY

**SYNTHESIS AND PREPARATION OF POLYMERIC DRUG CARRIER
MICELLES**

**M. Sc. Thesis by
Kerem KARAKUŞ**

Department : Chemistry

Programme : Chemistry

JUNE 2011

**SYNTHESIS AND PREPARATION OF POLYMERIC DRUG CARRIER
MICELLES**

**M.Sc. Thesis by
Kerem KARAKUŞ
(509091051)**

**Date of submission : 06 June 2011
Date of defence examination: 09 June 2011**

**Supervisor : Prof. Dr. Gülaçtı TOPÇU (ITU)
Co-supervisor : Prof. Dr. Gürkan HIZAL (ITU)
Members of the Examining Committee : Prof. Dr. Ümit TUNCA (ITU)
Prof. Dr. Ayla GÜRSOY (MU)
Assis. Prof. Dr. Melike ÜNER (IU)**

JUNE 2011

İSTANBUL TEKNİK ÜNİVERSİTESİ ★ FEN BİLİMLERİ ENSTİTÜSÜ

**İLAÇ TAŞIYICI POLİMERİK MİSELLERİN SENTEZİ VE
HAZIRLANMASI**

**YÜKSEK LİSANS TEZİ
Kerem KARAKUŞ
(509091051)**

Tezin Enstitüye Verildiği Tarih : 06 Mayıs 2011

Tezin Savunulduğu Tarih : 09 Haziran 2011

**Tez Danışmanı : Prof. Dr. Gülaçtı TOPÇU (İTÜ)
Eş Danışmanı : Prof. Dr. Gürkan HIZAL (İTÜ)
Diğer Jüri Üyeleri : Prof. Dr. Ümit TUNCA (İTÜ)
Prof. Dr. Ayla GÜRSOY (MÜ)
Doç. Dr. Melike ÜNER (İÜ)**

HAZİRAN 2011

FOREWORD

This master study has been carried out at İstanbul Technical University, Chemistry Department of Science & Letters Faculty.

I would like to express my gratitude to my thesis supervisor, Prof. Dr. Gülaçtı TOPÇU and co-supervisor Prof. Dr. Gürkan HIZAL for offering invaluable help in all possible ways, continuos encouragement and helpful critisms throughout this research.

I would like also extend my sincere gratitude to Fatemeh BAHADORİ, Aydan DAĞ, Hakan DURMAZ, İpek ÖSKEN, Aslı ÇAPAN and Ufuk Saim GÜNEY for their friendly and helpful attitudes and support during my laboratory works. In addition, I would like to thank both group members in Natural Product Laboratory and Complex Macromolecular Structure Center during my laboratory studies.

I would like to present the most gratitude to my family; Muzaffer KARAKUŞ, Adalet KARAKUŞ, my grandfather Süddik KARAKUŞ and to all my friends for their patience, understanding and morale support during all stages involved in the preparation of this research.

May 2011

Kerem KARAKUŞ

TABLE OF CONTENTS

	<u>Page</u>
TABLE OF CONTENTS.....	vii
ABBREVIATIONS	xi
LIST OF TABLES	xiii
LIST OF FIGURES	xv
LIST OF SYMBOLS	xvii
SUMMARY	xix
ÖZET	xxi
1. INTRODUCTION.....	1
2. THEORETICAL PART	7
2.1 Chemistry of Curcumin	7
2.2 Drug delivery systems and nanotechnology.....	10
2.2.1 The ‘NANO era’ of targeted or site-controlled drug delivery systems....	10
2.2.2 Nanoparticle Carriers based on Amphiphilic Polymers for Drug Delivery.....	14
2.3 Targeted Drug delivery	18
2.3.1 Passive tumor targeting.....	18
2.3.1 Active tumor targeting	20
2.4 Micelle structure and composition	23
2.4.1 Methods of micelle preparation	26
2.4.2 Micelle stability.....	27
2.4.2.1 Thermodynamic stability	28
2.4.2.2 Kinetic stability	29
2.4.4 Micelle size	30
2.5 Drug incorporation	33
2.5.1 Drug loading procedures	33
2.5.2 Loading capacity	35
2.5.3 Examples of drug-loaded polymeric micelles.....	36
2.6 Star Polymers	37
2.6.1 Preparation of star polymers	38
2.6.1.1 End Linking with Multifunctional Linking Agent (Arm-First Method).39	39
2.6.1.2 Use of multifunctional initiators (core-first method).....	40
2.6.1.3 Use of difunctional monomers (arm-first method)	40
2.7 Miktoarm star polymers	41
2.8 Amphiphilic Star Block Copolymers	42
2.9 Ring-Opening Polymerization (ROP)	43
2.9.1 Controlled Ring-Opening Polymerization of cyclic esters	44
2.9.2 Catalysts	45
2.9.3 Coordination-Insertion ROP	46
2.9.4 Poly(ϵ -caprolactone)	49

2.10 Click Chemistry.....	50
2.10.1 Copper(I)-catalyzed azide-alkyne cycloaddition (CuAAC).....	51
2.11 Diels-Alder reaction	52
2.11.1 Stereochemistry of Diels-Alder reaction.....	52
3. EXPERIMENTAL PART	57
3.1 Materials	57
3.2 Instrumentation.....	57
3.3 Synthesis Methods.....	58
3.3.1 Synthesis of 4,10-dioxatricyclo[5.2.1.0 _{2,6}]dec-8-ene-3,5-dione(1).....	58
3.3.2 Synthesis of 4-(2-hydroxyethyl)-10-oxa-4-azatricyclo[5.2.1.0 _{2,6}]dec-8-ene-3,5-dione (2).....	59
3.3.3 Synthesis of 2,2,5-trimethyl-[1,3]dioxane-5-carboxylic acid (3).....	59
3.3.4 Synthesis of adduct alcohol-acid ketal ester and hydrolysis to diol.....	60
3.3.5 Synthesis of 2 alkyne end functionalized core for synthesis of PEG ₂	60
3.3.6 Synthesis of Azide ended Me-PEG.....	60
3.3.7 Synthesis of the PEG ₂ by using click reaction	61
3.3.8 Synthesis of anthracene end-functionalized PCL (Anth-PCL)	61
3.3.9 Synthesis of PCL-PEG ₂ miktoarm star copolymer via Diels-Alder click reaction	62
3.3.10 Synthesis of Me-PEG ₂₀₀₀ -COOH.....	62
3.3.11 Synthesis of maleimide end-functionalized PEG (MI-PEG)	62
3.3.12 Synthesis of anthracen-9ylmethyl 2,2,5-trimethyl-[1,3]dioxane-5-carboxylate (4).....	63
3.3.13 Synthesis of anthracen-9ylmethyl 3-hydroxy-2-(hydroxymethyl)-2-methylpropanoate (5)	63
3.3.14 Synthesis of anthracene end-functionalized (PCL) ₂	64
3.3.15 Synthesis of miktoarm PEG-(PCL) ₂ star block copolymer via Diels-Alder click reaction	64
3.3.16 Modification of the Me-PEG with 2,2,5-trimethyl-[1,3]dioxane-5-carboxylic acid (PEG-AK)	65
3.3.17 Dehydrolization of the ketal moety (PEG-Diol)	65
3.3.18 Synthesis of PEG-PCL ₂ miktoarmstar copolymer with ROP via using PEG-Diol as initiator.....	65
3.4 Micellar Characterization of the amphiphilic block copolymers	66
3.4.1 Preparation of the micelle	66
3.4.2 Zeta-Sizer Measurements.....	66
3.4.3 CMC Analysis	67
3.4.4 Preparation of Curcumin loaded polymeric miselles and determination of the maximum curcumin loadin capacity.....	67
4. RESULTS AND DISCUSSION.....	69
4.1 Synthesis of the Amphiphilic Miktoarm Star Block Copolymers.....	69
4.1.1 Synthesis of PEG ₂ -PCL With Core-First Method By using both Diels-Alder and CuAAC Reactions	69
4.1.1.1 Synthesis of the Core.....	70
4.1.1.2 Modification of the Me-PEG for Click Reaction	71
4.1.1.3 Synthesis of the PCL Chain Via Using 9-anthracene Methanol as Initiator	72
4.1.1.4 Synthesis of the PEG ₂ Via Click Chemistry	73
4.1.1.5 Synthesis of the PEG ₂ -PCL with DA	74
4.1.2 Synthesis of PCL ₂ -PEG By Using DA.....	76

4.1.2.1 Modifications of Me-PEG ₂₀₀₀	77
4.1.2.2 The preparation of the Ant-PCL ₂	78
4.1.2.3 The Synthesis of PCL ₂ -PEG via DA.....	81
4.1.3 Synthesis of the PCL ₂ -PEG By Using Modified MePEG.....	83
4.1.3.1 Synthesis of the PEG-Diol	83
4.1.3.2 The Synthesis of the PCL ₂ -PEG via ROP	84
4.2 Preparation and Characterization of the Micelles.....	86
4.2.1 Preparation of the Micelles	86
4.2.2 Particle size Analyses.....	87
4.2.3 CMC Measurements	90
4.2.4 Encapsulation of the Curcumin with Polymeric Micelles	91
5.CONCLUSION.....	95
REFERENCES.....	97
CURRICULUM VITA	107

ABBREVIATIONS

FDA	: Food and drug administration
RES	: Reticuloendothelial system
DDS	: Drug delivery system
EPR	: Enhanced permeation and retention
CMC	: Critical micelle concentration
PDI	: Polydispersive index
DMSO	: Dimethyl sulfoxide
DMAc	: Dimethyl acetamide
AFM	: Atomic force microscopy
SEM	: Scanning electron microscopy
GPC	: Gel permeation chromatography
DLS	: Dynamic light scattering
¹H NMR	: Hydrogen Nuclear Magnetic Resonance Spectroscopy
ATRP	: Atom Transfer Radical Polymerization
CH₂Cl₂	: Dichloromethane
CDCl₃	: Deuterated chloroform
CuAAC	: Copper catalyzed azide-alkyne cycloaddition
DA	: Diels-Alder
DMF	: <i>N,N</i> -dimethylformamide
DVB	: Divinyl benzene
ε-CL	: ϵ -caprolactone
EtOAc	: Ethyl acetate
GC	: Gas Chromatography
GPC	: Gel Permeation Chromatography
MWD	: Molecular Weight Distribution
NMP	: Nitroxide Mediated Polymerization
PCL	: Poly(ϵ -caprolactone)
PDI	: Polydispersive Index
PEG	: Poly(ethylene glycol)
PMDETA	: <i>N,N,N',N''-Pentamethyldiethylenetriamine</i>
r-DA	: retro-Diels-Alder
TD-GPC	: Triple Detector-Gel Permeation Chromatography
TEA	: Triethylamine
THF	: Tetrahydrofuran
UV	: Ultra Violet
APT	: Attached proton test

LIST OF TABLES

	<u>Page</u>
Table 2.1: Commonly Used Block Segments of Copolymers for Micellar Drug Delivery Systems	25
Table 2.2: The various factors which influence the thermodynamic or kinetic stability of block copolymer micelles	30
Table 2.3: Examples of drugs and tracers loaded into polymeric micelles	37
Table 4.1: Molecular weight analyses of the PEG ₂ -PCL	75
Table 4.2: Molecular weight analyses of the PCL ₂ -PEG	82
Table 4.3: Molecular weight analyses of the PCL ₂ -PEG synthesized with macro-initiator	85
Table 4.4: DMF/H ₂ O (V/V) and the size of the micelles prepared with PCL ₂ -PEG	89
Table 4.5: The loaded curcumin amount to polymeric micelles	93

LIST OF FIGURES

	<u>Page</u>
Figure 2.1: Natural yellow dye, Curcumin (diferuloylmethane; 1, 7-Bis(4 hydroxy-3-methoxyphenyl)-1,6-heptadiene-3,5-dione) curcumin I, MW 368; curcumin II, MW 338; Curcumin III, MW 308	8
Figure 2.2: Passive drug targeting through the enhanced permeability and retention (EPR) effect. The polymeric nanoparticles preferentially accumulate in solid tumors, owing at least in part to leaky tumor vessels and an ineffective lymphatic drainage system The various factors which influence the thermodynamic or kinetic stability of block copolymer micelles.....	20
Figure 2.3: Receptor-mediated endocytosis of folate-conjugated drugs. The folate receptors recognize the conjugates, which are subsequently subjected to membrane invagination. As the endosomal compartment acidifies, the conjugate and the drugs are released from the receptor into the cytosol.....	23
Figure 2.4: Schematic illustration of the core-shell structure of a polymer micelle with intended functions of each component.....	25
Figure 2.5: In-vivo behaviour of the polymeric micelles	32
Figure 2.6: Drug loading of polymeric micelles by the dialysis (a) and the oil-in-water methods (b)	35
Figure 2.7: Illustration of a star polymer.....	38
Figure 2.8: Illustration of the synthesis of star polymers by arm-first method.....	39
Figure 2.9: Illustration of the synthesis of star and star block copolymers by “core-first” method	40
Figure 2.10: Illustration of the synthesis of star polymers by “arm-first” method	40
Figure 2.11: Illustration of the synthesis of star and star block copolymers by “core-first” method.Illustration of miktoarm star polymers structures where each letter represents different polymeric arms	41
Figure 2.12: Dilute solution of block copolymers into spherical micelles	43
Figure 4.1: ^1H NMR spectra of the core	71
Figure 4.2: The comparison of the ^1H NMR spectra of the Me-PEG-TsCl and Me-PEG- N_3	72
Figure 4.3: ^1H NMR spectrum of the Ant-PCL 1	73
Figure 4.4: 1H NMR spectrum of the PEG2 74	74
Figure 4.5: GPC analysis of PEG ₂ , Ant-PCL and PCL—PEG ₂ miktoarm star block copolymer	75
Figure 4.6: ^1H NMR Spectrum of the PEG ₂ -PCL.....	76
Figure 4.7: ^1H NMR spectrum of the MI-PEG	78

Figure 4.8: ^1H NMR spectra of: a) 2,2,5-trimethyl-[1,3]dioxane-5-carboxylic acid; b) anthracen-9ylmethyl 2,2,5-trimethyl-1,3-dioxane-5 carboxylate ; c) anthracen-9ylmethyl 3-hydroxy-2 (hydroxymethyl) - 2-methylpropanoate in CDCl_3	80
Figure 4.9: The ^1H NMR spectrum of the Ant-PCL ₂	80
Figure 4.10: GPC analyses of PEG ₂ , Ant-PCL and PEG ₂ -PCL miktoarm star block copolymer.....	81
Figure 4.11: ^1H NMR spectra of the PCL ₂ -PEG.....	82
Figure 4.12: ^1H NMR Spectrum of the PEG-Diol	84
Figure 4.13: GPC analyses of PEG ₂ , Ant-PCL and PEG ₂ -PCL miktoarm star block copolymer	85
Figure 4.14: The ^1H NMR and ^{13}C NMR spectrums of the PCL ₂ -PEG miktoarm star block copolymer.....	86
Figure 4.15: Particle size distribution of the PEG ₂ -PCL micelles	88
Figure 4.16: The particle size distribution of the PEG ₂ -PCL micelles after dilution.....	88
Figure 4.17: The size distributions of the polymeric micelles that prepared with different DMF/H ₂ O ratios.....	89
Figure 4.18: The fluorescense spectrum of the PCL ₂ -PEG and PEG ₂ -PCL	90
Figure 4.19: The CMC graphs of the polymeric micelles.....	91
Figure 4.20: The calibration curve of the curcumin standarts used in calculations	92

LIST OF SYMBOLS

λ	: Wavelength
\mathbf{R}^{\cdot}	: Radical
f	: Number of arm
nm	: Nanometer
g'	: Contraction factor
$[\eta]$: Intrinsic viscosity
R_h	: Hydrodynamic radius
C	: Concentration
A	: Absorbance
ϵ	: Molar extinction coefficient
k_{act}	: Activation rate constant
k_{deact}	: Deactivation rate constant
R_p	: Rate of polymerization
d_n/d_c	: Refractive index increment
K	: Mark-Houwink-Sakurada constant
ppm	: Parts per million
$^{\circ}\text{C}$: Celsius
M	: Molarity
T_g	: Glass-transition temperature
M_n	: The number average molecular weight
M_w	: The weight average molecular weight
M_w/M_n	: The molecular weight distribution

SYNTHESIS AND PREPARATION OF POLYMERIC DRUG CARRIER MICELLES

SUMMARY

Cancer is the biggest health problem in the modern world which is caused to death of millions of patients and at least millions waiting for a proper cure for this disease. Curcumin (diferuloylmethane) is a polyphenol derived from the rhizome of the plant *Curcuma longa*, commonly called turmeric which is one of the potent cytotoxic agents and investigated as a drug for the treatment of cancer. But solubility of the curcumin in water is very poor to be used intravenously. Encapsulation of the curcumin with micelles formed by the amphiphilic block copolymers thought to be a solution for enhancing solubility of the curcumin in water. A₂B type amphiphilic miktoarm star block copolymers consist of polyethylene glycol (PEG) and poly ε-caprolactone (PCL) are synthesized to prepare micelles and via self-assembly of these amphiphilic block copolymers in water. And the enhancement of curcumin's solubility is aimed by entrapment in the hydrophobic core.

Two different copolymers are synthesized with three different ways. PEG is commercially available in various molecular weights, so no need to be synthesized from monomers, and for the synthesis of the copolymers they can be easily functionalized from the hydroxy (-OH) end. PCL is synthesized by using ring opening polymerization (ROP) to produce exact chain lengths and it gives options for synthesis of the optimum hydrophobic ratio for micelle stability. During the synthesis of the block copolymers, either "arm-first" or "core-first" strategies are used and segments are gathered via Click chemistry and Diels-Alder (DA) reaction.

The first copolymer, PEG₂-PCL miktoarm star block copolymer is synthesized with core-first method by using both Diels-Alder and Click chemistry.

As a second type of block copolymer, PEG-PCL₂ copolymer is synthesized following by two different methods. In the first method, the synthesis was carried out through arm-first strategy using only Diels-Alder reaction, and the micellar characterization of PEG-PCL₂ copolymer was found to be very promising. Due to long steps of the synthesis of PEG-PCL₂ block copolymer, an alternative synthetical method was developed with less steps. This is achieved by using modified PEG chain as the macro-initiator of the ring opening polymerization. It gives very good results with high yield and easy way of synthesis, with no side product and also easy purification.

In the second part of the study, the micellar characterization of the synthesized amphiphilic star block copolymers are carried out. Partical size analyses are done by using Zeta-sizer. Critical micelle concentration analyses are done with spectrophotometric measurements by using pyrene as flourescent probe. Critical

micelle concentration values are determined by plotting I_3/I_1 with $\log C$ (g/mL). Curcumin is loaded to the prepared micelles and the maximum loading capacity of the micelles are determined with Ultra Fast Liquid Chromatography (UFLC) measurements. The loaded amount of the drugs are calculated via area under curve method.

The synthesized A₂B type block copolymers were characterized by NMR and GPC analyses. The micellar formation of the amphiphilic block copolymers was found to be sufficient as drug carriers for curcumin, and particularly for PCL₂-PEG copolymer with enhanced solubility to 321.7 $\mu\text{g}/\text{mL}$ from 0.6 $\mu\text{g}/\text{mL}$.

POLYMERİK İLAC TAŞIYICI MİSELLERİN SENTEZİ VE HAZIRLANMASI

ÖZET

Modern dünyanın en büyük problemi olan kanser, milyonlarca kişinin ölümüne sebep oldu, en az milyonlarca hasta bu hastalık için uygun bir tedavi beklemektedir. Halk arasındaki genel adı zerdeçal olarak bilinen ve *Curcuma longa* bitkisinin köklerinden elde edilen kürkimin polifenoldür. kürkimin sitotoksik özelliği nedeni ile kanser tedavisinde potent ilaç olarak araştırılmaktadır. Fakat kürküminin sudaki çözünürlüğü damardan verilebilmesi için yeterli değildir. Bu nedenle kürküminin amfifilik polymerik miseller ile enkapsülasyonu sudaki çözünürlüğünün arttırılması için uygun bir çözüm olarak düşünüldü. Misellerin hazırlanması için poli \square -kaprolakton (PCL) ve polietilenglikol (PEG) oluşan A₂B tipi miktoarm star blok copolimerler sentezlendi ve bu amfifilik block kopolimerlerin suda kendiliğinde misel oluşturarak kürkimin hidrofobik çekirdekte hapsedip çözünürlüğünün artırılması planlandı.

İki farklı kopolimer üç değişik yöntem ile sentezlendi. PEG'in değişik moleküller ağırlıktaki türevleri ticari olarak mevcuttur, bu nedenle monomerlerden sentezlenmesine gerek duyulmadı. Ayrıca kopolimerlerin sentezi için hidroksi (-OH) ucundan kolayca fonksiyonlandırılabılırler. PCL misel kararlılığı için gerekli olan optimum hidrofobik oranın elde edilmesi için uygun başlatıcılar ile halka açılması polimerizasyonu üzerinden istenen zincir uzunluklarında sentezlendi. Sentez aşamasında arm-first ve core-first metodları kullanıldı ve segmentler Click kimyası ve Diels-Alder (DA) reaksiyonları ile birleştirildi.

İlk kopolymer, PEG₂-PCL miktoarm star block kopolimeri; Click kimyası ve Diels-Alder reaksiyonları kullanılarak core-first metodu ile sentezlendi.

İkinci tür blok kopolimer, PEG-PCL₂ iki değişik yöntem takip edilerek sentezlendi. Birinci yöntemde, sadece Diels-Alder reaksiyonu kullanılarak, arm-first stratejisi üzerinden sentezlendi, ve PEG-PCL₂ blok kopolimerinin misel karakterizasyonu daha ileri araştırmalar için umut verici bulundu. PEG-PCL₂ blok kopolimerinin sentezi uzun sentez basamakları nedeniyle alternatif yöntem ile daha az basamakta sentezlendi. Modifiye PEG zincirinin halka açılması polimerizasyonunda makrobaşlatıcı olarak kullanılması ile bunun üstesinden gelindi. Bu yöntem yüksek verim ve kolay sentez yanında yan ürünsüz ve kolay saflaştırma sağladı. Kritik misel konsantrasyonu tayini piren floresans prob olarak kullanılarak spektrofotometrik yöntemle gerçekleştirildi. Kritik misel konsantrasyonu değerleri I₃/I₁ karşı Log C (g/ml) eğrisi çizilerek hesaplandı. kürkimin polimerik misellere yüklenikten sonra maksimum yükleme kapasitesi ultra hızlı sıvı kromatografi cihazı le tayin edildi. Yüklenen kürkümin miktarları eğri altındaki yöntemi üzerinden hesaplandı.

Sentezlenen A₂B tipi blok kopolimerler NMR ve GPC analizleri ile karakterize edildi. Amfifilik kopolimerlerin misel formları kürkümin için ilaç taşıyıcısı olarak yeterli bulundu, özellikle de PCL₂-PEG kopolimeri kürküminin çözünürlüğünü 0.6 μ g/ml'den 321.7 μ g/ml ye arttırdı.

1. INTRODUCTION

Todays world's biggest unchallenged health problem is the cancer with millions of patients. Because, a lot of reasons are mentioned for its formation, but there is no certain reason identified as a cause for this disease, and it now reaches nearly 2000 different types of cancer due to the changes in organs and tissues, especially in the critical organs and cells, so the cure is too complex. Because of all this difficulties, it does not left to the chance which cause to kill the cells without cancer.

But, how could a simple drug can differ between a healthy tissue and a tumor, and even the limited number of cures have lots of negative results, such as side effects, poor effectivitness and high costs, that makes it irrecoverable for poor countries. But scientists and companies continue to search trying to find solutions to similar problems of the chemotherapy with collaboration of the different disciplines. These efforts are focused on to find and develop new drug delivery systems. Drug delivery systems (DDS) are simply the transportation of the drugs to body in various ways by using even synthetic or natural macromolecules for better solutions to disease and new gateways due to the classic medical treatments.

Cancer occurs at a molecular level when multiple subsets of genes undergo genetic alterations, either activation of oncogenes or inactivation of tumor suppressor genes. Then malignant proliferation of cancer cells, tissue infiltration, and dysfunction of organs will appear. Tumor tissues are characterized with active angiogenesis and high vascular density which keep blood supply for their growth, but with a defective vascular architecture. Combined with poor lymphatic drainage, they contribute to what is known as the enhanced permeation and retention (EPR) effect. Tumor genes are not stable with their development and often show genovariation [1]. The inherent complexity of tumor microenvironment and the existence of P-glycoprotein (Pgp) usually act as barriers to traditional chemotherapy by preventing drug from reaching the tumor mass. Meanwhile, delivery of the therapeutic agents *in vivo* shares physiological barriers, including hepatic and renal clearance, enzymolysis and hydrolysis, as well as endosomal/lysosomal degradation. In addition, the efficiency

of anticancer drugs is limited by their unsatisfactory properties, such as poor solubility, narrow therapeutic window, and intensive cytotoxicity to normal tissues, which may be the causes of treatment failure in cancer.

Accordingly, there is a great need for new therapeutic strategies capable of delivering chemical agents and other therapeutic materials specifically to tumor locations. With the development of nanotechnology, the integration of nanomaterials into cancer therapeutics is one of the rapidly advancing fields which probably revolutionize the treatment of cancer. Nanotechnology is the creation and utilization of materials, devices, and systems through the control of matter on the nanometer (1 billionth of a meter) scale. Nanocarrier systems can be designed to interact with target cells and tissues or respond to stimuli in well-controlled ways to induce desired physiological responses. They represent new directions for more effective diagnosis and therapy of cancer [1]. The reduction of the side effects, sustained release of the drug in body, decreasing the cost, are the examples of the advantages aimed in DDS and the recent works are succeeded in most of them. Drug delivery systems are one of the most attractive headline in the last quarter of the 20 th century by the development of the nanotechnology and the application area of them is increased, and today it becomes a market that its value is mentioned with billions and expected to be reach trillions at the end of the first quarter of the 21 th century.

One of the goals of the DDS is targeted drug delivery and micelles, which are good candidates for this achievement. Addition to liposomes, amphiphilic block copolymers are used to form micelles with improved bioavailability for the drugs. They have many advantages with different properties depending on the polymer composition, and preparation conditions, such as: a pH sensitive polymer allow a delivery system which can release the drug where the micelle meets the proper pH value, by programming the synthesis of the block copolymer at the beginning, or by preparation of temperature sensitive micelles which are sensitive to the temperature of the environment. Thus, during circulation of the micelles in the blood vessels, the drug is released when it meets a tumoral area, where the temperature is higher than healthy tissues and organs of the body.

Liposomes are also used for the same targets but, micelles of amphiphilic block copolymers seem to have better properties, such as tunnable micelle size, lower CMC and higher drug loading capacity than the liposomes which are approved by the Food

and Drug Administration (FDA). Amphiphilic copolymers have also molecular architecture in which different domains, both hydrophilic and hydrophobic, present within the polymer molecules. This gives rise to unique properties of these materials in selected solvents, at surfaces as well as in the bulk, due to microphase separation [2]. The characteristic self-organization of these materials in the presence of selective media often results in the formation of aggregates such as micelles, microemulsions, and adsorbed polymer layers [3].

Polymers with a wide variety of functional groups can be produced by ring-opening polymerizations. Ring-opening polymerization (ROP) is a unique polymerization process [3-7], in which a cyclic monomer is opened to generate a linear polymer. Nowadays, increasing attention is paid to biodegradable and biocompatible polymers for applications in the biomedical and pharmaceutical fields, primarily because after use they can be eliminated from the body via natural pathways and also they can be a solution to problems concerning the global environment and the solid waste management. Aliphatic polyesters are among the most promising materials as biodegradable polymers. The commonly used biocompatible polymers are aliphatic polyesters, such as poly(ϵ -caprolactone) (PCL), poly(lactic acid) (PLA), poly(glycolic acid) (PGA), and their corresponding copolymers [8]. PCL and PEG are both well-known FDA approved biodegradable and biocompatible materials, which have been widely used in the biomedical field [9].

The “click chemistry” concept was introduced by Sharpless and co-workers in 2001 [10]. Selected reactions were classified as click chemistry if they were modular, stereospecific, wide in scope, resulted in high yields, and generated only safe byproducts. Several efficient reactions such as copper(I)-catalyzed azide-alkyne cycloaddition (CuAAC), Diels-Alder (DA) cycloadditions, nucleophilic substitution and radical reactions can be classified under this term. The Diels-Alder reaction is an organic chemical reaction (specifically, a cycloaddition) between a conjugated diene and a substituted alkene, commonly termed dienophile, to form a substituted cyclohexene system [11, 12]. Some of the Diels-Alder reactions are reversible; the decomposition reaction of the cyclic system is then called the Retro-Diels-Alder. For example, Retro-Diels-Alder compounds are commonly observed when a Diels Alder product is analyzed via mass spectrometry [12].

Star polymers are among the macromolecular architectures receiving growing interest, due to their distinct properties in bulk, melt and solutions. They often exhibit lower solution and melt viscosities compared to those of the linear counterparts [13]. The synthesis of star-shaped polymers is generally achieved by one of two approaches; the “arm-first” in which the polymer arms are coupled to a multifunctional coupling agent and the “core-first” based on a multifunctional core as initiator.

Amphiphilic star-shaped block copolymers have recently attracted much attention because these polymers can behave as unimolecular micelles or be designed to exhibit a very low critical aggregation concentration (CAC) [14-15]. However, star-block copolymers comprising hydrophobic biodegradable and hydrophilic biocompatible segments are of particular interest, especially for biomedical applications, this is the reason to prepare PCL-PEG amphiphilic copolymers in this these study.

Polymeric micelles (PMs) very stable, having low critical micelle concentration (CMC) values compared to surfactant micelles, as low as 10^{-6} M. All these issues related to PMs make them ideal carriers for anticancer drugs and tumor targeting. PMs have attracted a lot of attention as a carrier for poorly water-soluble drugs, genes [14-15] and imaging agents. Indeed, they have also been used for the delivery of hydrophobic agents. And the size of them led to be used for passive targetting of the cytotoxic drugs. Nanoparticles are solid, colloidal particles consisting of macromolecular substances that vary in size from 10 nm to 1000 nm (Kreuter, 1994a). However, particles >200 nm are not heavily pursued and nanomedicine often refers to devices <200 nm (i.e., the width of microcapillaries). Typically, the drug of interest is dissolved, entrapped, adsorbed, attached and/or encapsulated into or onto a nano-matrix. Depending on the method of preparation nanoparticles, nanospheres, or nanocapsules can be constructed to possess different properties and release characteristics for the best delivery or encapsulation of the therapeutic agent (Barratt, 2000; Couvreur et al., 1995; Pitt et al., 1981) [16].

Turmeric has been used historically as a component of Indian Ayurvedic medicine since 1900 BC to treat a wide variety of ailments. Research in the latter half of the 20th century has identified curcumin as responsible for most of the biological activity of turmeric. *In vitro* and animal studies have suggested a wide range of

potential therapeutic or preventive effects associated with curcumin especially its cytotoxic potent makes it a potent anti-cancer agent and researches still continue to become a drug on market. But, poor solubility of curcumin is one of the barrier behind this process.

In this study, we tried to get rid of solubility problem of the curcumin by its encapsulation with prepared micelles of the synthesized amphiphilic polymers. Poorly water-soluble, hydrophobic agents are known to be associated with problems in therapeutic applications such as poor absorption and bioavailability, as well as drug aggregation related complications such as embolism. On the other hand, poor water solubility is associated with many drugs, especially anticancer drugs. PMs promisingly increase the water solubility of such drugs by 10 to 5000 fold [17].

For this purpose; the two different AB₂ type miktoarm star amphiphilic copolymers (PEG₂-PCL and PCL₂-PEG) are synthesized with three different methods for encapsulation of curcumin to enhance its solubility in the plasma via using both Click chemistry and Diels-Alder reactions. The identification of the synthesized copolymers was made based on NMR and GPC analyses, and their micellar characterization was carried out by the measurements of CMC with fluorescent probe pyrene, of particle size analysis on Zeta-sizer, and of the max. loading capacity of curcumin on UFC.

2. THEORETICAL PART

2.1 Chemistry of *Curcumin*

Curcumin (diferuloylmethane; see Figure 2.1) is a natural yellow orange dye derived from the rhizome of *Curcuma longa* Linn, an East Indian plant. It is insoluble in water and ether but is soluble in ethanol, dimethylsulfoxide and other organic solvents. It has a melting point of 183°C and a molecular weight of 368.37. Commercial curcumin contains three major components: curcumin (77%), demethoxycurcumin (17%), and bisdemethoxycurcumin (3%), together referred to as curcuminoids (Figure 2.1). Spectrophotometrically, curcumin absorbs maximally at 415-420 nm in acetone and a 1% solution of pure curcumin has an optical density of 1650 absorbance units. It has a brilliant yellow hue at pH 2.5 to 7.0, and takes on a red hue at pH > 7.0. Curcumin fluorescence is a broad band in acetonitrile ($\lambda_{\text{max}} = 524$ nm), ethanol ($\lambda_{\text{max}} = 549$ nm), or micellar solution ($\lambda_{\text{max}} = 557$ nm). Curcumin produces singlet oxygen (${}^1\text{O}_2$) upon irradiation ($\lambda > 400$ nm) in toluene or acetonitrile ($\text{pH}_i = 0.11$ for 50 μM curcumin); in acetonitrile curcumin also quenched ${}^1\text{O}_2$ ($k_q = 7 \times 10^6 \text{ M/S}$). ${}^1\text{O}_2$ production was about 10 times lower in alcohols. Recently, Das and Das have studied the ${}^1\text{O}_2$ quenching activity of curcumin in detail. Curcumin photogenerates superoxide in toluene and ethanol. In contrast, it quenches superoxide ions in acetonitrile.

Curcumin is also phototoxic to mammalian cells, as demonstrated in a rat basophilic leukemia cell model, and this phototoxicity likewise requires the presence of oxygen. The spectral and photochemical properties of curcumin vary with environment, resulting in the potential for multiple or alternate pathways for the execution of photodynamic effects. For example, curcumin photogenerates singlet oxygen and reduced forms of molecular oxygen under several conditions relevant to cellular environments.

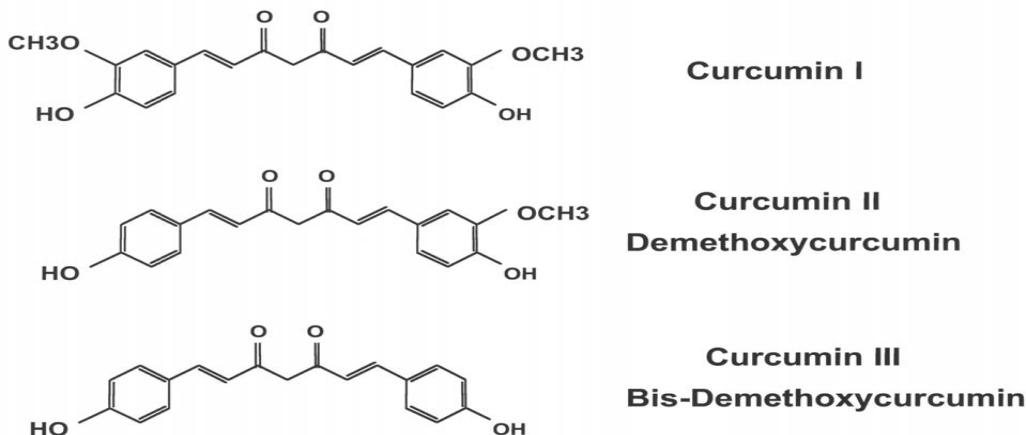


Figure 2.1: Natural yellow dye, Curcumin (diferuloylmethane; 1, 7-Bis(4-hydroxy-3-methoxyphenyl)-1,6-heptadiene-3,5-dione) curcumin I, MW 368; curcumin II, MW 338; Curcumin III, MW 308.

Tonnesen examined the kinetics of pH-dependent curcumin degradation in aqueous solution. A plot of the rate constant against pH indicated the pKa values of the acid protons. The graph also indicated the complexity of curcumin degradation. The same investigators also investigated the stability of curcumin when exposed to UV/visible radiation. The main degradation products were identified. The reaction mechanisms were investigated and the order of the overall degradation reactions and the half-lives of curcumin in different solvents and in the solid state were determined. These workers also examined the photobiological activity of curcumin using bacterial indicator systems. On irradiation with visible light, curcumin proved to be phototoxic for *Salmonella typhimurium* and *Escherichia coli*, even at very low concentrations. The observed phototoxicity makes curcumin a potential photosensitizing drug, which might find application in the phototherapy of, for example, psoriasis, cancer and bacterial and viral diseases. Recently, the same group, prepared a complexed curcumin with cyclodextrin to improve its water solubility and the hydrolytic and photochemical stability of the compound. Complex formation resulted in an increase in water solubility at pH 5 by a factor of at least 104. The hydrolytic stability of curcumin under alkaline conditions was strongly improved by complex formation, while the photodecomposition rate was increased compared to a curcumin solution in organic solvents. The cavity size and the charge and bulkiness of the cyclodextrin side-chains influenced the stability constant for complexation and the degradation rate of the curcumin molecule. Wang *et al.* examined the degradation kinetics of curcumin under various pH conditions and the stability of curcumin in physiological

matrices. When curcumin was incubated in 0.1 M phosphate buffer and serum-free medium, pH 7.2, at 37°C, about 90% decomposed within 30 minutes. A series of pH conditions ranging from 3 to 10 were tested and the results showed that decomposition was pH dependent and occurred faster at neutral-basic conditions. It is more stable in cell culture medium containing 10% fetal calf serum and in human blood; less than 20% of curcumin decomposed within 1 hour and, after incubation for 8 hours, about 50% of curcumin still remained. Trans- 6-(4'-hydroxy-3'-methoxyphenyl)2,4-dioxo-5-hexenal was predicted to be the major degradation product and vanillin, ferulic acid and feruloyl methane were identified as minor degradation products. The amount of vanillin increased with incubation time [18].

Wide arrays of phenolic substances, especially those present in dietary and medicinal plants, have been reported to possess substantial antioxidant, antiinflammatory, anticarcinogenic, and antimutagenic effects . The spice turmeric is used in curries as a coloring and flavoring agent in various parts of the world, especially in the Indian subcontinent, an area that has a low incidence of colorectal cancer .

Several animal model studies have shown that curcumin suppresses carcinogenesis in skin, stomach, colon, breast, and liver. Curcumin is reported to induce apoptosis in a wide variety of tumor cells, including B- and T-cell leukemias, colon, and breast carcinoma. Chemopreventive activities of curcumin are thought to involve up-regulation of carcinogen-detoxifying enzymes and antioxidants, suppression of cyclooxygenase-2 expression , and inhibition of nuclear factor-nB release . Inhibition of nuclear factor-nB release by curcumin also leads to the downregulation of various proinflammatory cytokines (e.g.,tumor necrosis factor and interleukins) and inhibition of the mRNAexpression of several proinflammatory enzymes (e.g., cyclooxygenase, lipoxygenases, metalloproteinases, and nitric oxide synthase). In animal studies, curcumin undergoes rapid metabolic reduction and conjugation, resulting in poor systemic bioavailability after oral administration. For example, an oral dose of 0.1 g/kg administered to mice yielded a peak plasma concentration of free curcumin that was only 2.25 µg/mL . In rats, curcumin completely disappeared from plasma within 1 h after a 40 mg/kg i.v. dose. When given orally at a 500 mg/kg dose, peak concentrations of 1.8 ng/mL of free curcumin were detected in plasma. The major metabolites of curcumin identified in rat plasma were curcumin glucuronide and curcumin sulfate based on enzymatic hydrolysis studies.

Hexahydrocurcumin, hexahydrocurcuminol, and hexahydrocurcumin glucuronide were also present in minor amounts .

Data on the pharmacokinetic properties and metabolism of curcumin in human are very limited. In a human study conducted in 25 patients with precancerous lesions, free curcumin concentrations in plasma after taking 4, 6, and 8 g of curcumin per day for 3 months were 0.19, 0.20, and 0.60 $\mu\text{g}/\text{mL}$, respectively. None of the curcumin conjugates or metabolites of curcumin were reported in that study. A study of six patients with advanced colorectal cancer dosed with 3.6 g of curcumin daily for up to 3 months yielded 4.3, 5.8, and 3.3 ng/mL mean plasma concentrations of curcumin, curcumin glucuronide, and curcumin sulfate, respectively, 1 h after administration .

In animal models, no toxicity has been reported to date. Similarly, in human to date, few adverse events due to curcumin even at very high doses have been reported. Whether the low toxicity is only a function of lack of bioavailability is an open question [19].

2.2 Drug Delivery Systems and Nanotechnology

2.2.1 The “NANO era” of targeted or site-controlled drug delivery systems

In the mid to late 1970s the concept of polymer-drug conjugates or “nanotherapeutics”, independently arose at various places around the world. Three key technologies were the major factors that stimulated the immense activity and clinical success of nanotherapeutics from the late 1980s to the present. The first was the concept of “PEGylation”, which refers to polyethylene glycol conjugated drugs or drug carriers. The second is the concept of “active targeting” of the drug conjugate by conjugating cell membrane receptor antibodies, peptides or small molecule cell ligands to the polymer carrier. The third was the discovery of the “enhanced permeation and retention effect” (EPR) by Hiroshi Maeda in Kumamoto, Japan, wherein nano-scale carriers are entrapped within solid tumors due to leaky vasculature of the fast-growing tumor. This is called “passive” targeting as contrasted with active targeting. These will be discussed and referenced below.

The first major success of polymer-drug conjugates was based on the conjugation of poly(ethylene glycol) or PEG to the drug, known by the term “PEGylation”. In the late 1960s, Frank Davis at Rutgers University conceived of the concept of

PEGylation to enhance both the circulation time and the stability (against enzyme attack or immunogenic recognition) of the recombinant protein drugs that were just being developed. This led to the founding of the PEGylation company called Enzon, at the beginning of the 1980s. The first clinical products were PEGylated enzymes such as asparaginase and glutaminase, which metabolized asparagine and glutamine, essential nutrients for leukemic cancer cells. Milton Harris, a chemistry professor at the University of Alabama, Huntsville later founded Shearwater Polymers, the other important PEGylation company, that subsequently collaborated with major pharmaceutical companies to introduce a number of PEGylated recombinant protein products to the clinic. Independent of Davis and around that same time in the 1970s, Helmut Ringsdorf at the University of Mainz sketched the idea of a targeted, polymer-drug conjugate and published it in 1975.

Independent of Ringsdorf, Jindra Kopecek in Prague conceived of a new polymer carrier called poly(hydroxypropyl methacrylamide) (PHPMA) which was first synthesized by Karel Ulbrich, his PhD student; the drug was conjugated to the PHPMA by pendant tetrapeptide linkages that were degradable by cathepsin B, a lysosomal enzyme. The polymer synthesis and characterization was carried out in Prague and the conjugate's drug action was tested in collaboration with Ruth Duncan, John Lloyd's PhD student, in the UK (Kopecek was introduced to Lloyd and Duncan by Ringsdorf). Duncan also contributed to the design of the polymer. Blanka Rihova in Prague found PHPMA to be non-immunogenic, and James Cassidy, MD, a UK clinician, led the clinical trials. The drugs included doxorubicin and other small molecule anti-cancer drugs. The drug-polymer conjugates could be actively targeted with ligands such as galactose, an asialo-glycoprotein membrane receptor ligand for hepatocytes, for liver cancer treatment. Etienne Schacht of Ghent later synthesized new degradable peptide sequences. This was truly an international success story of a remarkable team of scientists and clinicians, bringing a novel polymer-drug conjugate to the clinic. This success has had a great influence on the field of nanoscale polymeric therapeutics. Duncan has published several reviews of nano-carriers and nano-therapeutics, one along with Kopecek.

Other polymer-small drug conjugates are currently being developed; examples include: Cell Therapeutics in Seattle with Xytax®, a polyglutamic acid-paclitaxel

conjugate, in phase III trials, and Insert Therapeutics of Mark Davis, with IT-101, a PEG-cyclodextrin-camptothecin polymeric micelle in phase II trials. Polymeric micelle-small drug and nucleic acid DDS will be discussed in more detail below.

One of the earliest examples of active targeting was the use of a polyclonal antibody to target a drug in the late 1950s. The development and availability of monoclonal antibodies in the 1960s made it possible to deliver nano-therapeutics to specific cells. Other ligands have been discovered and have been used to target cells. One of the most notable has been the integrin receptor ligand, the peptide RGD, first published in 1980 in *Science* by Pierschbacher and Ruoslahti.

In 1984, Hiroshi Maeda of Kumamoto University discovered what he called the “Enhanced Permeation and Retention” effect, or EPR. He was carrying out animal studies with his novel polymerdrug conjugate, styrene-maleic anhydride (SMA) conjugated to the anti-cancer peptide drug, neocarcinostatin (NCS), which he called “SMANCS” and he had labeled the conjugate with a dye. He noted that the dye accumulated within the tumor tissue, and concluded that the rapidly forming vasculature in such solid tumors was “leaky”, while the lymph drainage system was not yet working efficiently, and that led to its entrapment or accumulation within the tumor tissue. This combination caused the nano-scale SMANCS to be trapped within the extra-vascular tumor tissue. He submitted a manuscript on this observation, and Maeda recalls that Folkman was one of the reviewers; Folkman encouraged him to publish that exciting finding “as soon as possible” . Recent evidence by various researchers suggests that the EPR effect is only effective close to the leaky vessels, and not throughout the tumor, due perhaps to the low diffusion coefficient of the nanocarriers within the tumor’s extravascular tissues.

In the late 1980s and early 1990s, other nano-scale DDS were developed, including PEGylated polymeric micelles and liposomes. Kazunori Kataoka, Teruo Okano and Masayuki Yokoyama in Tokyo synthesized A-B block copolymers of a PEG block conjugated to a hydrophobic amino acid block. These block copolymers spontaneously formed PEGylated polymeric micelles above a very low CMC. The hydrophobic cores of the micelles could be loaded with small hydrophobic drugs such as doxorubicin, either by physically loading the drug or by conjugating it to the

amino acid pendant acid groups, and the terminal OH groups of the PEGs could be conjugated with cell specific ligands for targeted delivery. Around essentially the same time, and independent of Kataoka et al.'s work, Alexander Kabanov in Nebraska developed drug-loaded PEGylated micelles based on PEO-PPO-PEO tri-block copolymers known as Pluronics® (where “PEO”=“PEG”) Many different PEGylated polymeric micelles are now in clinical trials for delivery of a number of small molecule drugs.

In the early 1990s, the emergence of important nucleic acid drugs, such as plasmid DNA (pDNA) and antisense ODNs (“oligos”) led to the development of cationically-condensed pDNA or ODN nanoparticles. Both cationic polymers and cationic liposomes were used to condense the nucleic acid drugs; the resultant complexes are called polyplexes or lipoplexes, respectively. One key polycation development was by Jean-Paul Behr, who proposed the use of poly(ethyleneimine) or PEI for complexation and intracellular delivery of nucleic acid drugs, where endosomal escape was enhanced by the PEI due to the “proton sponge” mechanism.

Block polymers of PEG-polycation (A-B) or PEG-polycation-PEG (AB- A) have been used to condense a nucleic acid drug, to form PEGylated micelles, with the water insoluble nucleic acid-polycation electrostatic complexes (polyplexes) forming the core of the PEGylated polymeric micelle. More recently, in the 2000s, a number of companies (e.g., Alnylam, Roche, Merck, Calando) have been involved in clinical trials for delivery of siRNA from similar lipoplexes and polyplexes.

Nano-scale albumin-based drug carriers have recently reached the clinic. Examples include Abraxane®, a nanoparticle of albumin and paclitaxel, and Albuferon- α ®, a conjugate of albumin and interferon- α .

During the 1990s Vladimir Torchilin developed many liposomal formulations, some for diagnostic imaging applications and others for drug delivery, where hydrophilic drugs could be loaded in the aqueous core of the liposome, or hydrophobic drugs could be loaded in the lipidbilayer shell. A PEGylated liposome-doxorubicin product called Doxil® was approved by the FDA for clinical use in 1995. Martin Woodle and Frank Martin developed this product at Liposome Technologies Inc., (LTI).

Nano-scale DDS with polymeric carriers that are still underdevelopment include dendrimers, dendronized polymers and other hyper-branched polymers. Most of

these have succeeded because of the emergence of three key technologies: (1) PEGylation, (2) active targeting to specific cells by ligands conjugated to the DDS, or passive targeting to solid tumors via the EPR effect [20].

2.2.2. Nanoparticle Carriers based on Amphiphilic Polymers for Drug Delivery

Polymeric micelles from of amphiphilic block copolymers [21, 22] are supramolecular core-shell-type assemblies of tens of nanometers in diameter, which can mimic naturally occurring biological transport systems such as lipoproteins and viruses [23]. Recently, polymeric micelles as carriers of anti-tumor drugs have drawn increasing research interests, due to their various advantages in drug delivery applications. First, polymeric micelles are highly stable in aqueous solution because of their intrinsic low critical micelle concentration (CMC), which prevents the drug-entrapped micelles from dissociation upon dilution in the blood stream after intravenous injection. Furthermore, the nanosize of polymeric micelles can facilitate their extravasations at tumor sites while avoiding renal clearance and nano-specific reticuloendothelial uptake. In these micellar delivery systems, the hydrophobic core of the micelles is a carrier compartment that accommodates anti-tumor drugs, and the shell consists of a brush-like protective corona that stabilizes the nanoparticles in aqueous solution [23-25].

The problem associated with the classical micelle structure can be overcome by developing molecules in which the lipophilic components are covalently bound together within the micelle core. Core polymerization is an effective method to prevent dissociation of the block copolymer micelle. Kataoka's group has successfully employed this idea. In their study, the micelles were prepared from an amphiphilic block copolymer in which the hydrophobic block contained a polymerizable end group. After micellation, the end groups on the hydrophobic block were polymerized to form a stable core for the star-shaped polymer structure. The resulting micelles showed fairly high stability and maintained small size. As anticipated, the core polymerized micelle showed excellent solubilization of rather large molecules such as taxol.

Another approach developed recently by Uhrich et al. with a three-arm star polymer composed of mucic acid substituted with fatty acid as the lipophilic inner block and with PEG as the hydrophilic outer block. This new type of molecule was capable of

encapsulating a hydrophobic model drug in aqueous media. However, due to the structural constraints, the free volume of the hydrophobic core was limited, and only one or two drug molecules could be encapsulated in each micelle. A series of star block copolymers with the number of arms ranging from three to eight have also been synthesized. The arms were composed of block copolymer with PEG as the inner hydrophilic block and PCL as the outer hydrophobic block. The application of this type of copolymer as an injectable drug delivery system was reported. It was found that a reversible sol-gel transition process exists for this system, which is useful for drug delivery. However, such star copolymers do not form micelles in aqueous media because the hydrophilic block is located in the interior of the star. A recent paper described the synthesis of a four-arm star block copolymer of PCL and PEG by the same route and similar chemistry as reported in this paper. Another paper described the preparation of a four-arm star PCL-*b*-PEG polymer with diethylzinc catalyst. However, the molecular weight distribution of the block copolymer was unacceptably wide.

Many studies have been carried out using dendrimers as drug delivery systems. Star polymers with a dendrimer as the hydrophobic core and multiple PEG chains as the hydrophilic arms have been synthesized and investigated as unimolecular micelles for drug delivery by Fre'chet and Kono. It has been demonstrated that the micelles with larger dendrimer core have a higher encapsulation capability than those with smaller cores. However, due to the structural limitations involved in the synthesis of dendrimers of higher generation, and the relatively compact structure of the dendrimers, it is difficult to increase significantly the size of the hydrophobic dendritic core in the dendrimer- PEG star polymer. Therefore, such dendrimer systems have limitations in terms of drug-loading capacity and delivery of compounds of large size [26].

Recently, more and more attention has been paid for applying biodegradable polymers, especially aliphatic polyesters such as poly(ϵ -caprolactone) (PCL), polylactide (PLA), and polyglycolide (PGA), as biomaterials due to their biocompatibility, degradability, and excellent shaping and molding properties. PCL is a kind of biodegradable materials with low toxicity, excellent biocompatibility and bioabsorbability *in vivo*. It has been widely used in biomedical applications, such as sustained drug delivery systems, implants for orthopedic devices and absorbable

fibers. However, the low hydrophilicity and high crystallinity of PCL reduce its degradation rate, which results in poorer soft tissue compatibility [25-28]. Anti-tumor drug, doxorubicin (DOX), is widely used in cancer chemotherapy. Major drawbacks of the drug is the acute toxicity to normal tissue and inherent multi-drug resistance effect. To reduce the acute toxicity of the free drug and improve their therapeutic efficacy, various liposome [29] and polymeric micelle systems were designed as delivery vehicles. The use of polymeric micelles as carriers of anticancer drugs has advanced greatly by the work of some researchers [30].

Micelles formed from amphiphilic block copolymer shape recently attracted significant attention in diverse fields of medicine and biology. In particular, polymeric micelles have been developed as drug and gene delivery systems as well as carriers for various contrasting agents in diagnostic imaging applications. In an aqueous environment, the hydrophobic blocks of the copolymer are expected to segregate into the core of the micelle, whereas the hydrophilic blocks form the corona or outer shell. Such a core-shell architecture of the polymeric micelles is essential for their utility as novel functional materials for pharmaceutical applications. The hydrophobic micelle core serves as a microenvironment for the incorporation of various therapeutic compounds; the corona, or outer shell, serves as a stabilizing interface between the hydrophobic core and the external medium. As a result, polymeric micelles can be used as efficient containers for reagents with poor solubility and/or low stability in physiological environments. Interest in polymeric micelles for drug delivery has increased rapidly since the late 1980s. Most of the work has focused on classical micelles formed by intermolecular aggregation of amphiphilic polymers as the drug delivery vehicle, and the advantages of using micelle structures as a drug delivery system have been demonstrated.

The major factors that influence the performance of polymeric micelles for drug delivery are loading capacity, release kinetics, circulation time, biodistribution, size, and stability. Micelle stability is particularly important. Recent studies have shown that the *in vivo* antitumor activity of a drug incorporated into the polymer micelles is positively correlated with the stability of micelles *in vitro*. The formation of classical micelles is thermodynamically favorable only above a specific concentration of the amphiphilic molecules (critical micelle concentration, cmc). Above the cmc, micelles are in dynamic equilibrium with the free copolymer molecules (unimers) in solution,

continuously breaking and reforming. When the concentration of the copolymer is below the cmc, micelles tend to disassemble. Such thermodynamic instability of micelles below the cmc is one of the concerns for their application *in vivo*. A delivery system is subject to a severe dilution upon intravenous injection into an animal or human subject. In the bloodstream, under dilution, micelles begin to disassemble, causing changes in micelle structure and size. Therefore, controlling the release rate of drugs is difficult. Sudden dissociation of micelles may cause serious toxicity problems due to potentially large fluctuations in drug concentrations.

The problem associated with the classical micelle structure can be overcome by developing molecules in which the lipophilic components are covalently bound together within the micelle core. Core polymerization is an effective method to prevent dissociation of the block copolymer micelle. Kataoka's group has successfully employed this idea. In their study, the micelles were prepared from an amphiphilic block copolymer in which the hydrophobic block contained a polymerizable end group. After micellation, the end groups on the hydrophobic block were polymerized to form a stable core for the star-shaped polymer structure. The resulting micelles showed fairly high stability and maintained small size. As anticipated, the core polymerized micelle showed excellent solubilization of rather large molecules such as taxol .

Another approach developed recently by Uhrich et al. with a three-arm star polymer composed of mucic acid substituted with fatty acid as the lipophilic inner block and with PEG as the hydrophilic outer block. This new type of molecule was capable of encapsulating a hydrophobic model drug in aqueous media. However, due to the structural constraints, the free volume of the hydrophobic core was limited, and only one or two drug molecules could be encapsulated in each micelle. A series of star block copolymers with the number of arms ranging from three to eight has also been synthesized. The arms were composed of block copolymer with PEG as the inner hydrophilic block and PCL as the outer hydrophobic block. The application of this type of copolymer as an injectable drug delivery system was reported. It was found that a reversible sol-gel transition process exists for this system, which is useful for drug delivery. However, such star copolymers do not form micelles in aqueous media because the hydrophilic block is located in the interior of the star. A recent paper described the synthesis of a four-arm star block copolymer of PCL and PEG by

the same route and similar chemistry as reported in this paper. Another paper described the preparation of a four-arm star PCL-*b*-PEG polymer with diethylzinc catalyst. However, the molecular weight distribution of the block copolymer was unacceptably wide.

Many studies have been carried out using dendrimers as drug delivery systems. Star polymers with a dendrimer as the hydrophobic core and multiple PEG chains as the hydrophilic arms have been synthesized and investigated as unimolecular micelles for drug delivery by Fréchet and Kono. It has been demonstrated that the micelles with larger dendrimer core have a higher encapsulation capability than those with smaller cores. However, due to the structural limitations involved in the synthesis of dendrimers of higher generation, and the relatively compact structure of the dendrimers, it is difficult to increase significantly the size of the hydrophobic dendritic core in the dendrimer-PEG star polymer. Therefore, such dendrimer systems have limitations in terms of drug-loading capacity and delivery of compounds of large size [31].

2.3 Targeted Drug delivery

There are two ways of targeted drug delivery.

2.3.1 Passive tumor targeting

Most anticancer drugs used in conventional chemotherapy have no tumor selectivity and are randomly distributed in the body, resulting in a relatively low therapeutic index. For this reason, the common solid tumors that are major causes of cancer mortality are difficult to treat with chemotherapy alone. Polymeric carriers bearing physically entrapped or chemically conjugated drugs are an attractive strategy for improving the efficiency of tumor targeting. These nanoscale drug delivery systems have shown promising pharmacokinetics at both the whole body and cellular levels. At first, it seemed as though receptor-mediated targeting was the only workable way to improve tumor selectivity, and thus, many researchers sought to develop conjugates bearing tumor-specific antibodies or peptides. However, more recent studies have shown that polymer-conjugated drugs and nanoparticles show prolonged circulation in the blood and accumulate passively in tumors even in the

absence of targeting ligands, suggesting the existence of a passive retention mechanism.

Tumor blood vessels are generally characterized by abnormalities such as a relatively high proportion of proliferating endothelial cells, increased tortuosity, pericyte deficiency and aberrant basement membrane formation. This defective vascular structure, which is likely the result of the rapid vascularization necessary to provide oxygen and nutrients for fast-growing cancers, decreases lymphatic drainage and renders the vessels permeable to macromolecules. Because of the decreased lymphatic drainage, the permeant macromolecules are not removed efficiently, and are thus retained in the tumor. This passive targeting phenomenon, first identified by Maeda et al. has been called the “enhanced permeation and retention (EPR) effect”. Since this first identification, numerous studies have shown that the EPR effect results in passive accumulation of macromolecules and nanosized particulates (e.g. polymer conjugates, polymeric micelles, dendrimers, and liposomes) in solid tumor tissues, increasing the therapeutic index while decreasing side effects. (Fig. 2.2) illustrates the concept of passive tumor targeting by EPR effects.

The optimum size of nanoparticles that can be accumulated in a tumor by the EPR effect is not yet precisely known. However, studies using liposomes and nanoparticles have indicated that the cutoff size of the pores in tumor vessels is as large as 200 nm–1.2 mm and direct observation of tumor vasculature has demonstrated a tumor dependent pore cutoff size ranging from 200nm to 2 mm. These size ranges seem to indicate that drug loaded nanoparticles may be accumulated in malignant tumor cells. Consistent with this, administration of liposomal formulations with entrapped DOX have been demonstrated to exhibit favorable pharmacokinetics due to EPR-mediated tumor targeting, as compared with free DOX. In addition, polymer-based nanoparticles bearing DOX were found to circulate in the blood for more than 3 days, and gradually accumulated in tumors via the EPR effect. In theory, the EPR effect could be used to generally deliver genes and proteins to primary or metastasized tumors, suggesting that a wide variety of polymer-based nanomedicines may be used for tumor targeting of anticancer drugs. However, it should be noted that the vessel permeability that forms a cornerstone of the EPR effect varies during tumor progression. In addition, extravasation of

polymeric nanomedicines will depend on the tumor type and anatomical location, as well as the physicochemical properties of the utilized polymer [32].

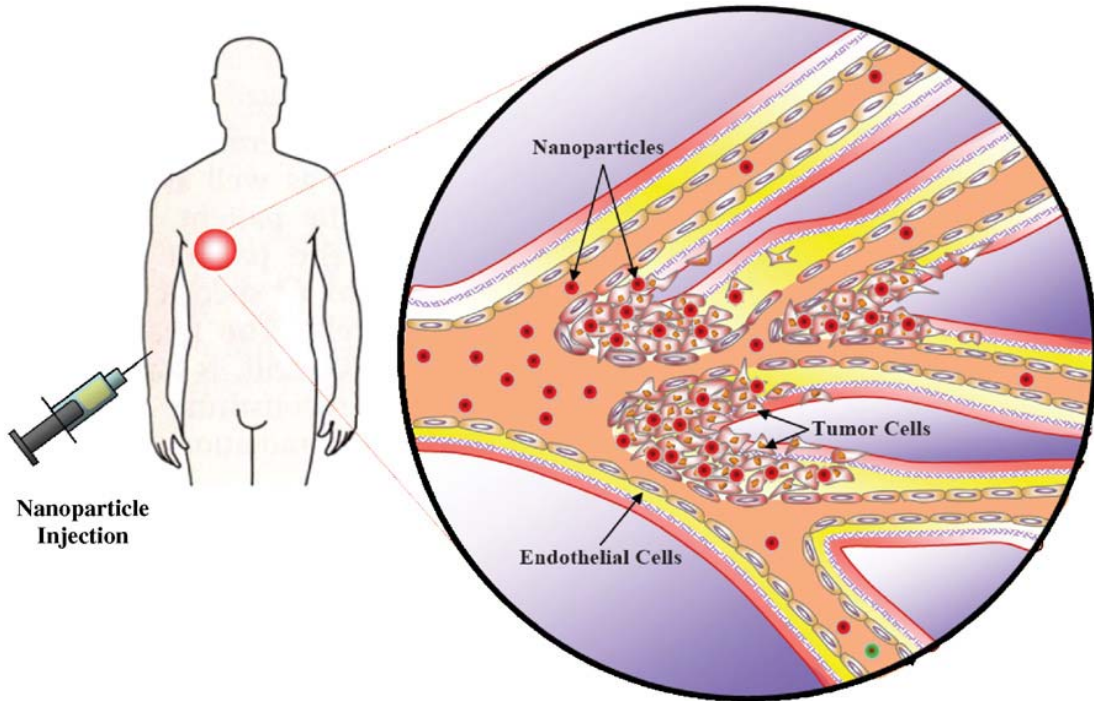


Figure 2.2: Passive drug targeting through the enhanced permeability and retention (EPR) effect. The polymeric nanoparticles preferentially accumulate in solid tumors, owing at least in part to leaky tumor vessels and an ineffective lymphatic drainage system [32].

2.3.2 Active tumor targeting

Researchers have expended a great deal of effort aimed at developing methods for efficiently delivering drugs to tumor cells through active targeting. Cancer cells often display increased cell surface expression of proteins that may be found at low levels on normal cells (tumor-associated antigens), as well as proteins that are found exclusively on cancer cell surfaces (tumor-specific antigens). Active drug targeting is usually achieved by chemical attachment to a targeting component that strongly interacts with antigens (or receptors) displayed on the target tissue, leading to preferential accumulation of the drug in the targeted organ, tissue, or cells. The use of a targeting moiety not only decreases adverse side effects by allowing the drug to be delivered to the specific site of action, but also facilitates cellular uptake of the drug by receptor mediated endocytosis, which is an active process requiring a significantly lower concentration gradient across the plasma membrane than simple endocytosis.

Active targeting often makes use of monoclonal antibodies, which were first shown to be capable of binding to specific tumor antigens in 1975. For successful cancer therapy, antigen targets for monoclonal antibody therapy should be expressed on the cancer cells but not on critical host cells, and there should be a low risk of mutation or structural variation among the antigens. Several monoclonal antibody-based therapeutic agents have been approved by the FDA. In addition, although monoclonal antibodies were initially used as therapeutic agents in their own right, they may also serve as carriers by conjugation to a drug or nanoparticulate drug delivery system.

Numerous other ligands have been used for active targeting. Folate targeting is an interesting approach for cancer therapy because it offers several advantages over the use of monoclonal antibodies. Folates are low molecular weight vitamins required by eukaryotic cells, and their conjugates have the ability to deliver a variety of drugs or imaging agents to pathological cells without causing harm to normal tissues. More importantly, elevated levels of folate receptors (FRs) are expressed on epithelial tumors of various organs such as colon, lung, prostate, ovaries, mammary glands, and brain. Folate is known to be non-immunogenic, and folate-conjugated drugs or nanoparticles are rapidly internalized via receptor-mediated endocytosis.

Furthermore, the use of folate as a targeting moiety is believed to bypass cancer cell multidrug-efflux pumps. The receptor-mediated uptake of folate conjugates proceeds through a series of distinct steps, as shown in Figure 2.3. The process begins with the conjugate binding to FRs on the cell surface. The plasma membrane then invaginates and eventually forms a distinct intracellular compartment. The endocytic vesicles (endosomes) become acidified to pH ca. 5, allowing the FR to release the folate conjugates. The membrane-bound FRs recycle back to the cell surface, allowing them to mediate the delivery of additional folate conjugates. Concurrently, the folate conjugates released from FRs escape the endosome, resulting in drug deposition in the cytoplasm. To date, a number of conjugates (including protein toxins, immune stimulants, chemotherapeutic agents, liposomes, nanoparticles, and imaging agents) have been successfully modified with folates and delivered to FR-expressing cells.

Transferrin, an 80kDa glycoprotein, is also suitable ligand for tumor targeting because its receptors are over-expressed on cancers, at levels correlating with the grade of malignancy. Transferrin is synthesized by the liver and secreted to plasma,

where it binds to endogenous iron, forming the iron-transferrin chelate, which is an important physiological source of iron for cells in the body. Transferrin receptors on cell surfaces recognize the chelate and mediate its endocytosis into acidic compartments. The low pH environment triggers dissociation of the iron and the iron-poor transferrin is released out of the cell for recycling. Transferrin receptors are often upregulated on the surface of malignant cells, and have thus become a target for cancer therapy. Bellocq et al. developed a transferrin-modified, cyclodextrin polymer- based gene delivery system composed of polymer/ DNA nanoparticles that were surface-modified to display PEG, yielding transferrin targeting of cancer cells. These transferrin-conjugated nanoparticles remained stable in a physiological solution and could be used to transfect leukemia cells with increased efficiency over untargeted particles, indicating the potential of transferrin-modified nanoparticles in cancer therapeutics. More recently, Sahoo and Labhasetwar prepared paclitaxel loaded nanoparticles with shells formed of the biodegradable polymer, poly(lactic–co–glycolic acid) (PLGA), conjugated to transferrin via epoxy linkages. The transferrin-conjugated nanoparticles demonstrated greater cellular uptake and reduced exocytosis, yielding greater antiproliferative activity and more sustained effects compared to the free drug or unconjugated nanoparticles.

Luteinizing hormone-releasing hormone (LHRH) is another targeting moiety; the LHRH receptor is barely present on the surfaces of most healthy human cells, but is over-expressed in ovarian and some other cancer cells. Dharap et al. recently developed the LHRH–PEG–camptothecin targeted anticancer drug delivery system, wherein LHRH targets the corresponding receptors in cancer cells: PEG is used as a carrier to prolong the circulation time in blood, and camptothecin functions as the anticancer drug. The targeted conjugate exhibited significantly higher cytotoxicity against cancer cells than the non-targeted PEG– camptothecin conjugate or the free drug *in vivo*, indicating the validity of actively targeted nanoparticles for anticancer therapy [32].

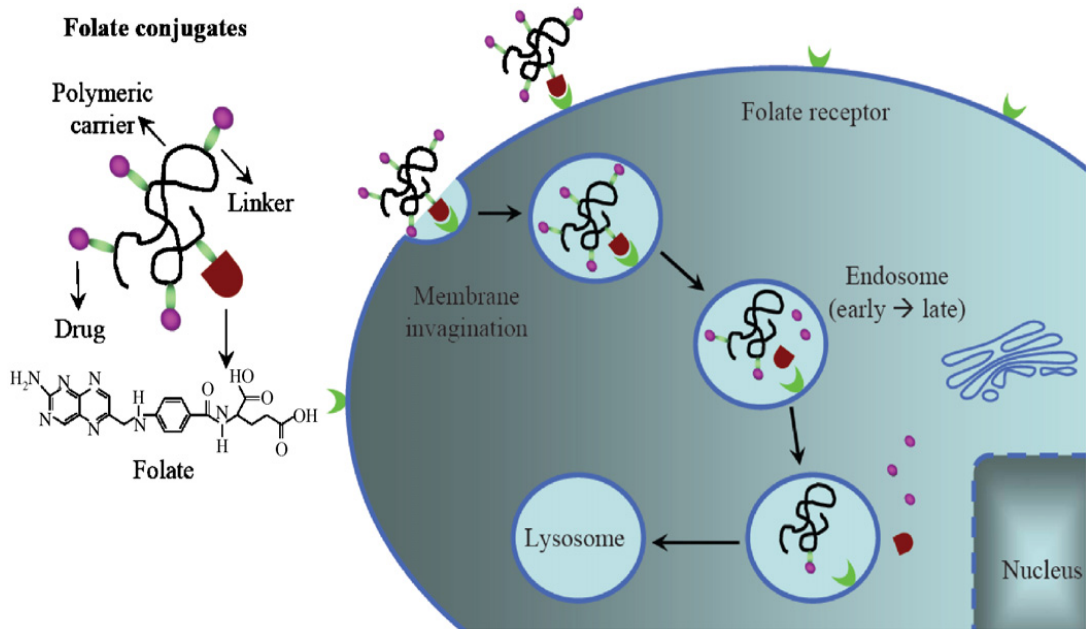


Figure 2.3: Receptor-mediated endocytosis of folate-conjugated drugs. The folate receptors recognize the conjugates, which are subsequently subjected to membrane invagination. As the endosomal compartment acidifies, the conjugate and the drugs are released from the receptor into the cytosol [32]..

2.4 Micelle structure and composition

Polymer micelles are composed of amphiphilic macromolecules that have distinct hydrophobic and hydrophilic block domains, with the structure of the copolymers usually being a di-block, tri-block, or graft copolymer. Within each copolymer system, aqueous exposure induces the hydrophobic and hydrophilic segments to phase separate and form nanoscopic supramolecular core/shell structures.

Depending on the relative size of the hydrophobic and hydrophilic segments and solvent conditions, Eisenberg et al. have demonstrated the formation of structures of many morphologies, including spheres, rods, vesicles, tubules, and lamellae. Although aggregates of different morphology may provide drastically different pharmacokinetic properties, as in the case of filamentous nanocarriers which can provide different flow behavior over spherical particles due to anisotropic alignment most current applications have focused on spherical micelles and thus will be the subject of this review. Many types of copolymers have been used for micelle formation, but the requirements of biocompatibility and oftentimes biodegradability have limited the choice of copolymers in clinical applications. Table 2.1 provides the names and structures of common copolymers for drug delivery applications. For the

hydrophilic segment, the most commonly used polymer is polyethylene glycol (PEG) with a molecular weight of 2-15 kD. PEG is completely water soluble, non-toxic, and uncharged, the latter property serving to lessen the possibility of undesired electrostatic interactions with plasma proteins. Other hydrophilic polymers such as poly(N-vinyl pyrrolidone) (PVP) or poly(N-isopropyl acrylamide) (pNIPAM) have also been used to form the micelle corona layer. For the hydrophobic segments, the most common materials are hydrophobic polyesters, but other materials, such as polyethers, polypeptides, or poly(β -amino ester) have also been used. Polyesters and polyamides can undergo hydrolytic and enzyme-catalyzed degradations, respectively, and are considered biodegradable. As an example of a micelle forming copolymer, Pluronic is a ternary copolymer of PEG and poly(propylene oxide) (PPO) oriented in a PEG-PPO-PEG configuration. Upon micellization, the hydrophobic PPO segments form the core while the PEG segments form the corona. The core-shell structure of polymer micelles affords several advantages for drug delivery applications. Firstly, drug encapsulation within the micelle core allows for solubilization of water insoluble drugs. For example, the water solubility of paclitaxel can be increased by several orders of magnitude from 0.0015 to 2 mg/mL through micelle incorporation. Secondly, micelles have prolonged blood half-lives because PEG prevents opsonization, effectively reducing micelle uptake by the reticuloendothelial system (RES). Thirdly, their small size (10-100 nm) makes them suitable for injection and enhanced tumor deposition due to the enhanced permeability and retention (EPR) effect stemming from the leakiness of tumor vasculature. Finally, their chemistry allows for the development of multifunctional modalities that can enhance micelle accumulation in cancerous tissues and facilitate drug internalization inside cancer cells [33].

Table 2.1: Commonly Used Block Segments of Copolymers for Micellar Drug Delivery Systems [33].

* Depending on stereochemistry

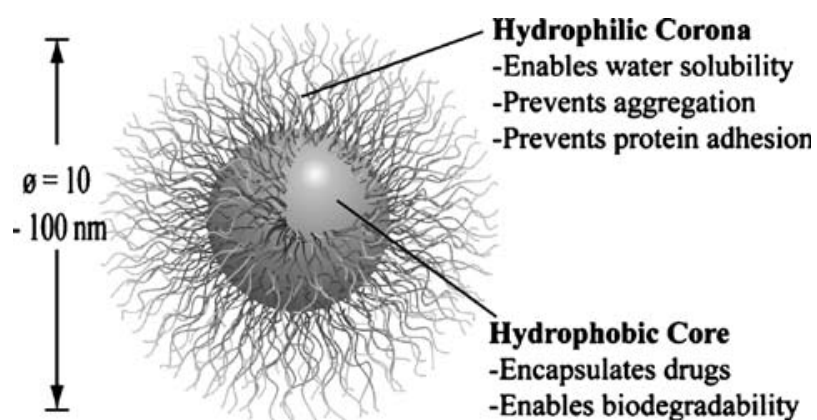


Figure 2.4: Schematic illustration of the core-shell structure of a polymer micelle with intended functions of each component

2.4.1 Methods of micelle preparation

There are two principal methods for the preparation of block copolymer micelles, the direct dissolution method and the dialysis method, as outlined in Fig. 2.5. The choice of which method to use depends mostly on the solubility of the block copolymer in water. To this point, mostly star-type micelles have been investigated as drug carriers. Star-type micelles are formed from block copolymers which have corona-forming blocks that are longer than the core-forming blocks. If the copolymer is marginally soluble in water, the direct dissolution method is employed, whereas if the copolymer is poorly soluble in water, the dialysis method is usually employed.

The direct dissolution simply involves adding the copolymer to water or another aqueous medium such as phosphate buffer saline. The micelles formed from the PEO-*b*-PPO-*b*-PEO copolymers are routinely formed by direct dissolution, but in some cases the copolymer and water are mixed at elevated temperatures to ensure micellization.

The dialysis method is often used when micelles are to be formed from a copolymer that is not easily soluble in water. In this case, the copolymer is first dissolved in a common organic solvent that is miscible with water such as dimethylformamide, tetrahydrofuran, or dimethylacetamide. The copolymer solvent mixture is stirred and then dialyzed against bidistilled water. During the process of dialysis micelle formation is induced and the organic solvent is removed.

The size and size population distribution of micelles produced using the dialysis method may vary depending on the organic solvent employed. In addition, the weight fraction or yield of micelles obtained was also found to vary with the choice of organic solvent. For example, in a study by La et al., the use of DMSO as the organic solvent gave rise to PEO-*b*-PBLA micelles which were only 17 nm in size; however, only 6% of the copolymer formed micelles. Yet, when DMAc was used, the micelles were obtained in high yield, with an average particle size of 19 nm and a narrow size distribution. In this way, the dialysis method provides a means of tailoring the size and size population distribution of the micelles.

Recently, our group has been worked on crewcut micelle systems formed from a variety of copolymers such as PS-*b*-PAA, PS-*b*-PEO and PCL-*b*-PEO. Crew-cut

aggregates are formed from copolymers which have core-forming blocks that are longer than the corona-forming blocks. These copolymers are thus insoluble in water and therefore must first be dissolved in a common organic solvent. For this reason, the method of preparation employed involves the initial dissolution of the copolymer in a common organic solvent followed by the slow addition of water at a very slow rate. Self-assembly occurs at some critical water content which depends on the physical properties of the block copolymer, primarily the length of the hydrophobic block and the copolymer concentration. The copolymer in the organic:water solvent mixture is then dialyzed against bidistilled water. Our studies have found that the size, size distribution and morphology of the micelles can depend on both the common organic solvent employed and the rate of water addition to the copolymer solvent mixture. Once again this demonstrates the many parameters of the micelles (size, size population distribution and morphology) that can be manipulated by simple variations within the method of preparation.

2.4.2 Micelle stability

The stability of block copolymer micelles includes two different concepts thermodynamic stability and kinetic stability. A micelle is thermodynamically stable relative to disassembly to single chains in pure water if the total copolymer concentration is above the critical micelle concentration (CMC). The critical micelle concentration (CMC) is the copolymer concentration below which only single chains exist but above which both micelles and single chains are present. However, even if a micelle system is below its CMC, it may still be kinetically stable and survive at least for some period or time, if the core is large and the core material is below the Tg or if it is crystalline and thus physically crosslinked. Table 2.2, discusses the way in which a number of parameters affect the stability of the micelle as a drug delivery vehicle.

The CMC of polymeric micelles can be estimated by fluorescence spectroscopy using pyrene, a hydrophobic fluorescence probe that preferentially partitions into the hydrophobic core of the micelle. Pyrene undergoes changes in its photophysical properties as a result of the change in the micropolarity and it experiences upon diffusion from bulk water (hydrophilic environment) into the micelle core (hydrophobic environment). Two methods exist for determining the CAC of

polymeric micelles with pyrene fluorescence. The original method, proposed by Kalyanasundaram et al. takes advantage of the changes in the vibronic fine structure of the pyrene emission and monitors the changes in the ratio of the intensities I_1 and I_3 of the [0,0] and [0,2] bands, respectively. More recently, it has been suggested that a more accurate determination of the CAC can be obtained by monitoring the changes in the ratio of the pyrene excitation spectra intensities at $\lambda = 333$ nm for pyrene in water and $\lambda = 336$ nm for pyrene in a hydrophobic medium. By plotting the I_{336}/I_{333} intensity ratios vs. the logarithm of the concentration of the aqueous solutions of copolymer, sigmoidal curves are obtained, where, at the CAC, a sharp increase is observed in the fluorescence intensity ratio (I_{336}/I_{333}) as the polymer concentration increases [34].

2.4.2.1 Thermodynamic stability

A delivery system is subject to ‘sink conditions’ or severe dilution upon intravenous injection into an animal or human subject. In an average individual, the total blood volume is approximately 5,L. For example, following the intravenous injection of 100 mL (i.e. $0.3 \text{ mL kg}^{-1} \text{ min}^{-1}$ for 5 min.) of a 2% (w:w) $\text{PCL}_{21}\text{-}b\text{-PEO}_{44}$ micelle solution, the concentration of copolymer in the blood would be 400 mg L^{-1} . Therefore it is very important to know the critical micelle concentration of a particular copolymer. The CMC for $\text{PCL}_{21}\text{-}b\text{-PEO}_{44}$ is 2.8×10^{-7} or 1.2 mg L^{-1} . However, the copolymer concentration of 400 mg L^{-1} may be below the value of the CMC of many of the other block copolymers that have been explored as micellar delivery vehicles.

The CMC values for PBLA-*b*-PEO have been reported to range between 5–18 mg L⁻¹ while the CMC for a PLA-*b*-PEO system was found to be 35 mg L⁻¹. The CMC values for several PEO-*b*-PPO-*b*-PEO systems were reported to range between 10 and 1000 mg L⁻¹. In some cases, injecting a larger volume or a more concentrated micellar solution would prevent the copolymer concentration from falling below the CMC immediately upon injection.

However, it may prove to be more advantageous to begin with a copolymer system with a lower CMC value. The CMC of a copolymer is determined by many factors, some of which are the nature and length of the coreforming block, length of the hydrophilic block and the presence of hydrophobic solubilizates. The nature and

length of the core-forming block have the most profound effect on the CMC. Amphiphilic copolymers which contain a highly hydrophobic block have lower CMC values in water than those which include the less hydrophobic blocks. The CMC values for PS-*b*-PEO copolymers, which contain the highly hydrophobic polystyrene block, range between 1 and 5 mg L⁻¹.

For a series of copolymers, if the corona-forming block is kept constant, an increase in the molecular weight of the core-forming block will decrease the CMC. To a lesser extent, if the length of the core-forming block is maintained at a constant length, than an increase in the length of the hydrophilic block will cause an increase in the value of the CMC.

The use of a copolymer system with a low CMC value may increase the *in vivo* stability of the micelles. However, in many papers, the disassembly of micelles into single chains is mentioned to be advantageous since this will facilitate elimination of the copolymer material from the body via the kidneys. Therefore, the ideal micelle system will be stable to sink conditions encountered upon injection and will facilitate elimination by eventual disassembly into single chains [35].

2.4.2.2 Kinetic stability

The disassembly of micelles at copolymer concentrations below the CMC has been reported to be quite slow for some copolymer systems. The rate of disassembly depends, among others, upon the physical state of the micelle core. Micelles formed from copolymers containing a hydrophobic block which has a high glass transition temperature will tend to disassemble more slowly than those with a low glass transition temperature.

The rate of disassembly is likely affected by many of the same factors which affect the rate of unimer exchange between micelles. The unimer exchange rate has been found to be dependent on many factors such as content of solvent within the core, the hydrophobic content of the copolymer and the lengths of both the hydrophilic and hydrophobic blocks. For example, Creuz et al. studied micelles formed from poly((dimethylamino)alkyl methacrylate)-*b*sodium methacrylate and found that the rate of unimer exchange decreased with an increase in the hydrophobic:hydrophilic balance of the copolymer.

In addition, there is also evidence that the incorporation of hydrophobic compounds into block copolymer micelles may enhance micelle stability (Table 2.2). For example, in a study by Kataoka's group, they found that both the physical entrapment and/or chemical conjugation of adriamycin (ADR) into the micelle core increased the structural stability of the poly(ethylene glycol)- poly(aspartic acid) (PEG-P(Asp)) micelles. In their study, they assessed the stability of the micelle by gel exclusion chromatography. They found that the stability of the micelle increased as the amount of chemically conjugated adriamycin was increased, and also that the physical entrapment of adriamycin into the PEG- P(Asp)ADR micelles further enhanced micellar stability. They suggested that the presence of both the physically entrapped and chemically conjugated drug increased the hydrophobic interactions within the core, producing micelles which were more tightly packed [35].

Table 2.2: The various factors which influence the thermodynamic or kinetic stability of block copolymer micelles [35].

Parameter		Micelle stability	Reference
CMC	Low	↑	[31]
	High	↓	
T _g	Low	↓	[18–20]
	High	↑	
Hydrophobic-hydrophilic block ratio	Low	↓	[48]
	High	↑	
Conjugated drug content	Low	↓	[12]
	High	↑	

2.4.4 Micelle size

The size of colloidal particles is one of the properties which largely influences the circulation time and organ distribution of the vehicle. Particles which are less than 200 nm are said to be less susceptible to RES clearance, and those less than 5 nm have access to small capillaries. Also, the size of the carrier may influence its mechanism of entry into cells, which may, in turn, influence the kinetics and extent of cell uptake.

The size of micelles is controlled by several factors, among which are the length of the coreforming block and the length of the corona forming block. Several different groups have contributed to this area of research, and as a result scaling relations have been developed [36].

Small size (10 ± 100 nm) is one of the most interesting features of polymeric micelles. Besides allowing the extravasation of the carriers, it permits the sterilization of the preparation to be done simply by filtration and minimizes the risks of embolism in capillaries, contrary to larger drug carriers. Micellar size seldom exceeds 100 nm, but depends on several factors including copolymer molecular weight, relative proportion of hydrophilic and hydrophobic chains and aggregation number. The size of micelles prepared by dialysis can be affected by the organic solvent used to dissolve the polymer. It was shown that PEO \pm PBLA micelles prepared by first dissolving the block copolymer in DMF and dialyzing the resulting solution against water, yielded larger micelles than micelles directly prepared in water. Size measurements can be done to study the interaction of polymeric micelles with biological media. For instance, PEO \pm PPO \pm PEO micelles were found to maintain their initial size in the presence of antibodies and bovine serum albumin, suggesting the apparent absence of interaction with plasma proteins.

Determination of micelle size is particularly useful for the characterization of thermo-responsive micelles. Polymers used to prepare such micelles exhibit a lower critical solution temperature (LCST) which can be defined as the temperature at which the polymer phase separates. Below the LCST the polymer is soluble, but it precipitates at temperatures above the LCST. The diameter of these micelles rapidly rises at temperatures above the LCST, of the micelles. This effect of temperature on size was shown to be reversible, since the micellar architecture was maintained after lowering the temperature below the LCST.

Micellar diameter and size polydispersity can be obtained directly in water or in an isotonic buffer by dynamic light scattering (DLS). DLS can also provide some information on the sphericity of polymeric micelles. By DLS, it was shown that the addition of a low molecular weight surfactant such as sodium dodecyl sulfate (1% w/v) can destroy the polymeric micelle structure and brings about a complete shift of the mean diameter from approximately 50 to 3 nm.

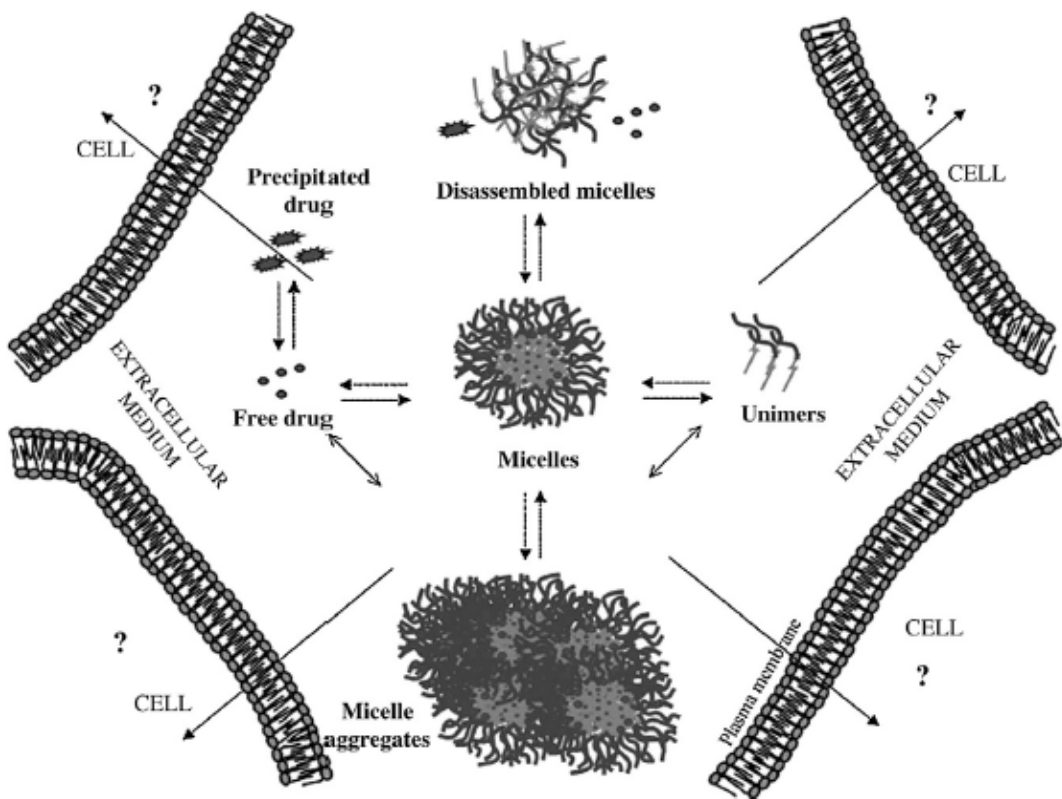


Figure 2.5: In-vivo behaviour of the polymeric micelles [37].

Micellar size can also be estimated by atomic force microscopy (AFM), transmission electron microscopy, scanning electron microscopy (SEM). These methods allow the characterization of the micelle shape and size dispersity. Conventional SEM is widely used in the field of colloidal carriers since it has high resolution and the sample preparation is relatively easy. However, to be analyzed, the samples must withstand high vacuum. Furthermore, the visualization of the particles requires them to be conductive, which is achieved by coating their surface with gold. The thickness of the coating, which can reach several nanometers, has to be taken into account in the size determination. New imaging tools such as AFM enable the visualization of polymeric micelles at atmospheric pressure without gold coating. By AFM, Cammas et al. showed that micelles of $\text{PNIPAA}\pm\text{b}\pm\text{PSt}$ had a discus shape with a 5 nm height and a 20 nm diameter, which was close to the 24 nm size measured by DLS. Finally, ultracentrifugation velocity studies are sometimes performed to assess the polydispersity of polymeric micelles [35].

2.5 Drug incorporation

The method of drug incorporation employed will depend mostly on the method of micelle preparation used for the particular block copolymer in question. If the micelles are formed by direct dissolution in water, then an aliquot of a copolymer water stock solution is often added to a vial which contains the drug to be incorporated. For example, a drug stock solution in acetone is made and then an aliquot is added to an empty vial, the acetone is allowed to evaporate, and then the copolymer:water mixture is added. However, the drug may also be incorporated by the oil in water emulsion method, in which case the drug is added dropwise in a solvent such as chloroform to the micelle solution in water. The drug is incorporated as the solvent evaporates.

Finally, if the micelles are prepared by the dialysis method, then the drug is added with the copolymer to the common organic solvent and then the preparation proceeds as described above for the micelles alone. In some cases, the oil in water emulsion method is also used for the incorporation of drugs into micelles prepared by the dialysis method.

In a study by La et al., the amount of indomethacin (IMC) entrapped into PEO-*b*-PBLA micelles was measured when both the dialysis method and the oil in water emulsion method were employed as methods of drug incorporation. The amount of IMC entrapped into the PEO-*b*-PBLA micelles was found to be 20.4% (w:w) and 22.1% (w:w) when the dialysis method and oil in water emulsion method were employed, respectively.

For the incorporation of drugs into crew-cut micelle systems, the slow addition of water method may be employed, as described previously. For example, the copolymer and drug are dissolved in the organic solvent and stirred for several hours. Water is then added at a slow rate and then the solutions are dialyzed against bidistilled water.

2.5.1 Drug loading procedures

Insoluble drugs can be incorporated in micelles by chemical conjugation or by physical entrapment through dialysis or emulsification techniques (Fig. 2.7). The simple equilibration of the drug and micelles in water may not result in high levels of incorporated drug. Chemical conjugation implies the formation of a covalent bond,

such as an amide bond, between specific groups on the drug and the hydrophobic polymer of the core. Such bonds are resistant to enzymatic cleavage mainly because of steric hindrance and cannot be readily hydrolyzed unless spacer groups are introduced. When possible, the incorporation of a drug by a physical procedure should be preferred. However, the insertion of hydrophilic compounds such as proteins may require the chemical hydrophobization of the molecule. Polyionic compounds can be incorporated through the formation of polyion complex micelles.

Physical entrapment of drugs is generally done by the dialysis (Fig. 2.6a) or oil-in-water emulsion procedure (Fig. 2.6b). The dialysis method consists in bringing the drug and copolymer from a solvent in which they are both soluble (e.g. ethanol, N,N-dimethylformamide) to a solvent that is selective only for the hydrophilic part of the polymer (e.g. water). As the good solvent is replaced by the selective one, the hydrophobic portion of the polymer associates to form the micellar core incorporating the insoluble drug during the process. Extending the dialysis over several days may ensure the complete removal of the organic solvent. The oil-in-water emulsion method consists in preparing an aqueous solution of the copolymer to which a solution of the drug in a water-insoluble volatile solvent (e.g. chloroform) is added in order to form an oil-in-water emulsion. The micelle-drug conjugate is formed as the solvent evaporates. The main advantage of the dialysis procedure over the latter method is that the use of potentially toxic solvents such as chlorinated solvents can be avoided. Both dialysis and oil-in-water emulsion methods were for the incorporation of DOX in PEO \pm PBLA micelles. The emulsification method was more efficient since the DOX content of the micelles was estimated to be 12% (w/w) compared to 8% (w/w) for the dialysis technique.

The drug loading procedure may affect the distribution of a drug within the micelle. Cao et al. showed that pyrene incorporated in micelles as they were forming was not protected from the aqueous environment as well as pyrene incorporated after micelles were formed, although the first method yielded a drug loading three times higher than the second method. Protection from aqueous environment may explain the improved chemical stability of DOX incorporated into polymeric micelles and the increased resistance of plasmid DNA in polyion complex micelles against enzymatic degradation.

Entrapment efficiency depends on the initial amount of drug added. Going over the maximum loading capacity results in precipitation of the drug and lower yield. Drug loading efficiency was also found to be dependent on the aggregation number of the copolymer. Micelles showing a higher aggregation number allow a greater amount of drug to be solubilized in their inner core [37].

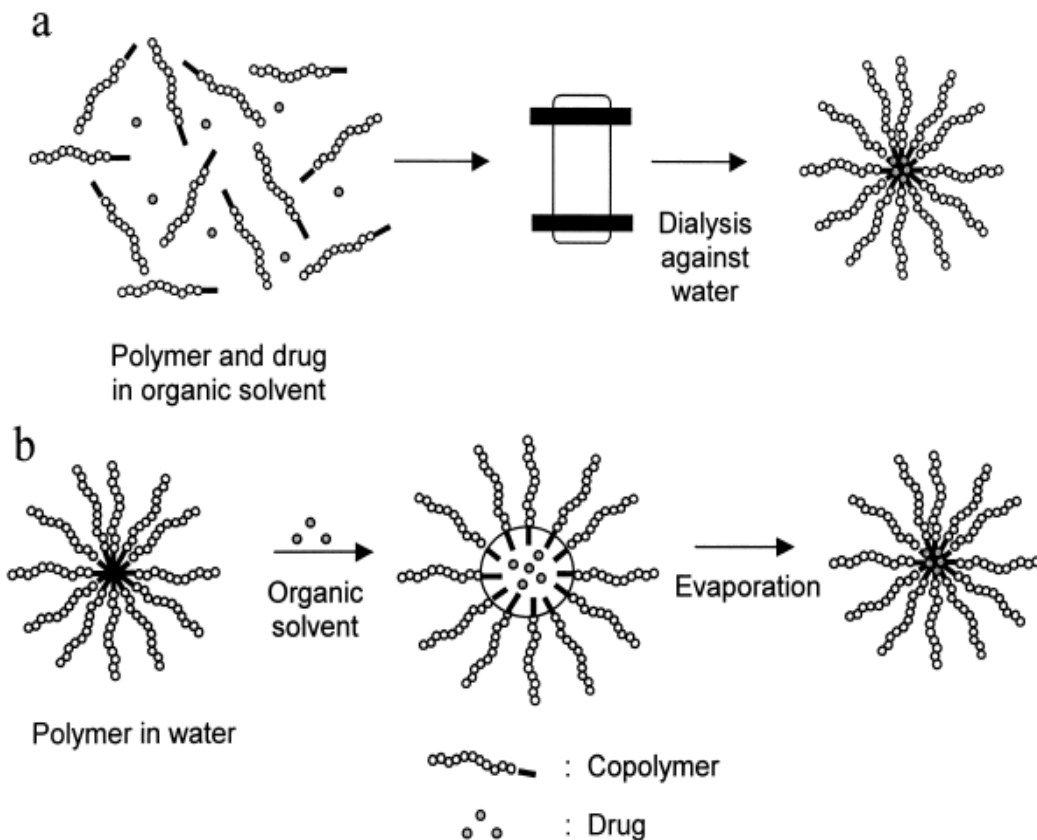


Figure 2.6: Drug loading of polymeric micelles by the dialysis (a) and the oil-in-water methods (b) [37].

2.5.2 Loading capacity

The micelle core serves as the cargo space for various lipophilic drugs. However, this cargo space is limited; for instance, a typical 1% (w:w) PCL-*b*-PEO (20-*b*-44) micelle solution contains only approximately 0.5% core volume. This means that in a 1 mL aliquot of this 1% (w:w) micelle solution only 5 mL is core volume. In order to exploit maximally the minimal loading space available, we must manipulate the many factors which control the loading capacity and loading efficiency.

Several of the major factors which influence both the loading capacity and loading efficiency of block copolymer micelles are nature of the solute, nature of the core-

forming block, core block length, total copolymer molecular weight, solute concentration and, to a lesser extent, the nature and block length of the corona. Many studies have indicated that the overriding factor is the compatibility between the solubilizate and the core-forming block [38].

2.5.3 Examples of drug-loaded polymeric micelles

Examples of compounds loaded into polymeric micelles as well as the corresponding drug loading procedure are given in Table 2.3. Although polymeric micelles have mostly been studied as delivery systems for anticancer drugs they could be used to transport plasmid DNA, antisense oligonucleotides or for the delivery of diagnostic agents to a specific organ in the body.

Evidence of drug incorporation can be obtained by GPC or DLS since both methods can detect a change in micellar size which usually increases in the presence of drugs. The location of a drug inside the micelle core is sometimes demonstrated by quenching experiments. For instance, iodide (I_2) which is a water soluble quencher of DOX, does not affect the fluorescence of the micelle incorporated drug but quenches the fluorescence of the free drug. Such experiments showed that DOX was retained in PEO \pm PBLA after freeze drying and reconstitution in water. In the case of DOX, the self-association of the drug in the micelle core also results in a decrease in the fluorescence intensity of the drug. More recently, the retention and slow release of amphotericin B from polymeric micelles was indirectly ascertained by measuring the decrease of its hemolytic activity after incorporation into PEO \pm PBLA micelles [39].

Table 2.3: Examples of drugs and tracers loaded into polymeric micelles [39].

Drug	Polymer	Incorporation mode	Micelle size with drug (nm)	Year
Amphotericin B	PEO-PBLA	P	26	1998
Antisense oligonucleotide	PEO-P(Lys)	EA	50	1996
Cisplatin	PEO-P(Asp)	C	16	1996
Cyclophosphamide	PEO-P(Lys)	C	Na	1984
Dequalinium	PEO-PE	P	15	1998
DOX	PEO-P(Asp)	C	50	1990
DOX	PEO-P(Asp)	C	14–131	1992
DOX	PEO-P(Asp)	C	17–42	1994
DOX	PEO-PBLA	P	30	1995
DOX	PEO-PDLLA	P	Na	1995
DOX	PEO-PBLA	P	37	1997
DOX	PEO-P(Asp)	P + C	Na	1998
DOX	PNIPA-PBMA	P	Na	1998
DOX	PAA-PMMMA	P	Na	1998
Gd-DTPA-PE	PEO-PE	P	20	1996
¹¹¹ In-DTPA-SA				
Haloperidol	PEO-PPO-PEO	P	Na	1989
Haloperidol	PEO-PPO-PEO	P	15	1992
Indomethacin	PEO-PBLA	P	25–29	1996
Indomethacin	PEO-PCL	P	145–165	1998
Indomethacin	PEO-PCL	P	114–156	1998
Iodine derivative of benzoic acid	PEO-P(Lys)	C	80	1997
KRN-5500	PEO-PBLA	P	71 ^b	1998
	PEO-(C ₁₆ ,BLA)			
	PEO-P(Asp,BLA)			
Paclitaxel	PEO-PDLLA	P	Na	1996
Paclitaxel	LCC	P	< 100	1998
Plasmid DNA	PEO-P(Lys)	EA	140–150	1998
Soybean trypsin inhibitor	PEO-PE	P	15	1998
Testosterone	PEO-PDLLA	P	Na	1996
Topoisomerase II inhibitor	PEO-PE	P	Na	1995
ellipticine				

^a Na, not available; P, physical entrapment; C, chemical bonding; EA, electrostatic association; DTPA, diethylenetriamine pentaacetic acid; PEO-P(Lys), poly(ethylene oxide)-poly(L-lysine); SA, stearylamine; LCC, N-lauroyl-carboxymethyl-chitosan; PE, phosphatidyl ethanolamine; PAA, poly(acrylic acid).

^b After the sonication of PEO(C₁₆,BLA) aggregates.

2.6 Star Polymers

Polymer properties are influenced by their structure and topology. Therefore, the synthesis of complex macromolecular architectures to control polymer properties is an ongoing field of study in polymer science. Branching in polymers is a useful structural variable that can be used advantageously to modify polymer physical properties and the processing characteristics as a result of changing the melt, solution, and solid-state properties of polymers [40]. It has been shown that branching results in a more compact structure in comparison to linear polymers of similar molecular weight, due to their high segment density, which affects the crystalline, mechanical, and viscoelastic properties of the polymer. A branched polymer structure was described as a nonlinear polymer comprised of molecules with more than one backbone chain radiating from branch points (junction points; atoms or small group from which more than two long chains emanate) [41]. Star polymers

constitute the simplest form of branched macromolecules where all the chains as arm segments of one molecule are linked to a centre (Figure 2.7).

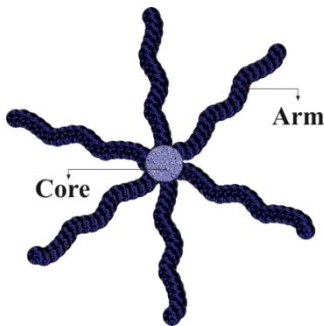


Figure 2.7: Illustration of a star polymer.

2.6.1 Preparation of star polymers

The methodology of living polymerization is ideally suited for the preparation of star polymers since it is possible to vary and control important structural parameters such as molecular weight, molecular weight distribution, copolymer composition and microstructure, tacticity, chain end functionality and the number of branches per molecule. Because termination and chain transfer reactions are absent and the chain-ends may be stable for sufficient time periods, these polymerizations have the following useful synthetic attributes for star polymer synthesis:

- I. One polymer is formed for each initiator molecule, so that the number average molecular weight of polymers or block segments can be predicted from the reaction stoichiometry. Multifunctional initiators with functionality n can form stars with n arms.
- II. If the rate of initiation is rapid or competitive with the rate of propagation, polymers with narrow molecular weight distributions are formed [42].
- III. When all of the monomer has been consumed, the product is a polymer with reactive chain ends that can be participate in a variety of post polymerization reactions:
 - a. block copolymerization by addition of a second monomer, and/or
 - b. end-linking with multifunctional linking agents to form the corresponding star polymers with uniform arm lengths.

There are three general synthetic methods for the preparation of star-shaped polymers. These methods have been based on two approaches: arm-first and core-first.

- I. End linking with multifunctional linking agent (arm-first)
- II. Use of multifunctional initiators (core-first)
- III. Use of difunctional monomers (arm-first)

2.6.1.1 End Linking with Multifunctional Linking Agent (Arm-First Method)

In the first method, referred to as the “arm-first” method, monofunctional living chains of known length and low polydispersity are used as precursor. Subsequently, the active sites located at chain end are reacted with a compound carrying a number of appropriate reactive functions, whereupon chemical links are formed. The number of arms corresponds to the functionality of the linking agent as shown in figure: 2.9. The precursor chains become the star branches, and the linking agent becomes the core.

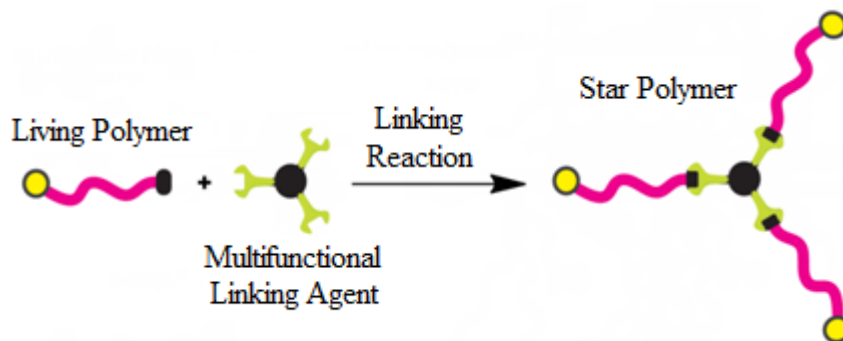


Figure 2.8: Illustration of the synthesis of star polymers by arm-first method.

The main advantage of this method is that the arms of the resulting star polymer are well-defined because the precursor arms can be characterized independently from the star. Because of the well-defined arms, the number of arms can be readily determined by measuring the molecular weight of the star. In principle, a variety of well defined, star polymers with different numbers of arms can be prepared using this methodology by varying the functionality of the linking agents. Disadvantages of the method can be observed. When long time required for the linking reaction and the need to perform fractionation in order to obtain pure star polymer, because in almost all cases a small excess of the living arm is used in order to ensure complete linking.

2.6.1.2 Use of multifunctional initiators (core-first method)

The “core-first” method involves the use of a multifunctional initiator (core). The number of arms per star polymer is determined by the number of initiating functionalities on each initiator (Figure 2.9). There are several requirements that a multifunctional initiator has to fulfill in order to produce star polymers with uniform arms, low molecular weight distribution, and controllable molecular weights. All the initiation sites must be equally reactive and have the same rate of initiation. Furthermore, the initiation rate must be higher than the propagation rate [43].

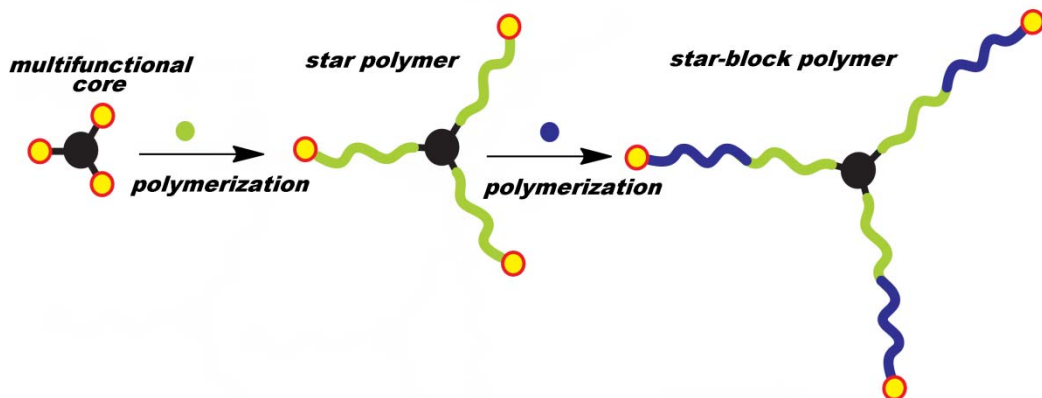


Figure 2.9: Illustration of the synthesis of star and star block copolymers by “core-first” method.

2.6.1.3 Use of difunctional monomers (arm-first method)

In this method, a living polymer precursor is used as macroinitiator for the polymerization of a small amount of a suitable cross-linker, such as ethylene glycol dimethacrylate (EGDMA) or divinyl benzene (DVB) [44]. Microgel nodules of tightly cross-linked polymer are formed upon the polymerization. These nodules serve as the branch point from which the arms emanate (Figure 2.10).

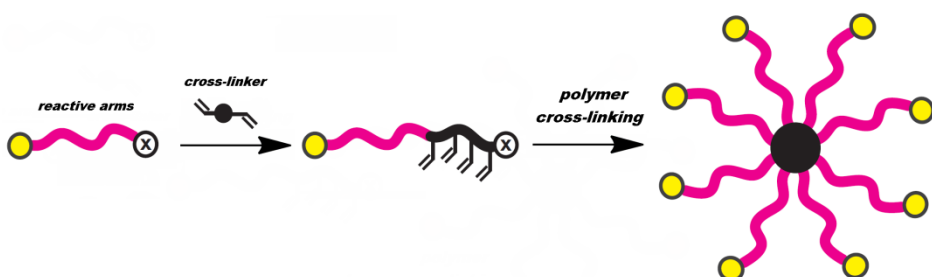


Figure 2.10: Illustration of the synthesis of star polymers by “arm-first” method.

The functionality of the stars prepared by this method can be determined by molecular weight measurements on the arms and the star product, but it is very difficult to predict and control the number of arms. The average number of arms attached to a star core depends on several experimental parameters, including the degree of polymerization (DP) and composition of the arm precursor, the chemical nature of cross-linker, the amount of cross-linker. Incomplete incorporation of linear arm precursors into the formed star is a common problem in this “arm-first” method, which could be explained by the loss of chain-end initiating sites or a buildup of steric hindrance around the core, as the coupling reactions proceed.

2.7 Miktoarm star polymers

The term “miktoarm” has been attributed to star polymers with three or more arms, at least two of which are molecularly and chemically different (chemical asymmetry). Miktoarm is a combination of Greek miktos, meaning “mixed”, and arm. This term was proposed by Hadjichristidis in 1992 and was widely accepted by the other research groups all over the world [45]. Although, the terms heteroarm star and A_nB_m -type star were also used for these types of star structures, miktoarm star (μ -star) will be used throughout this work to refer to star polymers with corresponding structure.

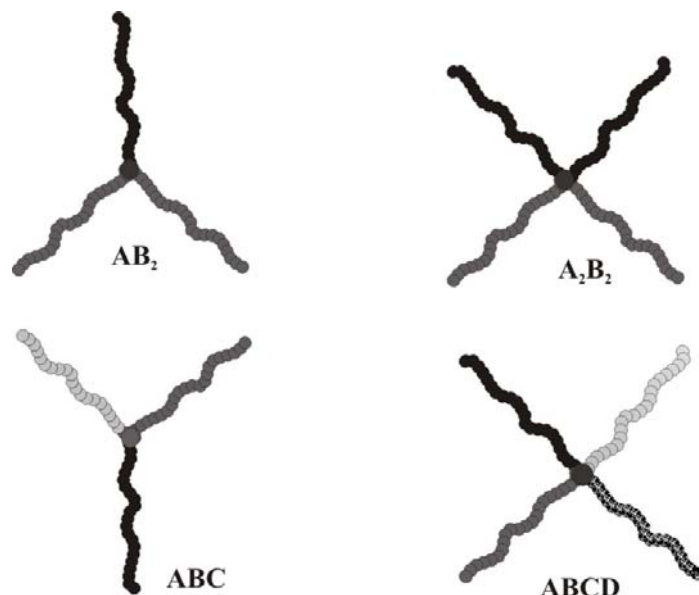


Figure 2.11: Illustration of the synthesis of star and star block copolymers by “core-first” method. Illustration of miktoarm star polymers structures where each letter represents different polymeric arms.

The most common examples of miktoarm stars are the A_2B , A_3B , A_2B_2 , A_nB_n ($n > 2$) and ABC types. Other less common structures, like the ABCD, AB_5 , and AB_2C_2 are also available (Figure 2.11).

2.8 Amphiphilic Star Block Copolymers

Amphiphilic block copolymers with hydrophilic and hydrophobic segments have been investigated extensively not only because of their unique self-organization characteristics but also for their wide range of potential applications such as drug delivery and separations technology [46]. At an aqueous interface, the amphiphilic property of block copolymers composed of hydrophilic and hydrophobic segments can cause the distal end of the hydrophilic chain to extend into the bulk aqueous solution, anchoring the hydrophilic block to the substrate surface through hydrophobic segments [47]. Amphiphilic block copolymers form micelles and hollow spheres having unique characteristics, such as nanosize, core-shell architecture, and low critical micelle concentration, and find potential applications as nanoreactors, nanoreservoirs, gene delivery vehicles, and reaction media for biocatalysis [48]. In an aqueous solution, micelles with core-shell structure are formed through the segregation of insoluble blocks into the core, which is surrounded by hydrophilic shell composed of hydrophilic blocks [49]. In general, drugs can be loaded into the hydrophobic cores of the micelles, which lowers their toxicity in the human body and prolongs their circulation time in the blood [50]. The use of block polymer micelles as drug-delivery vehicles, namely, micellar drug-delivery systems, was proposed in the 1980s with the aim to improve the curative effect of sparingly soluble pharmaceuticals [51]. The micellar characteristics of amphiphilic diblock copolymers depend on the nature of each block. The surface properties of self-organized micelles would be highly dependent on the structure of hydrophilic block. For example, poly(ethylene oxide) (PEO) block would provide a biocompatible surface environment for micellar aggregates. On the other hand, the micellar core characteristics would be determined by the structure of hydrophobic blocks [52].

Amphiphilic star-shaped block copolymers have recently attracted much attention because these polymers can behave as unimolecular micelles or be designed to exhibit a very low critical aggregation concentration (CAC) [53]. So far, several

amphiphilic star-block copolymers have been synthesized including star-poly(ethylene oxide)-*block*-poly(styrene) [54], star-poly(methyl vinyl ether)-*block*-poly(isobutylene) [55], star-poly(2,3-dihydroxypropylacrate)-*block*-poly(methyl methacrylate) [56], star-poly(ethylene glycol)-*block*-poly(isobutylene) [57] and star-poly(methacrylic acid)-*block*-poly(isobutylene) [58]. However, star-block copolymers comprising hydrophobic biodegradable and hydrophilic biocompatible segments are of particular interest, especially for biomedical applications.

Choi et al. [59] synthesized star-poly(ethylene oxide)-*block*-poly(L-lactic acid) (star-PEO-*b*-PLA) and star-PEO-*block*-poly(ϵ -caprolactone) (star-PEO-*b*-PCL) by initiating ring-opening polymerization of L-lactide and ϵ -caprolactone, respectively, with four and eight arm PEO at 110 °C in the bulk. Hedrick et al. [60] reported combination of ring-opening and atom transfer radical polymerization (ATRP). These authors synthesized dendrimer like multiarm poly(ϵ -caprolactone)-2-bromoisobutyrate which was used as macroinitiator in ATRP of 2-hydroxyethyl methacrylate and PEG-methacrylate, respectively.

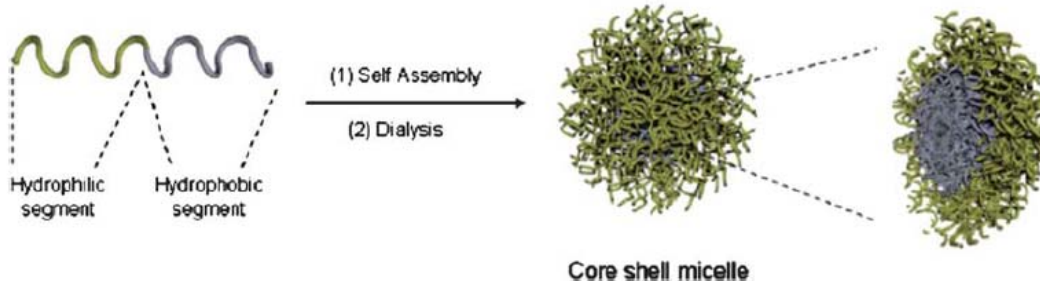


Figure 2.12: Dilute solution of block copolymers into spherical micelles [61].

2.9 Ring-Opening Polymerization (ROP)

Ring-opening polymerization (ROP) is a unique polymerization process, in which a cyclic monomer is opened to generate a linear polymer. It is fundamentally different from a condensation polymerization in that there is no small molecule byproduct during the polymerization. Polymers with a wide variety of functional groups can be produced by ring-opening polymerizations. Preparation of cyclic monomers, studies of catalysis and mechanisms are active areas of research both in academia and industry [62-65].

Nowadays, increasing attention is paid to degradable and biodegradable biocompatible polymers for applications in the biomedical and pharmaceutical fields,

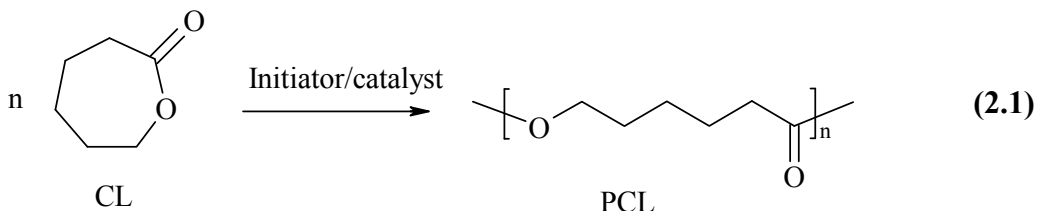
primarily because after use they can be eliminated from the body via natural pathways and also they can be a solution to problems concerning the global environment and the solid waste management. Aliphatic polyesters are among the most promising materials as biodegradable polymers.

2.9.1 Controlled Ring-Opening Polymerization of cyclic esters

The ring opening polymerization (ROP) of lactones and lactides to produce poly(ester)s provides versatile biocompatible and biodegradable polymers possessing good mechanical properties. These advantages have seen aliphatic poly(ester)s receive increasing attention over the last few years driven by their application as biodegradable substitutes for conventional commodity thermoplastics and applications in the biomedical field [66].

Aliphatic poly(ester)s can be either synthesized by polycondensation of hydroxyl-carboxylic acids or by the ring-opening polymerization (ROP) of cyclic esters. The polycondensation technique yields low molecular weight polyesters ($M_n < 30,000$) with poor control of specific end groups [67]. In contrast, high molecular weight aliphatic polyesters can be prepared in short periods of time by ROP. There has been much research directed towards the controlled ROP of commercially available cyclic esters including glycolide, lactide and ϵ -caprolactone resulting in aliphatic poly(ester)s with high molecular weights [68].

In practice, the ROP of lactones and lactides requires an appropriate catalyst to proceed in reasonable conditions and to afford polymers with controlled properties (2.1). Since the pioneering work of Kleine et al. in the 1950s metal-based catalytic systems have been the focus of considerable attention for the polymerization of cyclic esters, and numerous studies have been carried out to elucidate the mechanism of such coordination polymerizations. Through variation in the nature of the metal center and of the surrounding ligands, a broad range of initiators have been prepared and evaluated [69-73].

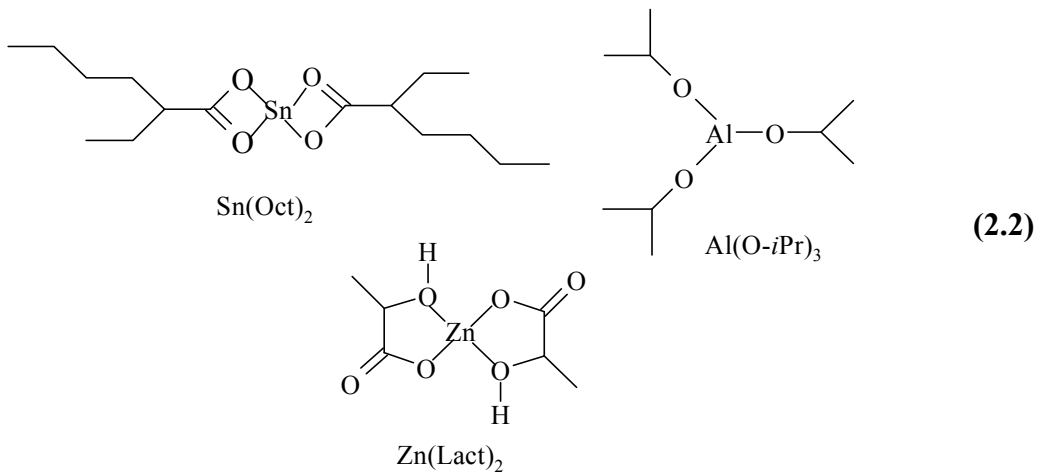


Besides the coordination-insertion mechanism, alternative strategies based on anionic, nucleophilic, or cationic promoters have also been recently (re)evaluated, the preliminary results reported in these fields being rather promising [74, 75].

2.9.2 Catalysts

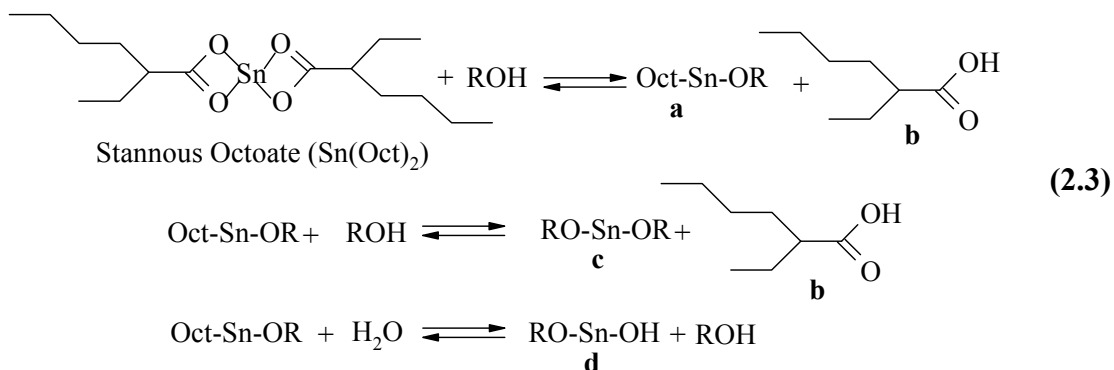
A large variety of organometallic compounds, such as metal alkoxides and metal carboxylates, has been studied as initiators or catalysts in order to achieve effective polymer synthesis [76]. The covalent metal alkoxides with free p or d orbitals react as coordination initiators and not as anionic or cationic initiators [77]. The most widely used complex for the industrial preparation of polylactones and polylactides is undoubtedly $\text{Sn}(\text{Oct})_2$. It is commercially available, easy to handle, and soluble in common organic solvents and in melt monomers. It is highly active and allows for the preparation of high-molecular-weight polymers in the presence of an alcohol [78]. Aluminum alkoxides have also proved to be efficient catalysts for the ROP of cyclic esters. The common example, namely, aluminum (III) isopropoxide, $\text{Al}(\text{O-i-Pr})_3$, has been largely used for mechanistic studies. However, it has been revealed to be significantly less active than $\text{Sn}(\text{Oct})_2$ [79]. Moreover, an induction period of a few minutes is systematically observed with $\text{Al}(\text{O-i-Pr})_3$ attributed to aggregation phenomenon [80]. For all these reasons, $\text{Al}(\text{O-i-Pr})_3$ is much less used for the preparation of biodegradable polyesters, and especially since aluminum ions do not belong to the human metabolism and are suspected of supporting Alzheimer's disease.

Much interest has thus been devoted to zinc derivatives as potential nontoxic catalysts. Zinc powder itself is a relatively good polymerization catalyst that is used industrially [81]. With reaction times of several days at 140 °C in bulk, it is roughly as active as $\text{Al}(\text{O-i-Pr})_3$. Numerous zinc salts have also been investigated [82].



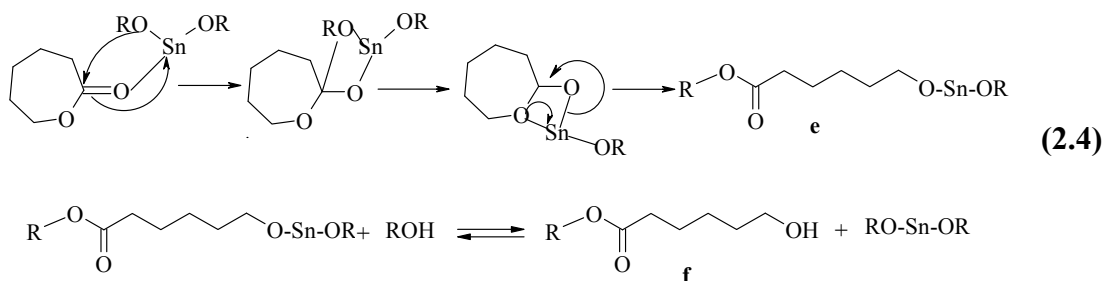
2.9.3 Coordination-Insertion ROP

Covalent metal carboxylates, particularly tin(II) bis(2-ethylhexanoate) usually referred to as tin(II) octanoate, $\text{Sn}(\text{Oct})_2$ belong to the most frequently used initiators for polymerization of cyclic esters due to its low cost, low toxicity, and high efficiency. Although, there are controversial reports in the literature about the nature of $\text{Sn}(\text{Oct})_2$ activity in the polymerization of lactones, two basic types of mechanism have been proposed. The first one is directly catalytic type where the catalyst serves to activate monomer through coordination with its carbonyl oxygen [83, 84]. The second mechanism is the monomer insertion type mechanism where the catalyst acts as co-initiator along with either purposely added or adventitious hydroxyl impurities, and polymerization proceeds through an activated stannous alkoxide bond [85,86].



Kricheldorf and co-workers have recently illustrated how the structure of the alcohol initiator may influence the strength of the catalyst/alcohol interaction [84, 86]. According to these authors, this interaction, in the early stages of reaction, is

responsible for formation of the “true” initiating species, subsequent ring opening, and formation of the active, propagating chain end. Prior to the beginning of polymerization, adventitious hydroxyfunctional impurities (e.g., water) or purposely added alcohol first complex and subsequently react with $\text{Sn}(\text{Oct})_2$ producing a stannous alkoxide species (**a**) and free 2-ethylhexanoic acid (**b**) as shown in 2.3. Further reaction with **a** second equivalent of alcohol produces the stannous dialkoxide initiator (**c**) and releases a second equivalent of 2-ethylhexanoic acid (**b**) as depicted in 2.3 [86, 87]. Adventitious water, meanwhile, serves mainly as a catalyst deactivator via a reversible reaction with **a** or **c**, thereby decreasing the concentration of active initiator and producing a stannous alcohol derivative (**d**), such as shown in 2.3, which is more thermodynamically stable than the stannous dialkoxide and is less efficient as an initiator [86].

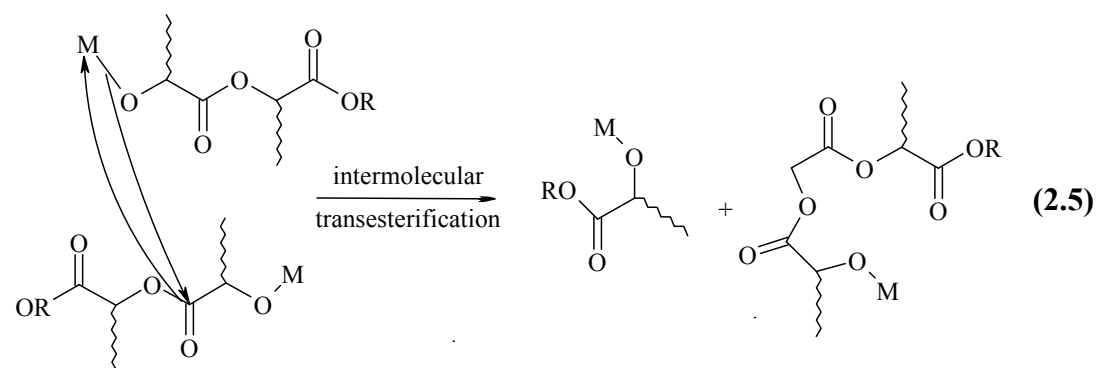


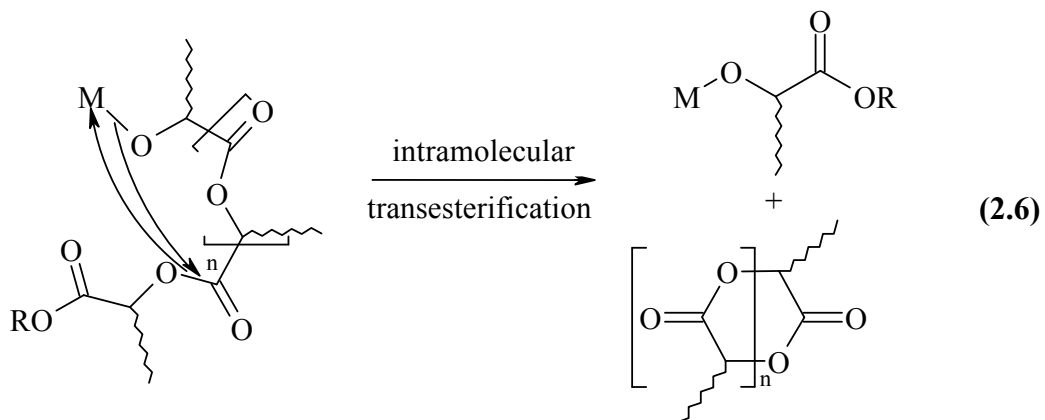
Reaction of **c** with monomer by means of coordination- insertion generates the first actively propagating chain end (**e**) consisting of not only the initiating alcohol fragment but also the active propagating center derived from the first monomer unit and stannous alkoxide. The **e** species may either propagate or undergo rapid intermolecular exchange of the stannous alkoxide moiety for a proton from either hydroxyl groups of initiator (if remaining) or another hydroxy chain end, either **e** or polymeric in nature. This rapid exchange of protons and stannous alkoxide moieties results in a dynamic equilibrium between activated and deactivated chain ends as depicted in 2.4, where $\text{R} =$ unreacted alcohol initiator or hydroxy chain ends generated in situ. This process eventually consumes the remaining unreacted alcohol initiator not involved in the initial formation of **c**. ROP based on coordination-insertion mechanism has been thoroughly investigated since it may yield well-defined polyesters through living polymerization [77, 88].

In such coordination-insertion polymerizations the efficiency of the molecular-weight control depends from the ratio $k_{\text{propagation}}/k_{\text{initiation}}$ but also from the extent of transesterification side reactions. These transesterification reactions can occur both intramolecularly (backbiting leading to macrocyclic structures and shorter chains) and intermolecularly (chain redistributions) (2.5-2.6) [89]. Intermolecular transesterification reactions modify the sequences of copolylactones and prevent the formation of block co-polymers. Intramolecular transesterification reactions cause degradation of the polymer chain and the formation of cyclic oligomers.

The polymerization/depolymerization equilibrium should also be taken into account as a particular case of intramolecular transesterification reaction. All of these side reactions result in broader molecular-weight distributions, sometimes making the molecular weights of the resulting polymers irreproducible. The extent of these undesirable transesterification reactions was found to strongly depend on the metallic initiator [79]. Side reactions occur from the very beginning of the polymerization with $\text{Sn}(\text{Oct})_2$, leading to rather broad MWD (PDI indexes around 2) but only at high or even complete conversion with $\text{Al}(\text{O}i\text{-Pr})_3$, yielding lower PDI indexes (less than 1.5) [79,90].

Parameters that influence the number of transesterifications are temperature, reaction time, and type and concentration of catalyst or initiator. Depending on the metal used, the initiator is more or less active towards transesterification reactions [90].





The promising results obtained with $\text{Sn}(\text{Oct})_2$, $\text{Al}(\text{O}i\text{-Pr})_3$, and $\text{Zn}(\text{Lact})_2$ have given rise to a growing interest in metal-based initiators that would display higher catalytic activity and better control the extent of the undesirable transesterification reactions.

2.9.4 Poly(ϵ -caprolactone)

Poly(ϵ -caprolactone) (PCL) is a semicrystalline polymer which represents one of several aliphatic polyesters that undergo degradation and absorption in vivo [91, 92]. The repeating molecular structure of PCL homopolymer consists of five non-polar methylene groups and a single relatively polar ester group. Although not produced from renewable raw materials, PCL is a fully biodegradable thermoplastic polymer due to the presence of the hydrolytically unstable aliphatic-ester linkage. PCL has good water, oil, solvent and chlorine resistance.

PCL has some unusual properties, including a low Tg (~ -60 °C) and Tm (~ 60 °C) and a high thermal stability. These properties are related to PCL's chain of carbons, as longer chains are give rise to less mobility and lower Tm's and Tg's. PCL is also highly permeable, which results from its low Tg and subsequent rubbery state at room temperature.

PCL is one of biodegradable polymers which have been used to prepare functional materials [93]. Copolymers containing poly(ϵ -caprolactone) (PCL) are especially interesting because they are miscible with a wide range of polymers, and they have features like crystallizability, lack of toxicity, ability to disperse pigments, low-temperature adhesiveness, and printability [94].

PCL has been increasingly studied in the scientific community and applied for drug delivery and tissue engineering [95]. Owing to its high crystallinity and strong

hydrophobicity of polymer backbone, PCL homopolymer usually show slow biodegradation and drug-release rate [96].

PCL is compatible with numerous other polymers, has the possibility of blending this aliphatic polyester with a number of commercial polymers such as poly(vinyl chloride) and bisphenol A polycarbonate. PCL is of interest as a packaging material and in biomedical applications since it is degradable and its degradation products are non-toxic. PCL and other copolymers have been evaluated for medical uses such as drug delivery systems, an external casting material for broken bones, as a material for use in making custom dental impression trays.

In addition to above, it is used mainly in thermoplastic polyurethanes, resins for surface coatings, adhesives and synthetic leather and fabrics. It also serves to make stiffeners for shoes and orthopedic splints, and fully biodegradable compostable bags, sutures, and fibres. Because the homopolymer has a degradation time on the order of 2 years, copolymers have been synthesized to accelerate the rate of bioabsorption. In Sweden there has been an attempt to produce PCL bags, but they degraded before reaching the customers.

2.10 Click Chemistry

“Click chemistry” is a chemical term introduced by Sharpless in 2001 and describes chemistry tailored to generate substances quickly and reliably by joining small units together [97]. Click chemistry can be summarized only one sentence: Molecules that are easy to make. Sharpless also introduced some criteria in order to fulfill the requirements as reactions that: are modular, wide in scope, high yielding, create only inoffensive by-products, are stereospecific, simple to perform and that require benign or easily removed solvent. Nowadays there are several processes have been identified under this term in order to meet these criterias such as nucleophilic ring opening reactions; non-aldol carbonyl chemistry; thiol additions to carbon–carbon multiple bonds (thiol-ene and thiol-yne); and cycloaddition reactions. Among these selected reactions, copper(I)-catalyzed azide-alkyne (CuAAC) and Diels-Alder (DA) cycloaddition reactions and thiol-ene reactions have gained much interest among the chemists not only the synthetic ones but also the polymer chemists.

2.10.1 Copper(I)-catalyzed azide-alkyne cycloaddition (CuAAC)

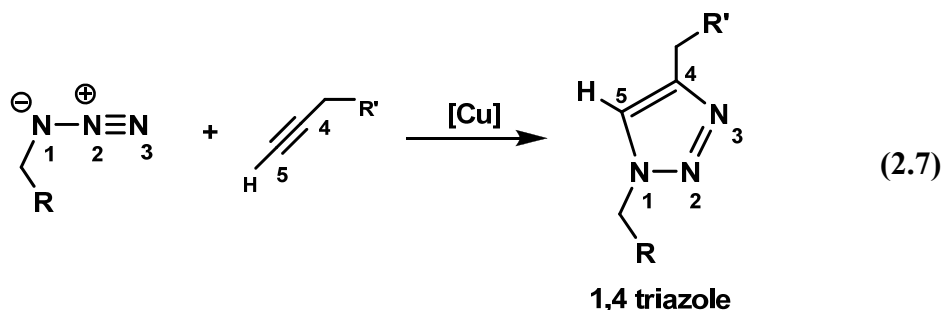
Huisgen's 1,3-dipolar cycloaddition of alkynes and azides yielding triazoles is, undoubtedly, the premier example of a click reaction [98]. Recently, 1,3-dipolar cycloadditions, such as reactions between azides and alkynes or nitriles, have been applied to macromolecular chemistry, offering molecules ranging from the block copolymers to the complexed macromolecular structures [99].

Sharpless and co-workers have identified a number of reactions that meet the criteria for click chemistry, arguably the most powerful of which discovered to date is the Cu(I)-catalyzed variant of the Huisgen 1,3-dipolar cycloaddition of azides and alkynes to afford 1,2,3-triazoles [100]. Because of Cu(I)-catalyzed variant of the Huisgen 1,3-dipolar cycloaddition of azides and alkynes reactions' quantitative yields, mild reaction condition, and tolerance of a wide range of functional groups, it is very suitable for the synthesis of polymers with various topologies and for polymer modification [101]. Because of these properties of Huisgen 1,3-dipolar cycloaddition, reaction is very practical. Moreover, the formed 1,2,3-triazole is chemically very stable [102].

In recent years, triazole forming reactions have received much attention and new conditions were developed for the 1,3-dipolar cycloaddition reaction between alkynes and azides [103]. 1,2,3-triazole formation is a highly efficient reaction without any significant side products and is currently referred to as a click reaction [104].

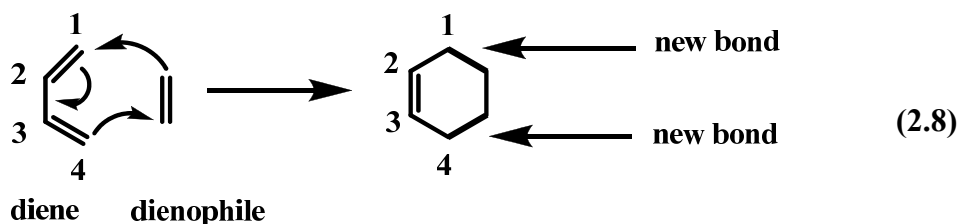
Copper(I)-catalyzed reaction sequence which regiospecifically unites azides and terminal acetylenes to give only 1,4-disubstituted 1,2,3-triazoles (2.7).

In fact, the discovery of Cu(I) efficiently and regiospecifically unites terminal alkynes and azides, providing 1,4-disubstituted 1,2,3-triazoles under mild conditions, was of great importance. On the other hand, Fokin and Sharpless proved that only 1,5-disubstituted 1,2,3-triazole was obtained from terminal alkynes when the catalyst switched from Cu(I) to ruthenium(II) [102].



2.11 Diels-Alder reaction

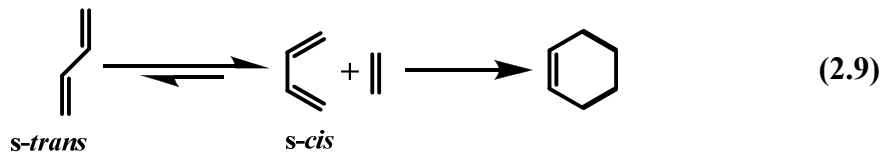
The Diels-Alder (DA) reaction is a concerted $[4\pi+2\pi]$ cycloaddition reaction of a conjugated diene and a dienophile. This reaction is one of the most powerful tools used in the synthesis of important organic molecules. The three double bonds in the two starting materials are converted into two new single bonds and one new double bond to afford cyclohexenes and related compounds (equation 2.8). This reaction is named for Otto Diels and Kurt Alder, who received the 1950 Nobel prize for discovering this useful transformation [103-105].



Typically, the DA reaction works best when either the diene is substituted with electron donating groups (like -OR, -NR₂, etc) or when the dienophile is substituted with electron-withdrawing groups (like -NO₂, -CN, -COR, etc) [106].

2.11.1 Stereochemistry of Diels-Alder reaction

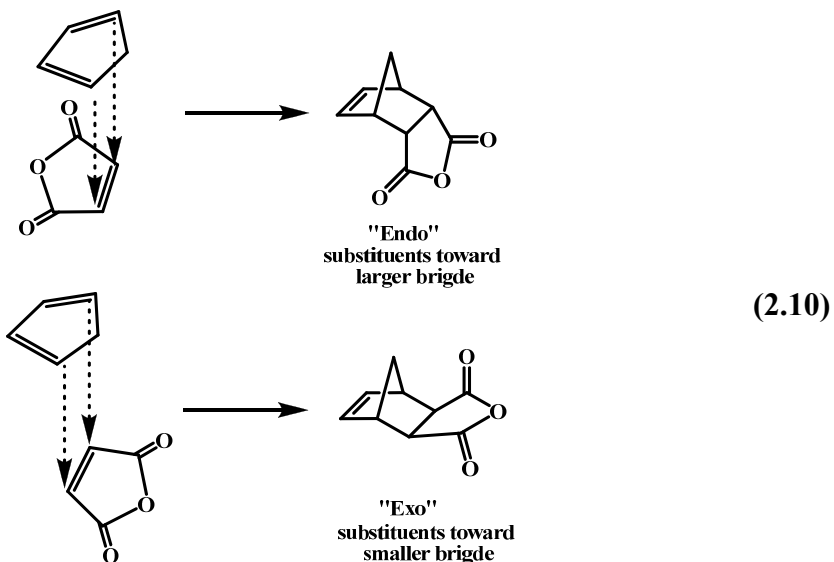
There are stereochemical and electronic requirements for the DA reaction to occur smoothly. First, the diene must be in an s-cis conformation instead of an s-trans conformation to allow maximum overlap of the orbitals participating in the reaction (equation 2.9).



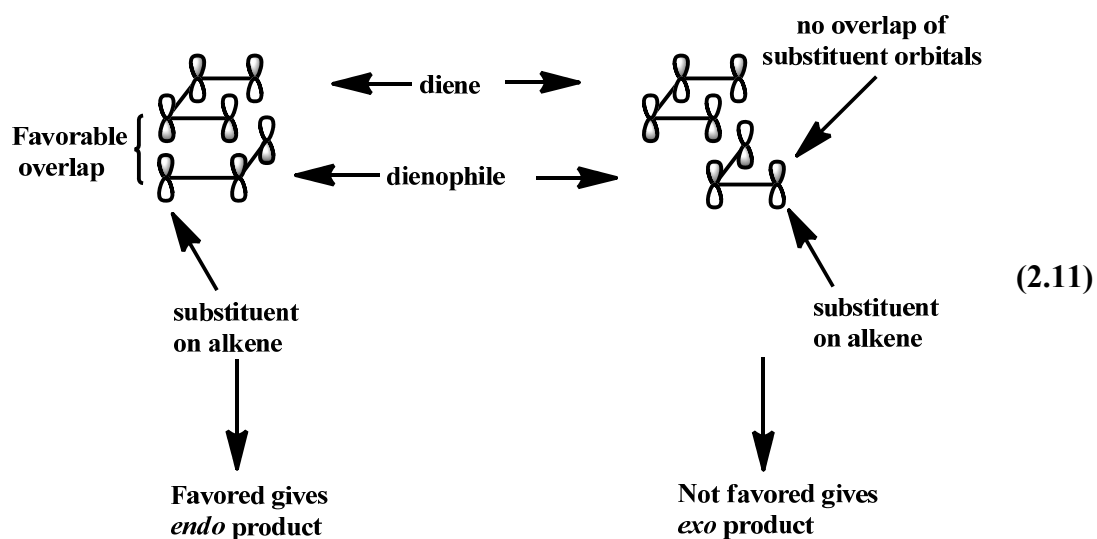
The “s” in *s-cis* and *s-trans* refers to “sigma”, and these labels describe the arrangement of the double bonds around the central sigma bond of a diene. Dienes often exist primarily in the lower energy *s-trans* conformation, but the two conformations are in equilibrium with each other. The *s-cis* conformation is able to react in the DA reaction and the equilibrium position shifts towards the *s-cis* conformer to replenish it. Over time, all the *s-trans* conformer is converted to the *s-cis* conformer as the reaction proceeds.

A unique type of stereoselectivity is observed in DA reactions when the diene is cyclic. In the reaction of maleic anhydride with cyclopentadiene, for example, the *endo* isomer is formed (the substituents from the dienophile point to the larger bridge) rather than the *exo* isomer (the substituents from the dienophile point away from the larger bridge) (equation 2.10).

The preference for *endo*-stereochemistry is “observed” in most DA reactions. The fact that the more hindered *endo* product is formed puzzled scientists until Woodward, Hoffmann, and Fukui used molecular orbital theory to explain that overlap of the p orbitals on the substituents on the dienophile with p orbitals on the diene is favorable, helping to bring the two molecules together [107, 108].



Hoffmann and Fukui shared the 1981 Nobel Prize in chemistry for their molecular orbital explanation of this and other organic reactions. In the illustration below, notice the favorable overlap (matching light or dark lobes) of the diene and the substituent on the dienophile in the formation of the endo product (equation 2.11):



Oftenly, even though the endo product is formed initially, an exo isomer will be isolated through a DA reaction. This occurs because the exo isomer, having less steric strain than the endo which is more stable, and because the DA reaction is often reversible under the reaction conditions. In a reversible reaction, the product is formed, reverts to starting material, and forms again many times before being isolated. The more stable the product, the less likely it will be to revert to the starting material. If the reaction is not reversible under the conditions used, the kinetic

product will be isolated. However, if the first formed product is not the most stable product and the reaction is reversible under the conditions used, then the most stable product, called the thermodynamic product, will often be isolated.

3. EXPERIMENTAL PART

3.1 Materials

ϵ -Caprolactone (ϵ -CL, 99%, Aldrich) was dried over CaH_2 and distilled in vacuum prior to use. Succinic anhydride (97%, Aldrich), 9-anthracenemethanol (97%, Aldrich), α -bromo isobutryl bromide (98%, Aldrich), triethylamine (Et_3N , 99.5%, Aldrich), toluene-4-sulfonyl Chloride (TsCl , 99%, Fluka), pyrene (Sigma, 99%), NaN_3 (99.5%, Aldrich), 4-Pentylic acid (95%, Aldrich) N,N' -dicyclohexylcarbodiimide (DCC, 99%, Aldrich), 4-dimethylaminopyridine (DMAP, 99%, Aldrich), tin(II)-2-ethylhexanoate (Aldrich, 98%), divinylbenzene (DVB, 80%, Aldrich), CuBr (99.9%, Aldrich), were used as received. N, N, N', N'', N'' -pentamethyldiethylenetriamine (PMDETA, 99%, Aldrich) was distilled over NaOH prior to use. Poly(ethylene glycol) monomethylether (Me-PEG-OH, $M_n = 2000$ and 550, Fluka) were dried by azeotropic distillation with anhydrous toluene. Tetrahydrofuran (THF, 99.8%, J.T. Baker) was dried and distilled from benzophenone-Na. Dichloromethane (CH_2Cl_2 , 99%, J. T. Baker) was dried and distilled over and P_2O_5 . Diethyl ether (99.7%, Aldrich), 1,4-dioxane (99.8%, Aldrich), toluene (99.8%, Aldrich), methanol (99.8%, Aldrich) were used without further purification. Ethyl acetate (EtOAc) and hexane were in technical grade and distilled prior to use, Spectra/Por dialysis membrane (MWCO:3500, Nominal Flat Width:18.0 mm, Diameter:11.5 mm, Vol/Length: 1.1 mL/cm). Curcumin ($\geq 90\%$, Merck)

3.2 Instrumentation

The ^1H and ^{13}C (250 MHz) spectra were recorded on Bruker NMR AC 250 and Varian Mercury-VX (400 MHz) spectrometer in CDCl_3 . The conventional Gel Permeation Chromatography (GPC) measurements were carried out with an Agilent instrument (Model 1100) consisting of a pump, refractive index, and UV detectors. Four Waters Styragel columns (HR 5E, HR 4E, HR 3, HR 2), (4.6 mm internal diameter, 300 mm length, packed with 5 μm particles) were used in series. The

effective molecular weight ranges were 2000- 4.000.000, 50-100.000, 500-30.000, and 500–20.000, respectively. THF was used as eluent at a flow rate of 0.3 mL/min at 30 °C. Toluene was used as an internal standard. The molecular weights of the polymers were calculated on the basis of linear PS standards (Polymer Laboratories). The second GPC system with an Agilent model isocratic pump, four Waters Styragel columns (guard, HR 5E, HR 4, HR 3, and HR 2), a Viscotek TDA 302 triple detector (RI, dual laser light scattering (LS) ($\lambda = 670$ nm, 90° and 7°) and a differential pressure viscometer) (TD-GPC) was conducted to measure the absolute molecular weights in THF with a flow rate of 0.5 mL/min at 35 °C. All three detectors were calibrated with a PS standard having narrow molecular weight distribution ($M_n = 115,000$ g/mol, $M_w/M_n = 1.02$, $[\eta] = 0.519$ dL/g at 35 °C in THF, $dn/dc = 0.185$ mL/g) provided by Viscotek company. Typical sample concentrations for GPC-analysis were in the range of 2–8 mg/mL depending on molecular weight of analyzed polymers. Data analyses were performed with OmniSec 4.5 software from Viscotek Company. Malvern Zetasizer NanoZS Particle size of particles and molecules from a maximum size range 0.3nm to 10 microns using NIBS technology and Dynamic Light Scattering, Zeta potential in aqueous and non-aqueous dispersions using M3-PALS technology with the range 3.8nm - 100 μ m and molecular weight range of 1000-2x10⁷ Da. Hitachi F-4500 Fluorescence Spectrophotometer, Telstar cryodos laboratory freeze-drier, Fisher scientific sonicator, Centrifuge VWR compactstar CS-4, UFC Shimadzu DGU-20A3 equipped with Shimadzu fluorescence detector RF-10XL, Prominence-diode array detector SPD-M20A, Prominence communications bus module CBM-20A, Shimadzu column oven CTO-10AS VP, Prominence Degasser DGU-20A3, Prominence Liquid chromatograph LC-20AB, and Prominence auto sampler SIL-20AC.

3.3 Synthesis methods

4,10-dioxatricyclo[5.2.1.0^{2,6}]dec-8-ene-3,5-dione (**1**) [109], 4-(2-hydroxyethyl)-10-oxa-4-azatricyclo[5.2.1.0^{2,6}]dec-8-ene-3,5-dione (**2**) [109] were prepared according to published procedures.

3.3.1 Synthesis of 4,10-dioxatricyclo[5.2.1.0^{2,6}]dec-8-ene-3,5-dione (**1**)

Maleic anhydride (60.0 g, 0.6 mol) was suspended in 150 mL of toluene and the mixture warmed to 80 °C. Furan (66.8 mL, 0.9 mol) was added via syringe and the

turbid solution was stirred for 6 h. The mixture was then cooled to ambient temperature white solids formed during standing were collected by filtration and washed with 2×30 mL of petroleum ether and once with diethyl ether (50 mL) afforded **1** as white needless. Yield: 80.2 g (80%). Mp: 114-115 °C (DSC). ^1H NMR (CDCl_3 , δ) 6.57 (s, 2H, $\text{CH}=\text{CH}$, bridge protons), 5.45 (s, 2H, - CHO , bridge-head protons), 3.17 (s, 2H, $\text{CH}-\text{CH}$, bridge protons).

3.3.2 Synthesis of 4-(2-hydroxyethyl)-10-oxa-4-azatricyclo[5.2.1.0_{2,6}]dec-8-ene-3,5-dione (2)

1 (10.0 g, 60.0 mmol) was suspended in methanol (150 mL) and the mixture cooled to 0 °C. A solution of ethanolamine (3.6 mL, 60.0 mmol) in 30 mL of methanol was added dropwise (10 min) to the reaction mixture, and the resulting solution was stirred for 5 min at 0 °C, then 30 min at ambient temperature, and finally refluxed for 6 h. After cooling the mixture to ambient temperature, solvent was removed under reduced pressure, and residue was dissolved in 150 mL of CH_2Cl_2 and washed with 3×100 mL of water. The organic layer was separated, dried over Na_2SO_4 and filtered. Removal of the solvent under reduced pressure gave white-off solid which was further purified by flash chromatography eluting with ethylacetate (EtOAc) to give the product as a white solid. Yield: 6.7 g (50%). Mp = 138-139 °C (DSC). ^1H NMR (CDCl_3 , δ) 6.51 (s, 2H, $\text{CH}=\text{CH}$, bridge protons), 5.26 (s, 2H, - CHO , bridge-head protons), 3.74-3.68 (m, 4H, $\text{NCH}_2\text{CH}_2\text{OH}$), 2.88 (s, 2H, $\text{CH}-\text{CH}$, bridge protons).

3.3.3 Synthesis of 2,2,5-trimethyl-[1,3]dioxane-5-carboxylic acid (3)

The 2,2-bis(hydroxymethyl)propanoic acid (8 g, 59.6 mmol) along with *p*-TSA (0.45 g, 2.32 mmol), and 2,2-dimethoxypropane (11.2 mL, 89.4 mmol) dissolved in 40 mL of dry acetone, and stirred 2h at room temperature. In the vicinity of 2h, while stirring continued the reaction mixture was neutralized with 6 mL of totally NH_4OH (25%), and absolute ethanol (1:5), filtered off by-products and subsequent dilution with dichloromethane (100 mL), and once extracted with distilled water (40 mL). The organic phase dried with Na_2SO_4 , concantrated to yield 7.4 g (71%) as white solid after evaporation of the solvent. ^1H NMR (CDCl_3 , δ) 4.18 (d, 2H, CCH_2O), 1.38 (s, 3H, CCH_3) 1.36 (s, 3H, CCH_3), 1.18 (s, 3H, $\text{C}=\text{OC}(\text{CH}_2\text{O})_2\text{CH}_3$).

3.3.4 Synthesis of adduct alcohol-acid ketal ester and hydrolysis to diol

2 (0.8g, 5.0 mmol) and 3 (1.05g, 5.0 mmol) DMAP (0.06g, 5mmol) DCC (0,124g, 6mmol) was dissolved in CH_2Cl_2 (50 mL), The reaction mixture was stirred for overnight at 25 °C, then extracted with 1 M HCl and distilled water organic phase was dried over Na_2SO_4 . The crude product was purified by flash chromatography eluting with ethylacetate (EtOAc), DCM and MeOH to give the viscous light yellow product (Yield = 1.5 g; 81 %). .

2-3 ester (1.5 g, 4.1 mmol) was dissolved in a mixture of 20 mL of THF and 10 mL of 1 M HCl. The reaction mixture was stirred for 2 h at room temperature. The reaction mixture was filtered off and reaction mixture was concentrated and extracted with 160 mL of CH_2Cl_2 and 40 mL of water. The combined organic phase was dried with Na_2SO_4 and concentrated and 1.09 g product is obtained (Yield = 1.09 g; 70 %). ^1H NMR (CDCl_3 , δ) 4.18 (d, 2H, CCH_2O), 3.63 (d, 2H, CCH_2O), 1.38 (s, 3H, CCH_3) 1.36 (s, 3H, CCH_3), 1.18 (s, 3H, $\text{C=OC(CH}_2\text{O)}_2\text{CH}_3$), 6.51 (s, 2H, CH=CH , bridge protons), 5.26 (s, 2H, - CHO , bridge-head protons), 3.92-4.18 (m, 4H, $\text{NCH}_2\text{CH}_2\text{OH}$), 2.88 (s, 2H, CH-CH , bridge protons).

3.3.5 Synthesis of 2 alkyne end functionalized core for synthesis of PEG₂ (Core)

Adduct-diol (0.83g, 2.55 mmol), 4-Pentynoic acid (0.53g, 5.63 mmol), DMAP (0.31g, 2.55 mmol), DCC (1.16g, 5.63 mmol) was dissolved in 80 mL of CH_2Cl and left for stirring overnight at 25 °C. The product was purified by flash chromatography eluting with ethylacetate (EtOAc), DCM and Hexane after extracted with distilled water and 0.9. g product was obtained (Yield = 0.90 g; 82 %). NMR spectra of the proves the ester formation with 4-pentynoic acid with ^1H NMR (CDCl_3 , δ) 1.16 (s, 3H, CCH_3), 1.96 (s, 1H, CH_2CCH), 2.48-2.53 ($\text{OC=OCH}_2\text{CH}_2\text{C}$), 2.88 (s, 2H, CH-CH , bridge protons), 3.84 (t, 2H, $\text{NCH}_2\text{CH}_2\text{OC=O}$), 4.18-4.30 (m, 2H, $\text{CCH}_2\text{OC=O}$ and $\text{NCH}_2\text{CH}_2\text{O}$), 5.25 (s, 2H, - CHO , bridge-head protons), 6.50 (s, 2H, CH=CH , bridge protons).

3.3.6 Synthesis of Azide ended Me-PEG

Me-PEG (Mn 550 g/mol) (5.0 g, 9.09 mmol) was dissolved in 100 mL of CH_2Cl . To this solution 4- toluene sulfonylchloride (2.57 g, 13.5 mmol), DMAP (1.10 g, 9.0 mmol) and triethylamine was added (1.87 mL, 13,5 mmol). Reaction mixture was

then left overnight at room temperature to stir. It was firstly extracted with 1 M HCl then 2 times with distilled water and dried over Na₂SO₄. After evaporation of the solvent 5.85 g viscous colorless product obtained.

Me-PEG-Tos (5.0 g, 0.79 mmol) was dissolved in DMF and Na₃ (1.02 g, 15.8 mmol) added to solution and left for mixing overnight at room temperature. The reaction mixture firstly filtered then extracted with CH₂Cl and water three times and dried over Na₂SO₄ after evaporation of the solvent 3.5 g viscous product gained (Yield = 3.5 g; 70 %). ¹H NMR (CDCl₃, δ) 3.62 (repeating units of the PEG), 3.34 (s, 3H, PEG-OCH₃), 3.39 (b, 2H, PEG-CH₂CH₂N₃), 2.27 (s, 2H, OCH₂CH₂N₃)

3.3.7 Synthesis of the PEG₂ by using click reaction

The core (0.78 g, 1.61 mmol) and PEG-N₃ (2.09 g, 3.53 mmol) were placed in a schlenk tube then dissolved in DMF. PMDETA (0.35 mL, 1.61 mmol) and CuBr (0.23 g, 1.61 mmol) added to solution and fastly transported to vacuum line after degassing reaction mixture was left to mixing in room temperature for overnight. For purificaiton polymer solution was passed through alumina column to remove copper salt and precipitated in cold diethylether (Yield = 2.25 g; 85 %). . white solid product is gained. ¹H NMR (CDCl₃, δ) 1.15 (s, 3H, CCH₃), 2.72 (t, 2H, triazole-CH₂), 2.88 (s, 2H, CH-CH, bridge protons), 2.98 (t, 2H, OC=OCH₂CH₂), 3.36 (s, 3H, PEG-OCH₃), 3.62 (repeating units of the PEG), 3.84 (t, 2H, NCH₂CH₂OC=O), 4.18 (s, 3H, CCH₂OC=O), 4.49 (t, 2H, NCH₂CH₂OC=O), δ 6.50 (s, 2H, CH=CH, bridge protons), 5.25 (s, 2H, -CHO, bridge-head protons), 7.51 (s, 1H, triazole proton)

3.3.8 Synthesis of anthracene end-functionalized PCL (Anth-PCL)

Anthracene end-functionalized poly(ϵ -caprolactone) (anth-PCL) was prepared by ROP of ϵ -caprolactone (ϵ -CL) (5.0 mL, 0.047 mol) in bulk using tin(II)-2-ethylhexanoate (Sn(Oct)₂) as a catalyst and 9-anthracene methanol (0.20 g, 0.94 mmol) as an initiator at 110 °C for 3 h. The degassed monomer, catalyst, and initiator were added to a previously flamed schlenk tube equipped with a magnetic stirring bar in the order mentioned. The tube was degassed with three FPT, left in argon, and placed in a thermostated oil bath. After the polymerization, the mixture was diluted with THF, and precipitated into an excess amount of cold methanol. It was isolated by filtration and dried at 40 °C in a vacuum oven for 24 h. Yield: 4.4 g

(82%). ^1H NMR (CDCl_3 , δ) 8.50 (s, 1H, ArH of anthracene), 8.31 (d, 2H, ArH of anthracene), 8.01 (d, 2H, ArH of anthracene), 7.60-7.42 (m, 4H, ArH of anthracene), 6.2 (s, 2H, CH_2 -anthracene), 4.0 (t, 2H, $\text{CH}_2\text{OC=O}$ of PCL), 3.60 (t, 2H, CH_2OH , end-group of PCL), 2.2 (t, 2H, C=OCH_2 of PCL), 1.2-1.8 (m, 6H, CH_2 of PCL)

3.3.9 Synthesis of PCL-PEG₂ miktoarmstar copolymer via Diels-Alder click reaction

In a 100 mL of two-necked round bottom flask were added anth-PCL (1.14 g, 0.3 mmol, based on Mn, ^1H NMR) and PEG₂ (1.00 g, 0.6 mmol, based on Mn, ^1H NMR) in 75 mL of toluene. The mixture was bubbled with nitrogen for 30 min. at room temperature and then refluxed for 48 h under nitrogen in the dark. After that time, toluene was evaporated under high vacuum and the residual solid dissolved in THF, and subsequently precipitated into methanol-diethylether. The obtained product was dried in a vacuum oven at 40 °C for 24 h. (Yield = 1.4 g; 85 %). ^1H NMR (CDCl_3 , δ) 1.18 (s, 3H, CCH_3), 2.30-1.30 (s, 2H, aliphatic CH_2 of PCL), 2.72 (s, 2H, triazole- CH_2), 2.98 (t, 2H, NCH_2CH_2), 3.35 (s, 3H, PEGOCH_3) 3.62 (repeating units of the PEG), 4.04 (s, 2H, $\text{O=CCH}_2\text{CH}_2$ repeating unit of PCL) 4.48 (s, 2H, CCH_2O and $\text{NCH}_2\text{CH}_2\text{OC=O}$) 4.8 (bridge protons) 5.46 (s, 2H, $\text{CCCCH}_2\text{OC=O}$) 7.1-7.4 (aromatic protons) 7.51 (s, 1H, triazole proton)

3.3.10 Synthesis of Me-PEG₂₀₀₀-COOH

Me-PEG₂₀₀₀ (5 g, 2.5 mmol) was dissolved in 150 mL of DCM. To the reaction mixture were added Et_3N (3.5 mL, 119.6 mmol), DMAP (1.22 g, 10.0 mmol), and succinic anhydride (1.0 g, 10.0 mmol) in that order. The reaction mixture was stirred for overnight at 25 °C, then poured into ice-cold water and extracted with CH_2Cl_2 . The organic phase was washed with 1 M HCl, dried over Na_2SO_4 and concentrated. The crude product was precipitated in diethylether. Yield: 4.5 g (86%). ^1H NMR (CDCl_3 , δ) 4.22 (s, 2H, $\text{OCH}_2\text{CH}_2\text{OC=O}$), 3.61 (s, repeating units of the PEG), 3.52 (s, 2H, $\text{OCH}_2\text{CH}_2\text{OC=O}$), 3.34 (s, 3H, CH_3PEG), 2.62 (s, 2H, $\text{O=CCH}_2\text{-CH}_2\text{C=O}$),

3.3.11 Synthesis of maleimide end-functionalized PEG (MI-PEG)

Me-PEG-COOH ($M_n = 2100$ based on Mn, ^1H NMR) (5.0 g, 2.38 mmol) was dissolved in 100 mL of CH_2Cl_2 . To the reaction mixture were added DMAP (0.24 g, 2.00 mmol) and 4-(2-hydroxyethyl)-10-oxa-4-azatricyclo[5.2.1.0_{2,6}]dec-8-ene-3,5-

dione (1.25 g, 6.0 mmol) in that order. After stirring 5 min at room temperature, a solution of DCC (1.24 g, 6.00 mmol) in 10 mL of CH_2Cl_2 was added. Reaction mixture was stirred for overnight at room temperature. After filtration off the salt, the solution was concentrated and the viscous brown color product was purified by column chromatography over silica gel eluting with $\text{CH}_2\text{Cl}_2/\text{EtOAc}$ mixture (1:1, v/v) and then with $\text{CH}_2\text{Cl}_2/\text{methanol}$ (90:10, v/v) to obtain MI-PEG as white solid. Yield: 5.0 g (88%). ^1H NMR (CDCl_3 , δ) 6.50 (s, 2H, $\text{CH}=\text{CH}$ as bridge protons), 5.25 (s, 2H, - CHO , bridge-head protons), 4.23 (m, 4H, $\text{CH}_2\text{OC=O}$), 3.75-3.51 (m, OCH_2CH_2 repeating unit of PEG, C=ONCH_2 , and CH_2 -PEG repeating unit), 3.36 (s, 3H, PEG- OCH_3), 2.87 (s, 2H, $\text{CH}-\text{CH}$, bridge protons) 2.61-2.56 (m, 4H, $\text{C=OCH}_2\text{CH}_2\text{C=O}$).

3.3.12 Synthesis of anthracen-9ylmethyl 2,2,5-trimethyl-[1,3]dioxane-5-carboxylate (4)

9-Anthracene methanol (2 g, 9.6 mmol) was dissolved in 50 mL of CH_2Cl_2 and **3** (2 g, 11.5 mmol), and DMAP (1.17 g, 9.6 mmol) were added to the reaction mixture in that order. After stirring 5 minutes at room temperature, DCC (2.37 g, 11.5 mmol) dissolved in 20 mL of CH_2Cl_2 was added. Reaction mixture was stirred overnight at room temperature and urea byproduct was filtered. Then reaction mixture was extracted with water/ CH_2Cl_2 (1:4) two times and combined organic phase was dried with Na_2SO_4 . Solvent was evaporated and the remaining product was purified by column chromatography over silica gel eluting with hexane/ethyl acetate (4:1) to give pale yellow oil (Yield = 2.97 g; 85 %). ^1H NMR (CDCl_3 , δ) 8.50 (s, 1H, ArH of anthracene), 8.32 (d, 2H, ArH of anthracene), 8.02 (d, 2H, ArH of anthracene), 7.60-7.45 (m, 4H, ArH of anthracene), 6.2 (s, 2H, CH_2 -anthracene), 4.14 (d, 2H, CCH_2O), 3.58 (d, 2H, CCH_2O), 1.38 (s, 3H, CCH_3), 1.35 (s, 3H, CCH_3), 1.08 (s, 3H, $\text{C=OC(CH}_2\text{O)}_2\text{CH}_3$).

3.3.13 Synthesis of anthracen-9ylmethyl 3-hydroxy-2-(hydroxymethyl)-2-methylpropanoate (5)

9-anthrylmethyl 2,2,5-trimethyl-1,3-dioxane-5-carboxylate (2.95 g, 8.1 mmol) was dissolved in a mixture of 20 mL of THF and 10 mL of 1 M HCl. The reaction mixture was stirred for 2 h at room temperature. The precipitated product was filtered off and reaction mixture was concentrated and extracted with 160 mL of

CH₂Cl₂ and 40 mL of water. The combined organic phase was dried with Na₂SO₄ and concentrated. Hexane was added to the reaction mixture and it was kept in deep freeze overnight to give white solid (Yield = 2.4 g, 91 %). ¹H NMR (CDCl₃, δ) 8.52 (s, 1H, ArH of anthracene), 8.30 (d, 2H, ArH of anthracene), 8.03 (d, 2H, ArH of anthracene), 7.60-7.45 (m, 4H, ArH of anthracene), 6.2 (s, 2H, CH₂-anthracene), 3.85 (d, 2H, CH₂OH), 3.66 (d, 2H, CH₂OH), 2.17(br, 2H, OH), 1.01 (s, 3H, CCH₃).

3.3.14 Synthesis of anthracene end-functionalized (PCL)₂

Anth-(PCL)₂ was prepared by ROP of ε-CL (5.0 mL, 0.047 mol) in bulk using tin(II)-2-ethylhexanoate as a catalyst and **5** (0.30 g, 0.94 mmol) as an initiator at 110 °C for 9 h. The degassed monomer, catalyst, and initiator were added to a previously flamed schlenk tube equipped with a magnetic stirring bar in the order mentioned. The tube was degassed with three FPT, left in argon, and placed in a thermostated oil bath. After the polymerization, the mixture was diluted with THF, and precipitated into an excess amount of cold methanol. It was isolated by filtration and dried at 40 °C in a vacuum oven for 24 h. ¹H NMR (CDCl₃, δ) 8.50 (s, 1H, ArH of anthracene), 8.30 (d, 2H, ArH of anthracene), 8.03 (d, 2H, ArH of anthracene), 7.60-7.47 (m, 4H, ArH of anthracene), 6.2 (s, 2H, CH₂-anthracene), 4.0 (t, 2H, CH₂OC=O of PCL), 3.60 (t, 2H, CH₂OH, end-group of PCL), 2.3 (t, 2H, C=OCH₂ of PCL), 1.2-1.8 (m, 6H, CH₂ of PCL).

3.3.15 Synthesis of miktoarm PEG2-PCL star block copolymer via Diels-Alder click reaction

In a 100 mL of two-necked round bottom flask were added anth-(PCL)₂ (1.0 g, 0.187 mmol, based on Mn, ¹H NMR) and MI-PEG (1.2 g, 0.224 mmol, based on Mn) in 75 mL of toluene. The mixture was bubbled with nitrogen for 30 min. at room temperature and then refluxed for 48 h under nitrogen in the dark. After that time, toluene was evaporated under high vacuum and the residual solid dissolved in THF, and subsequently precipitated into methanol. The obtained product was dried in a vacuum oven at 40 °C for 24 h. Yield: 1.2 g (60%). ¹H NMR (CDCl₃, δ) 7.2 (ArH of cycloadduct), 5.4 (br, 2H, cycloadduct-CH₂OC=O), 4.83 (s, 1H, CH, bridge-head proton), 4.0 (repeating unit of PCL), 3.62 (br, 6H, -OCH₂CH₂, repeating unit of PEG and NCH₂CH₂OC=O), 2.4 (m, 4H, C=OCH₂CH₂C=O), 2.4-0.9 (aliphatic protons of PCL and PEG).

3.3.16 Modification of the Me-PEG with 2,2,5-trimethyl-[1,3]dioxane-5-carboxylic acid (PEG-AK)

Me-PEG Mn 2000 g/mol (5.00 g, 2.50 mmol), 2,2,5-trimethyl-[1,3]dioxane-5-carboxylic acid (1.20 g, 7.50 mmol) DMAP (0.30 g, 2.50 mmol) was placed in 250 mL round bottom flask and dissolved in 95 mL of CH₂Cl. After stirring 5 min at room temperature, a solution of DCC (1.55 g, 7.50 mmol) in 10 mL of CH₂Cl₂ was added and left to mixing overnight. For purification, after filtration of the reaction mixture solvent was evaporated then precipitated in cold diethylether and placed in vacuum drying-oven overnight and 5.0 g of product is gained with % 92 yield. ¹H NMR (CDCl₃, δ) 3.36 (s, 3H, PEG-OCH₃), 4.30 (t, 2H, CH₂OC=O) 3.51-3.75 (m, OCH₂CH₂ repeating unit of PEG, 1.38 (s, 3H, CCH₃) 1.36 (s, 3H, CCH₃), 1.18 (s, 3H, C=OC(CH₂O)₂CH₃).

3.3.17 Dehydrolization of the ketal moiety (PEG-Diol)

PEG-AK (5.00 g, 2.38 mmol) was dissolved in a mixture of 50 mL of THF and 10 mL of 1 M HCl. The reaction mixture was stirred for 2 h at room temperature. The reaction mixture was filtered off and reaction mixture was concentrated and extracted with 250 mL of CH₂Cl₂. The combined organic phase was dried with Na₂SO₄ after filtration the solvent evaporated and concentrated then precipitated in cold diethylether and placed in vacuum drying-oven 4.50 g of pure product obtained with % 92 yield. ¹H NMR (CDCl₃, δ) 1.18 (s, 3H, CCH₃), 3.60 (s, 2H, CCH₂OH), 3.36 (s, 3H, PEG-OCH₃), 4.30 (t, 2H, CH₂OC=O), 3.51-3.75 (m, OCH₂CH₂ repeating unit of PEG),

3.3.18 Synthesis of PEG-PCL₂ miktoarmstar copolymer with ROP via using PEG-Diol as initiator

PEG-PCL₂ was prepared by ROP of ε-CL (2.0 mL, 0.047 mol) in bulk using tin(II)-2-ethylhexanoate (22.2 µg) as a catalyst and PEG-Diol (0.57 g, 0.27 mmol) as an initiator at 110 °C for 5 h. The degassed monomer, catalyst, and initiator were added to a previously flamed schlenk tube equiped with a magnetic stirring bar in the order mentioned. The tube was degassed with three FPT, left in argon, and placed in a thermostated oil bath. After the polymerization, the mixture was diluted with THF,

and precipitated into an excess amount of cold diethylether. It was isolated by filtration and dried at 40 °C in a vacuum oven for 24 h and 2.2 g of product is obtained with % 84 conversion . ¹H NMR (CDCl₃, δ) 4.02 (repeating unit of PCL), 3.62 (t, 4H, -OCH₂CH₂, repeating unit of PEG), 3.36 (s, 3H, PEG-OCH₃), 4.04, 2.25, 1.6 and 1.30 (m, 2H, aliphatic protons of PCL), 1.18 (S, 3H, CCH₃) 4.20 (s, 2H, CCH₂OC=O) ¹³C NMR (APT) (CDCl₃, δ) 174 (repeating carbonyl carbon of the PCL chain), 7.05 (repeating ester CH₂ of the PEG chain), 64.1, 34.2, 28.3, 25.5, 24.6 (repeating CH₂ units of the PCL), 59.0 (CH₃ at the end of the PEG chain), 19 (CCH₃), 46.3 (OC=OC(CH₂)₂C) 173 (PEGOC=OC)

3.4 Micellar Characterization of the amphiphilic block copolymers

3.4.1 Preparation of the micelle

Micelles were prepared with the dialysis method. 100 mg of the copolymers were dissolved in DMF and left to stirring for over night. Water was added slowly to vial till the water content become 67% percent of the total volume then left to stirring for over night. 3 Different water content (50, 67 and 75%) dialysis was done to observe the effect of the DMF over water ratio on the size of the micelles. The solution was transported to the dialysis membrane (MWCO 3500) and placed in 3 L distilled water carrying tank and stirred at 300 rpm. Water of the tank is changed periodically until the rigidity of the dialysis membrane was lost. After the dialysis, polymer solution placed in vials and placed in freeze-drier and lyophilized at -50 °C for removal of the water. After the lyophilisation process the products seems like white fluffy cotton in the vials

3.4.2 Zeta-Sizer Measurements

4 mg polymer was dissolved in 1 mL deionized water (18.4 µQ) and filtered with 0.2 µm filter to remove aggregates then started to dilute to half till to prepare 20 samples before the measurements samples were waited 20 min. for reformation of the micelles.

The measurements were carried out with Malvern Zetasizer NanoZS and 173° angle of lazer beam. Every analyze is repeated 5 times with 3 minute measurement time

Dynamic light scattering (DLS) is a technique used for particle sizing of samples, typically in the sub-micron range. The technique measures the time-dependent fluctuations in the intensity of scattered light from a suspension of particles

undergoing random, Brownian motion. Analysis of these intensity fluctuations allows for the determination of the diffusion coefficients, which in turn yield the particle size through the Stokes- Einstein equation.

Conventional DLS instruments use a detection angle of 90° and this optical configuration may not be sensitive enough for the successful measurement of surfactant micelles.

The Zetasizer Nano range of instruments incorporates non-invasive back scatter (NIBS) optics. The scattered light is detected at an angle of 173° and this novel optics arrangement maximizes the detection of scattered light while maintaining signal quality. This provides exceptional sensitivity that is required for measuring the size of nanoparticles, such as surfactant micelles, at low concentrations. [110]

3.4.3 CMC Analysis

Pyrene was used as fluorescent probe for determination of the CMC. 20 samples of 1 mL 6×10^{-7} M pyrene solutions are prepared by solving pyrene in acetone and then acetone was evaporated under vacuum. For polymer solutions, firstly 10 mg/ mL polymer solution was prepared and by twice dilution, 20 samples were prepared via solving polymers with phosphate buffer solution (PBS) and left to stirring overnight. The polymer solutions were transferred to pyrene vials, then 1 min vortex and 6 min sonication applied and left to stirring for overnight.

The CMC was determined as the point of cross-section of the extrapolation of the change in absorbance over a wide range of concentration of polymer. CMC was determined by comparing the peak intensities at 339 nm to 336 nm for PEG₂-PCL 338 nm to 335 nm for PEG-PCL₂ and these values plotted with the concentrations of the polymers to observe the change of the emission of the pyrene due to change in the environment from nonpolar micelle core to polar water surrounding.

3.4.4 Preparation of Curcumin loaded polymeric micelles and determination of the maximum curcumin loading capacity

For determination of the maximum loading capacity of the polymeric micelles curcumin was chosen because of its high potent anti-cancer effect on various tumors. Curcumin fluorescence is a broad band in acetonitrile ($\lambda_{\text{max}} = 524$ nm) and it makes it a suitable drug for UFLC measurements which is a better method for

determination of the maximum loading drug capacity of the drug carrier polymeric micelles

For the measurement of the maximum drug loading capacity, firstly a series of standart solutions (0.125-100 $\mu\text{g}/\text{mL}$) of the curcumin were prepared with MeOH for drawing the calibration curve. Then, series of curcumin solutions were prepared in CCl_3H (0.2-4.0 mg/mL) for drug loading and the solvent was evaporated under vacuum and 20 mg/mL polymer solutions were prepared. Polymer solutions are left to stirring for overnight and they then transferred to curcumin vials. Before left them to stirring for overnight, vortex and sonication was applied. After one night stirring, the samples are placed in centrifuge and rotated at 6000 rpm for a half hour to precipitate and unencapsulated curcumin in the water then 100 μL of the supernatant solution was taken into vials and diluted with MeOH to 1mL.

UFLC measurments were carried out with Column: XR-ODS 50 x 3 mm, 2.2 um ID, Column temperature: 30 °C, Mobile phase: MeCN:% 2 Asetik asit (50:50,v/v), Flow rate: 0.5 mL/min, Wavelenght: 420 nm, Injection volume: 10 μL and amount of the loaded drug is calculated by area under curve method.

4. RESULTS AND DISCUSSION

4.1 Synthesis of the Amphiphilic Miktoarm Star Block Copolymers

The objective of this thesis is to design A₂B type miktoarm star block copolymers in order to use in massive targeted drug delivery system. For this purpose PEG₂-PCL and PCL₂-PEG miktoarm star block copolymers were synthesized in three different ways and the characterization of the synthesized products. ¹H NMR and GPC analysis were carried out where necessary for polymers. Data of this analysis are used to prove the formation of the targeted molecular structure. $M_{n,GPC}$ of the products based on linear PS standards (RI detector). However, determination of more precise molecular weight for PCL, a correction formula was used: $M_{n,PCL} = 0.259 \times M_{n,GPC}^{1.073}$

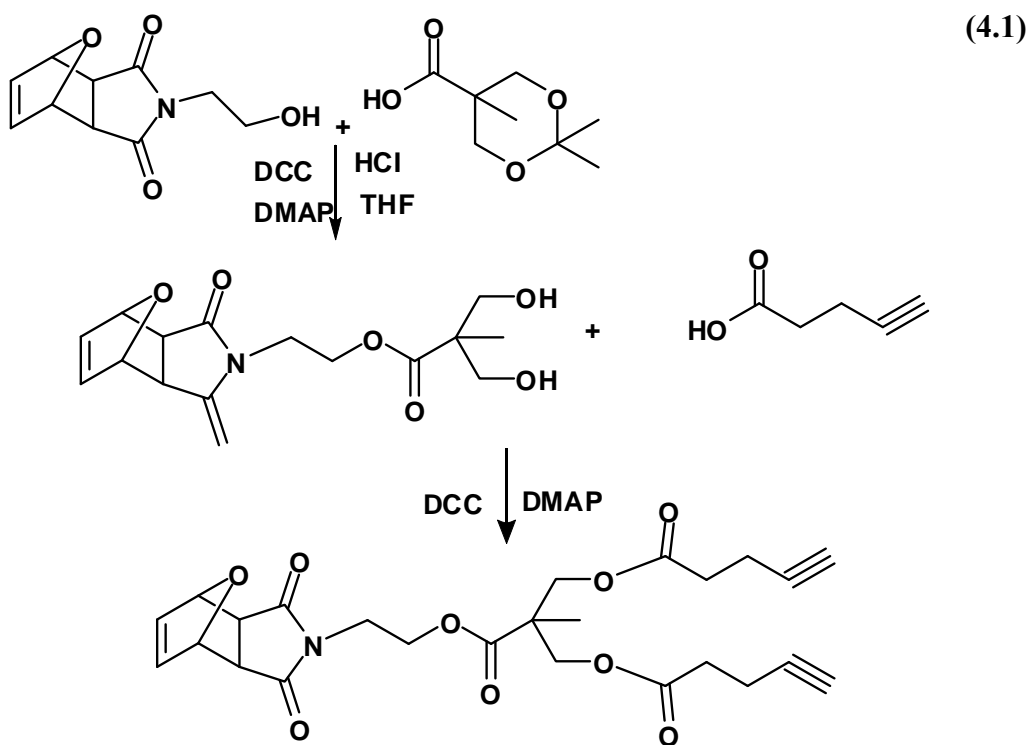
4.1.1 Synthesis of PEG₂-PCL With Core-First Method By using both Diels-Alder and CuAAC Reactions.

Core-First strategy was used for the synthesis of the PEG₂-PCL miktoarm star block copolymer. Due to this strategy high yield reactions are required for junction of the PEG and PCL moieties.

Copper catalyzed reactions are not preferred by the FDA but before this final procedure two different procedures are experienced but the reactions did not work out. So, it was decided to use CuAAC, but if the micellar characterization gives good results the miktoarm star block copolymer, new pathway will be searched for this polymer. Diels-Alder (DA) reaction and the CuAAC (click) was used for the synthesis because both of them has high yield and with no side products. DA was used for the junction of the PCL chain and click for the PEG chains. For the PEG chains click is preferred because the purification of the unreacted PEG is very hard and the reaction yield of the click was very high and has a simple process for purification as mentioned in experimental section.

4.1.1.1 Synthesis of the Core

The core have two different functional groups, first one is dienophile group for DA and alkyne group for the click. 4,10-dioxatricyclo[5.2.1.0_{2,6}]dec-8-ene-3,5-dione has a dienophile group and for gaining two alkyne group for junction of the PEG chains (4.1)



4-(2-hydroxyethyl)-10-oxa-4-azatricyclo[5.2.1.0_{2,6}]dec-8-ene-3,5-dione esterified with 2,2,5-trimethyl-[1,3]dioxane-5-carboxylic acid and hydrolyzed to give two -OH functional group. The addition of the acid to diol group can be easily followed by the ¹H NMR with formation of the 1.18 (C=OC(CH₂O)₂CH₃), 3.63 (CCH₂O) and signal shift of the CH₂ protons from 3.68 ppm (NCH₂CH₂OH) to 4.18 ppm

Secondly, -OH groups of the product turn to alkyne groups by esterification with 4-Pentynoic acid. Formation of the product is proved with ¹H NMR spectra.

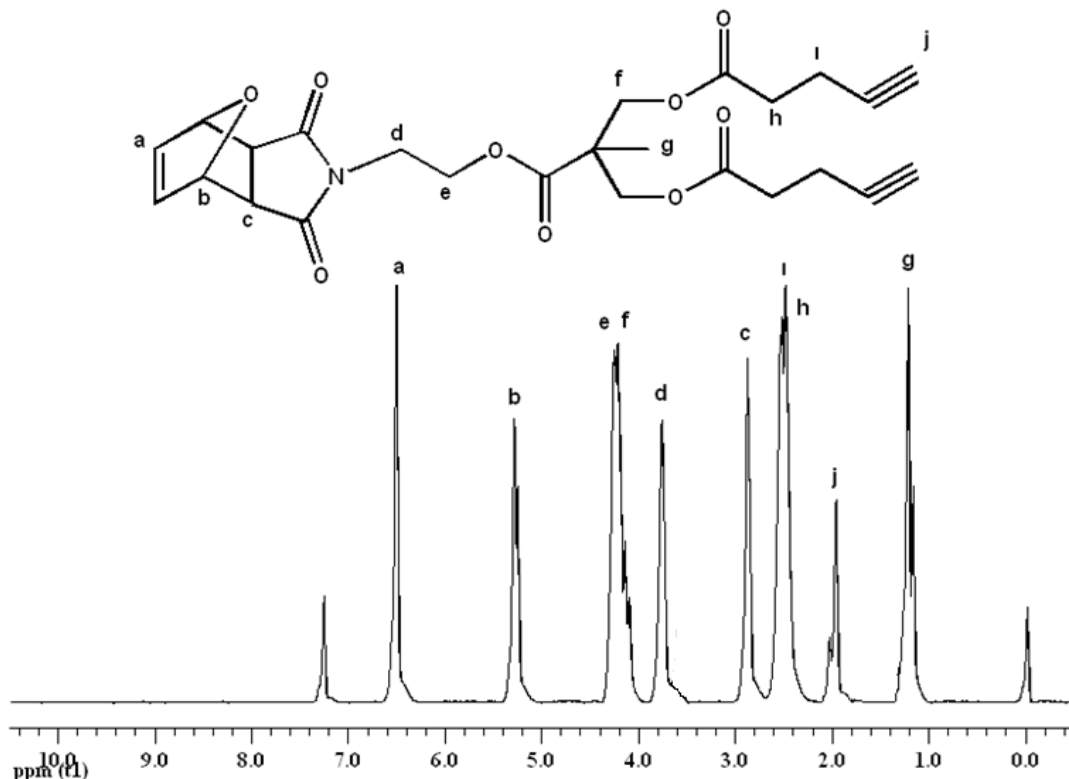
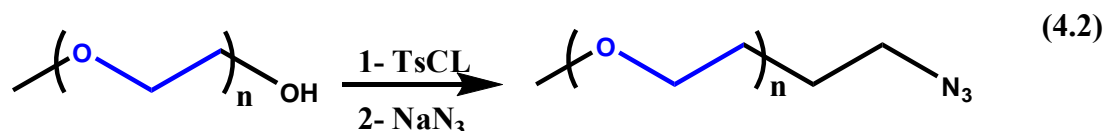


Figure 4.1: ^1H NMR spectra of the core

4.1.1.2 Modification of the Me-PEG for Click Reaction

The core was ready for the click reaction with two alkyne groups to prepare the Me-PEG moiety –OH end of the Me-PEG was turned to azide group in two steps.



In first step –OH group turn to tosyl group as mentioned in previous part and in the second step tosyl group is substituted with azide group that was used in click reaction (4.2) between Me-PEG-N₃ to core Formation of the tosyl end can be observed with formation of the aromatic signals between 7.0-8.0 ppm and the substitution of the tosyl group with azide group is can be followed with loss of aromatic signals and formation of the peak at 2.27 ppm

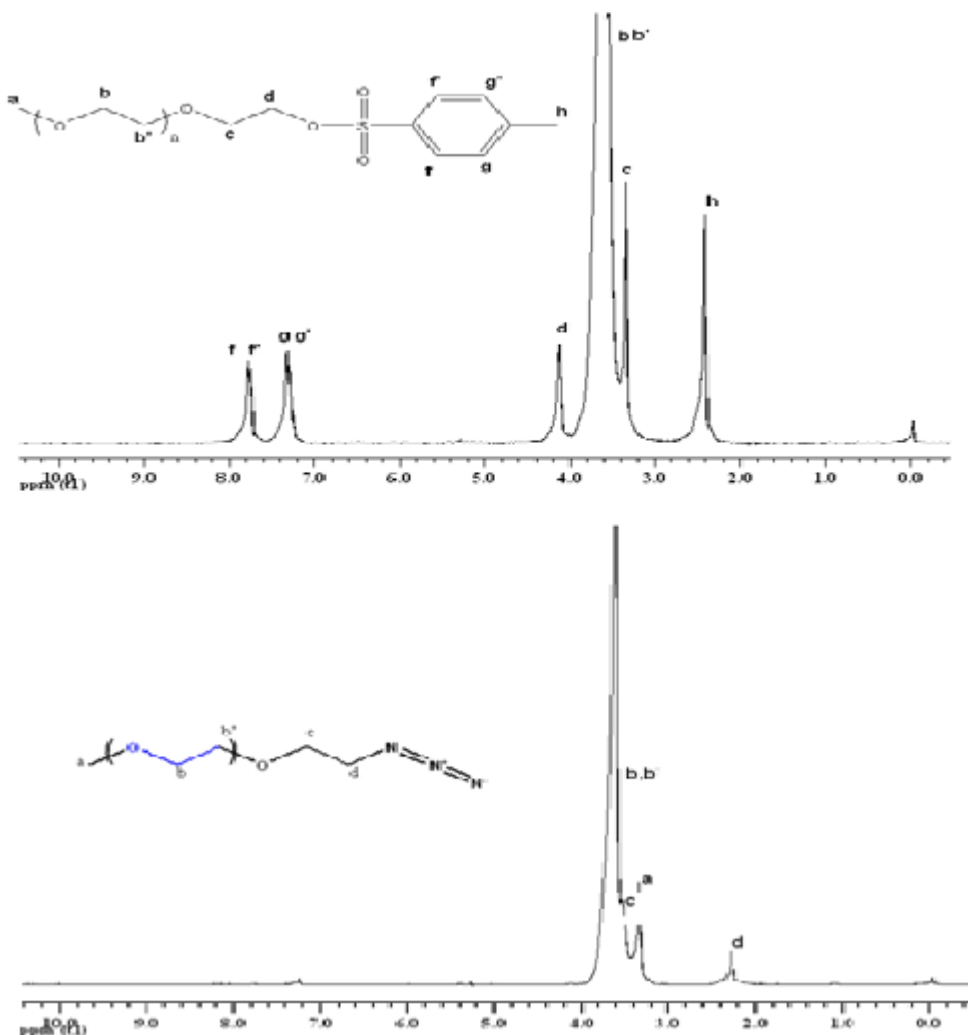
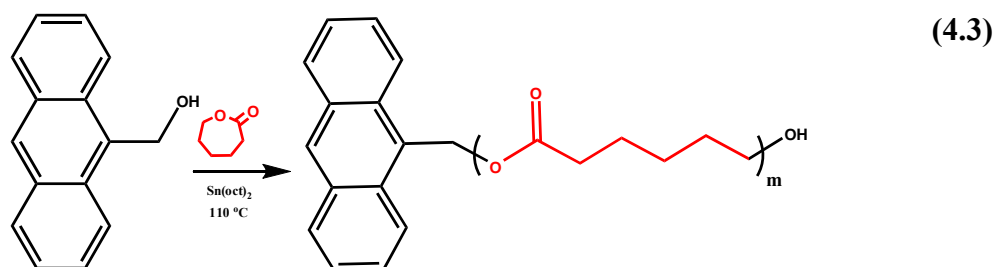


Figure 4.2: The comparison of the ^1H NMR spectra of the Me-PEG-TsCl and Me-PEG- N_3

4.1.1.3 Synthesis of the PCL Chain Via Using 9-anthracene Methanol as Initiator

PCL was synthesized with ROP that allows various type of initiators and for bonding the PCL chain to core. 9-anthracene methanol is a proper initiator because it has got a diene group that gives ability for bonding to core with DA (4.3).



The product was characterized with both GPC and ^1H NMR. $M_{\text{n,NMR}} = 3450$ of the polymer was determined accordingly from the integration of the peaks at 4.02 and 8.28 ppm related to PCL's repeating unit and anthracene end-group protons, respectively.

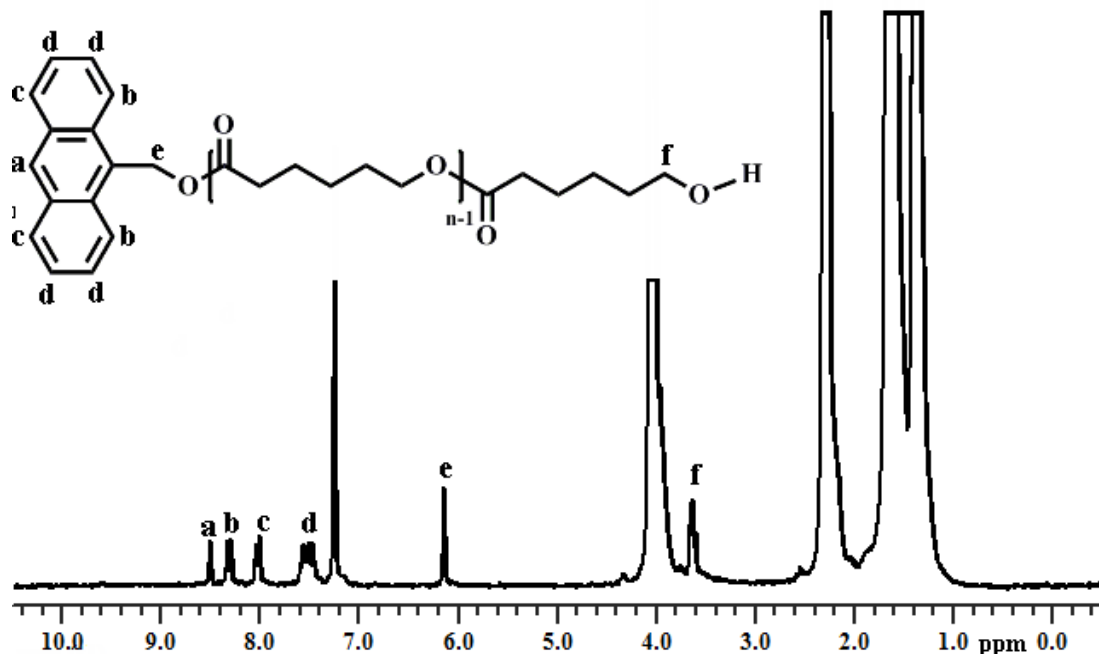


Figure 4.3: ^1H NMR spectrum of the Ant-PCL

4.1.1.4 Synthesis of the PEG_2 Via Click Chemistry

The Me-PEG- N_3 was bonded to core with click reaction between azide end of the PEG chain and alkyne functional group of the core. 2.2 equivalent of the Me-PEG- N_3 was used in the reaction to ensure the bonding of the both alkyne end of the core (**4.4**) and excess amount of the was removed in the last step of the reactions with precipitation in cold diethylether-methanol mixture.

The product was characterized with both ^1H NMR and GPC analysis. The formation of the triazole ring proves the bonding of the Me-PEG to core and it can be followed with the signal at 7.51 ppm and the signals at 3.62 is belongs to PEG chain.

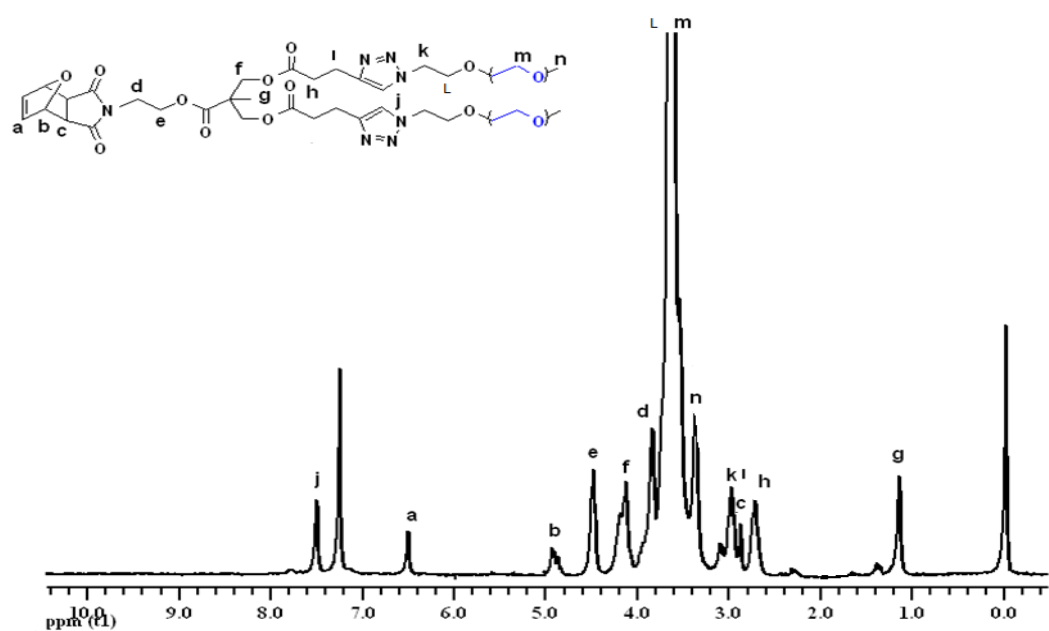
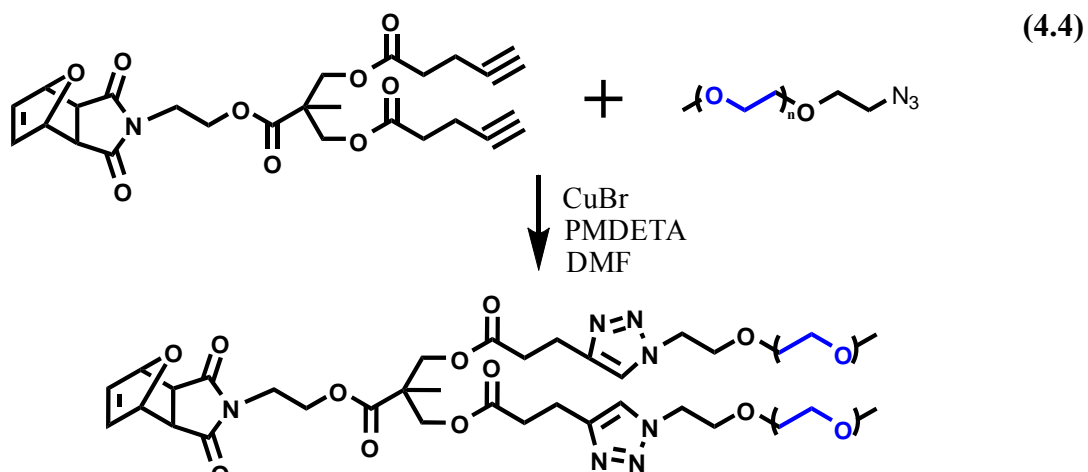


Figure 4.4: ^1H NMR spectrum of the PEG_2

4.1.1.5 Synthesis of the $\text{PEG}_2\text{-PCL}$ with Diels-Alder Reaction

At the final step Ant-PCL was bonded to core via Diels-Alder reaction with procedure mentioned in the experimental part and characterized with both ^1H NMR and GPC analysis. From the GPC trace chromatogram the reaction can be followed. The products peak is not good separated from the Ant-PCL because PEG chains are absorbed by the column and it causes a longer retention time and it seems the molecular weight is lowered although it is increasing with the addition of the MI- PEG_2 to PCL chain (4.4)

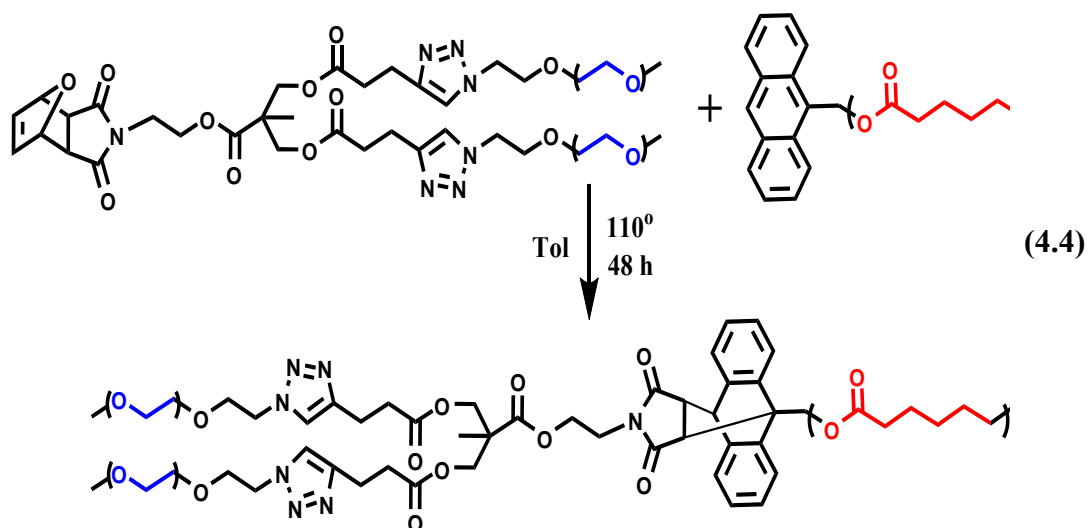


Table 4.1: Molecular weight analyses of the PEG₂-PCL

Polymer	Precursor	M_n,theo (g/mol)	M_n,NMR (g/mol)	M_n,GPC (g/mol)	M_w/M_n
PCL- (PEG) ₂	Anth-(PCL)+ MI-PEG ₂	5000	5200	7000	1.07

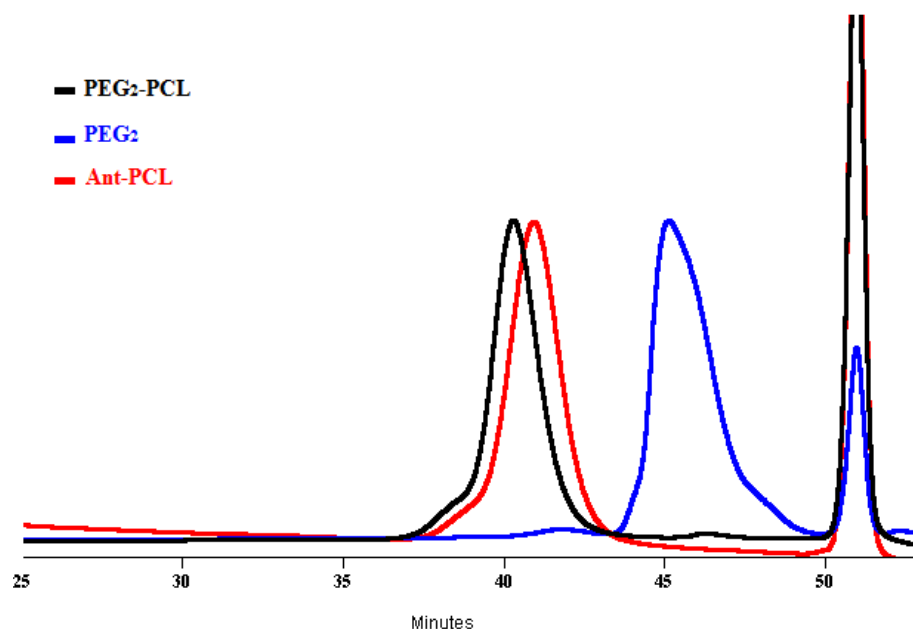


Figure 4.5 GPC analysis of PEG₂, Ant-PCL and PCL—PEG₂ miktoarm star block copolymer.

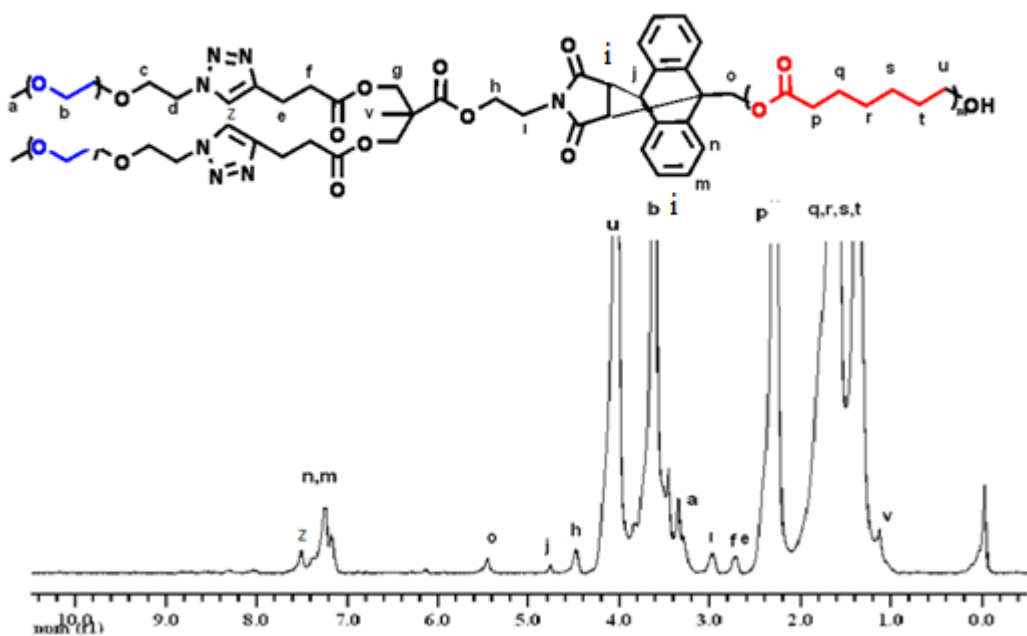


Figure 4.6: ^1H NMR Spectrum of the PEG₂-PCL

4.1.2 Synthesis of PCL₂-PEG By Using DA

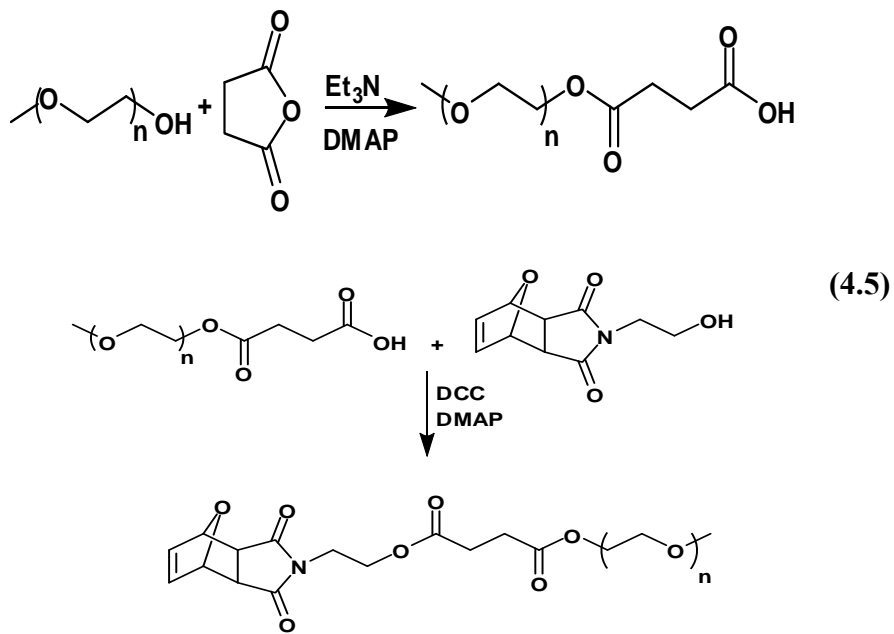
The second synthesized miktoarm star copolymer was PCL₂-PEG. For the synthesis of the aimed product arm-first method was chosen. The synthesis of second copolymer was easier than the first one because the production of the PCL₂ part was available with little modification on the ROP initiator by using 2,2,5-trimethyl-[1,3]dioxane-5-carboxylic acid for getting 2-OH functional group for synthesis of the two arm and also it has a diene group already for DA. And Me-PEG's -OH end was prepared for the DA by using Succinic anhydride as linker for modifying the Me-PEG end as a dieneophile with 4,10-dioxatricyclo[5.2.1.0_{2,6}]dec-8-ene-3,5-dione for DA. Me-PEG is commercially available in various chain lengths and Me-PEG₂₀₀₀ was chosen to produce a optimum hydrophobe to hydrophile chain ratio for formation of the micelle because other available options are Me-PEG₅₅₀ and Me-PEG₅₀₀₀. The first one would cause less soluble block copolymer that could cause a precipitation in water without forming micelle and the second can be totally soluble in water again without forming any micellar structure.

The second synthesized polymer have sent to USA Chicago Illinois and micellar characterization of the product was carried out by Fatemeh BAHADORI and the results found to be very promising for drug carrying polymeric micelle so the

synthesis of the copolymer was modified for a shorter and a cleaner pathway as mentioned in the coming section.

4.1.2.1 Modifications of Me-PEG₂₀₀₀

The Me-PEG's -OH end was not available for bonding 4-(2-hydroxyethyl)-10-oxa-4-azatricyclo[5.2.1.0_{2,6}]dec-8-ene-3,5-dione to have a dieneophile end. So, firstly -OH end of it turned into -COOH by Succinic anhydride via ring opening in the presence of TEA/DMAP catalyst system (4.5). And, secondly 4,10-dioxatricyclo[5.2.1.0_{2,6}]dec-8-ene-3,5-dione was bonded to PEG chain with esterification reaction between COOH functional end of the PEG end -OH group of the 4-(2-hydroxyethyl)-10-oxa-4-azatricyclo[5.2.1.0_{2,6}]dec-8-ene-3,5-dione as shown in the experimental part.



The characterization of the products were done with ¹H NMR and GPC analyses. From the NMR analysis, the peak at 2.87 (CH-CH, bridge protons)) 6.50 (CH=CH as bridge protons), 5.25 (-CHO, bridge-head protons), 4.23 (CH₂OC=O), 3.75-3.51 (OCH₂CH₂) and 2.62 ppm (O=CCH₂-CH₂C=O) proved the adding of the 4,10-dioxatricyclo[5.2.1.0_{2,6}]dec-8-ene-3,5-dione and succinic anhydride linking. And GPC analysis shows that no degradation was occurred during the process by the observation of a single peak on the chromatogram.

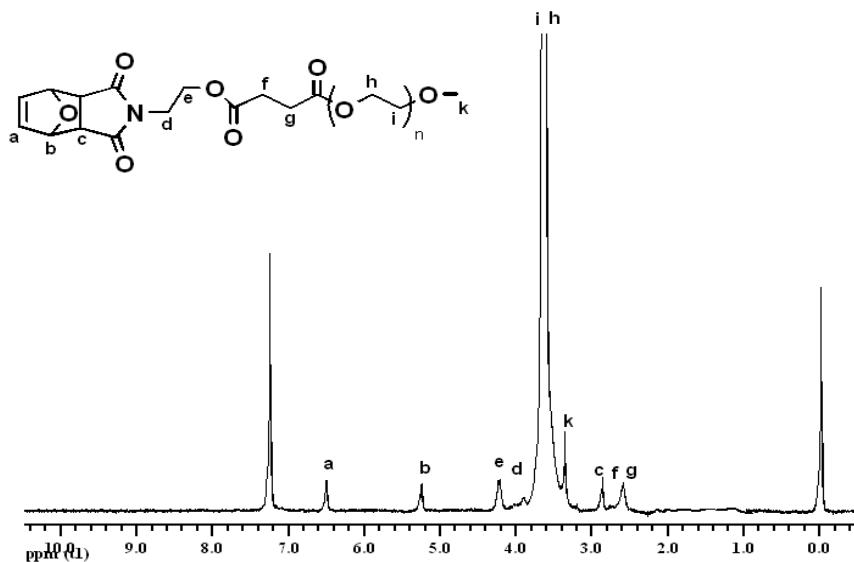


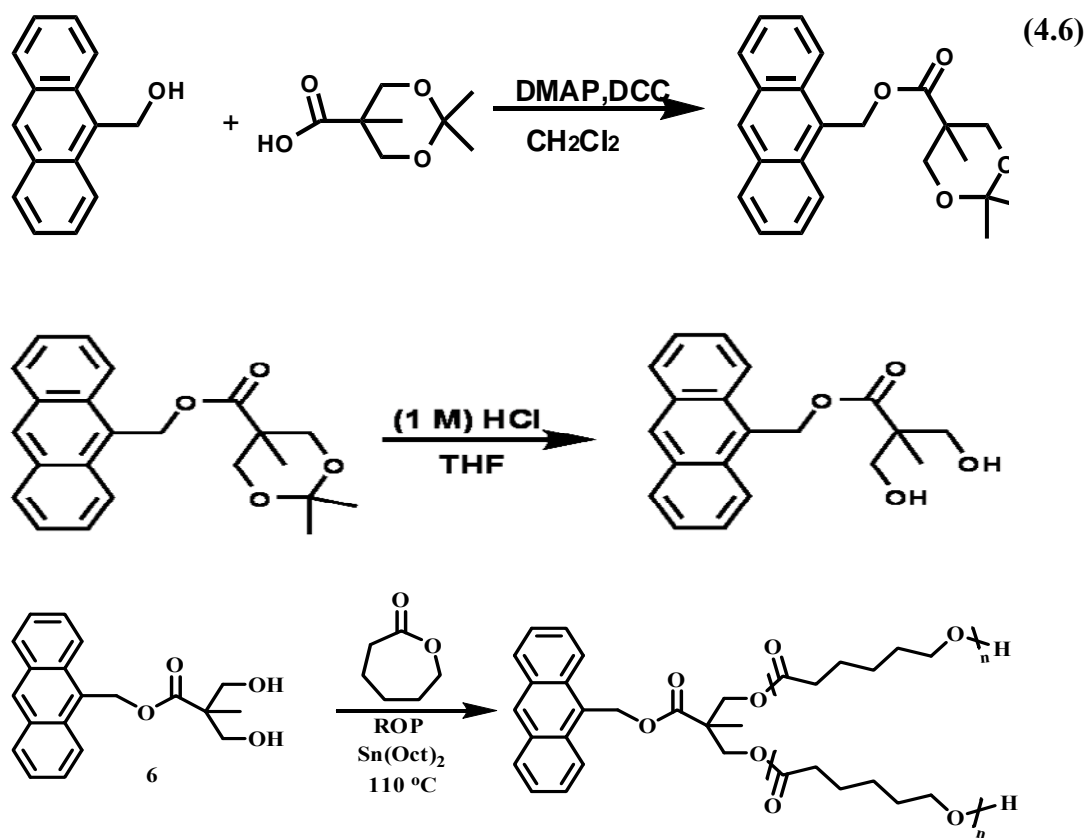
Figure 4.7: ¹H NMR spectrum of the MI-PEG

4.1.2.2 The preparation of the Ant-PCL₂

The PCL moiety of the miktoarm star block copolymer was synthesized in 3 steps. In first 2 steps initiator of the ROP was prepared and at the last step Ant-PCL₂ was synthesized with ROP via using anthracenediol as initiator.

Firstly -OH functionality of the 9-anthracenemethanol was esterified with the -COOH moiety of the 2,2,5-trimethyl-[1,3]dioxane-5-carboxylic acid. DCC was used as a coupling agent and catalytic amount of DMAP as catalyst to give anthracen-9-ylmethyl 2,2,5-trimethyl-1,3-dioxane-5-carboxylate. The observation of proton signals at 4.14 ppm (CCH₂O), 3.58 ppm (CCH₂O), 1.38 ppm (CCH₃), 1.35 ppm (CCH₃), 1.08 ppm (C=OC(CH₂O)₂CH₃) and the shift of CH₂-anthracene signal to 6.2 ppm proves the addition of the 2,2,5-trimethyl-[1,3]dioxane-5-carboxylic acid group to 9-anthracenemethanol (**4.6**).

Secondly, ketal protection of the diol group was removed with hydrolysis. Formation of the diol can be followed by the loss of the 1.38 ppm (CCH₃), 1.35 ppm (CCH₃) and the change of the chemical shift of the CCH₂O signals from 4.14 ppm to 3.66 ppm. The product was obtained as yellow needle like solid



At the final step, Ant-PCL₂ was synthesized via ring opening polymerization by using anthracen-9-ylmethyl 3-hydroxy-2-(hydroxymethyl)-2-methylpropanoate as initiator. The product was characterized by both ¹H NMR and GPC. The proton signals at 4.0 ppm (CH₂OC=O of PCL), 3.60 ppm (CH₂OH, L), 2.3 ppm (C=OCH₂), 1.2-1.8 ppm (CH₂) indicated PCL and the signals in the aromatic region indicated to initiator.

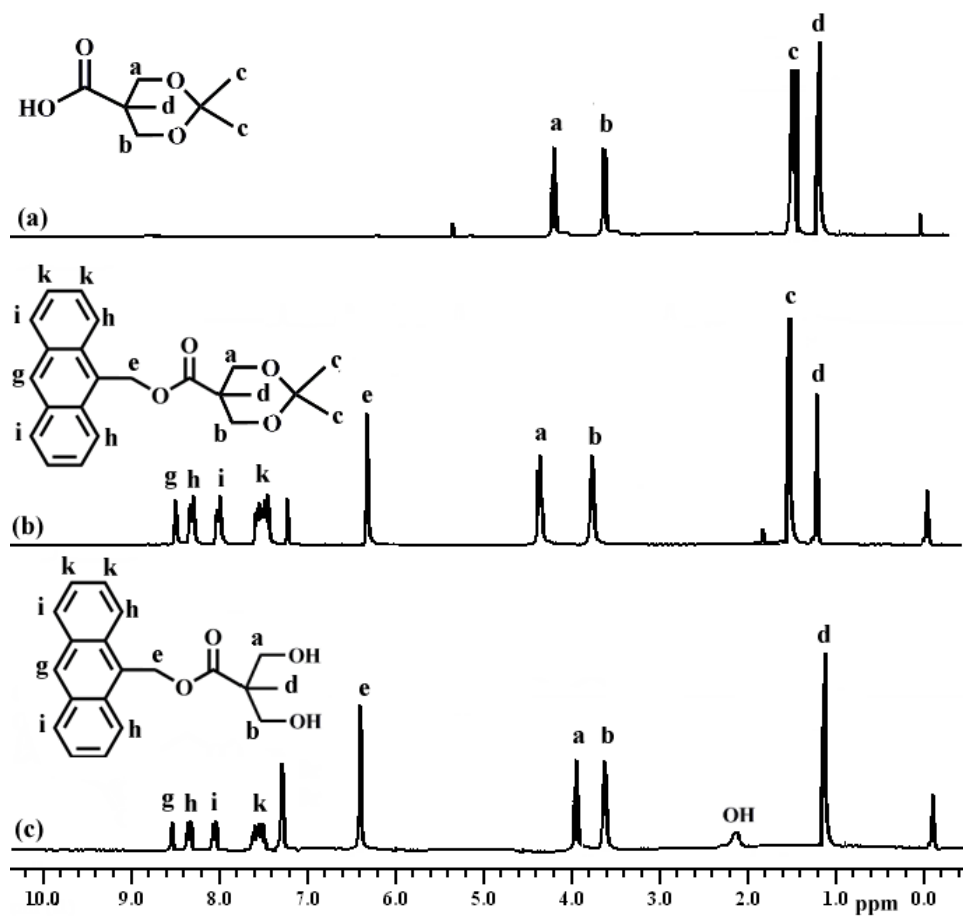


Figure 4.8: ^1H NMR spectra of: a) 2,2,5-trimethyl-[1,3]dioxane-5-carboxylic acid; b) anthracen-9-ylmethyl 2,2,5-trimethyl-1,3-dioxane-5-carboxylate ; c) anthracen-9-ylmethyl 3-hydroxy-2-(hydroxymethyl)-2-methylpropanoate in CDCl_3

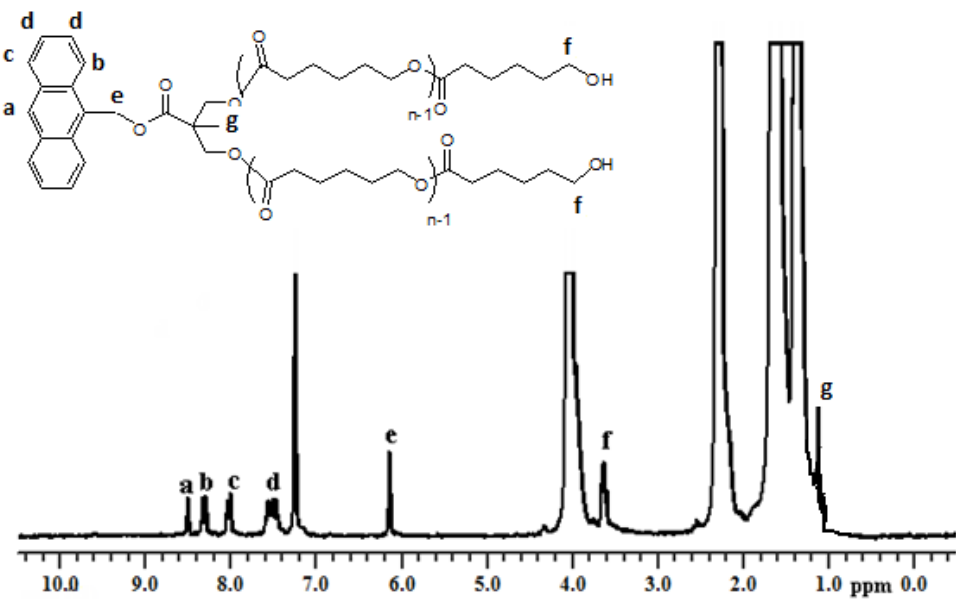


Figure 4.9: The ^1H NMR spectrum of the Ant-PCL₂

4.1.2.3 The Synthesis of $\text{PCL}_2\text{-PEG}$ via DA

In the final step of the procedure, MI-PEG and Ant-PCL₂ were coupled with DA reaction at high temperature (110 °C). During the reaction firstly the furan protection of the MI-PEG was removed due to retro Diels-Alder reaction. After removal of the furan, the end of the PEG was still dieneophile, so DA reaction occurs between PEG and PCL chains to give the $\text{PCL}_2\text{-PEG}$ product (4.7).

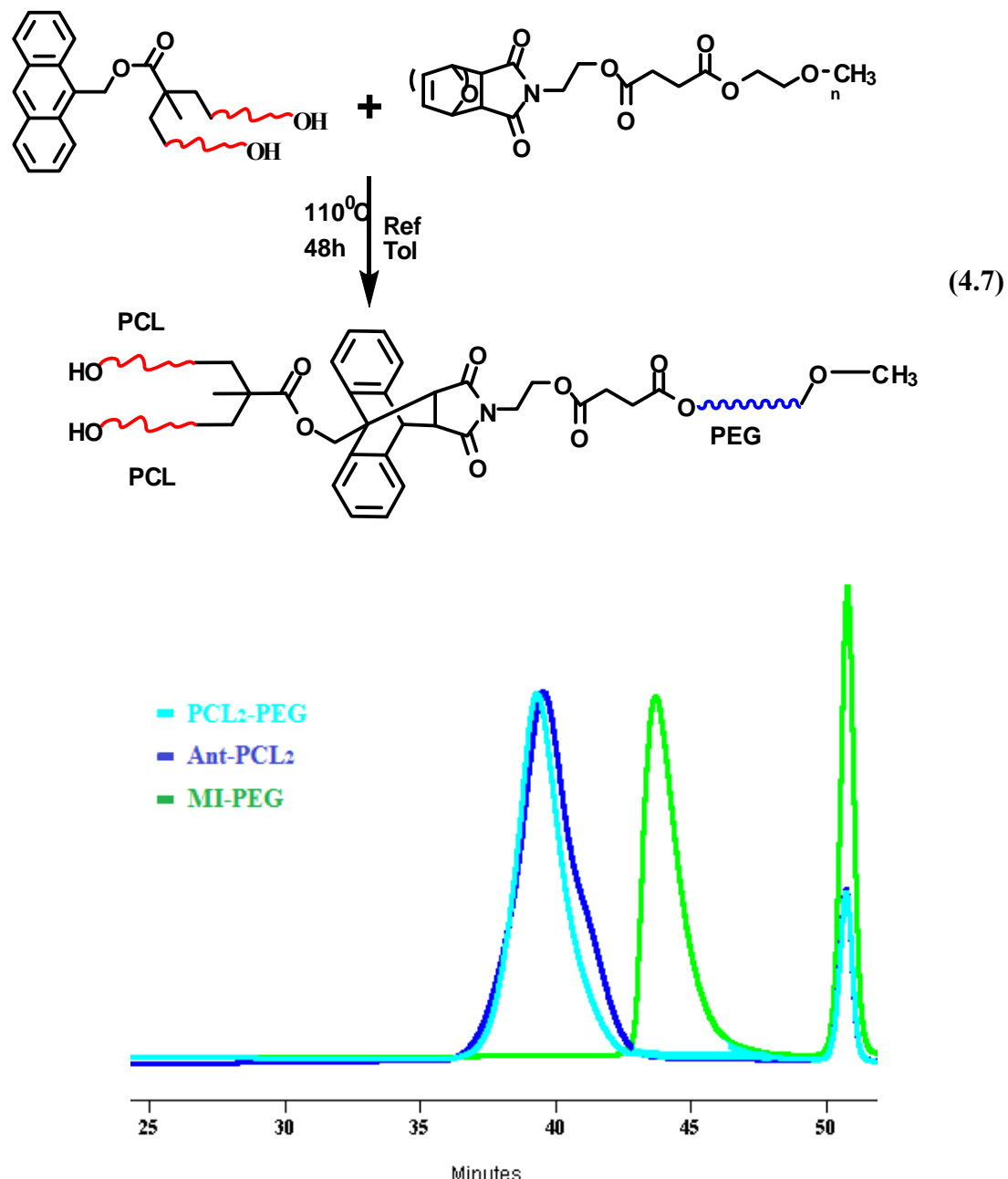


Figure 4.10: GPC analyses of PEG_2 , Ant-PCL and $\text{PEG}_2\text{-PCL}$ miktoarm star block copolymer.

The product was characterized by both ^1H NMR and GPC analyses. From the GPC analysis the signal of the product was observed near Ant-PCL₂ precursor because even the molecular weight was increased with the joining of the two chains, and the retention of the PEG moiety in the column was due to the adsorption behaviour of the PEG. Molecular weight of the product observed near to PCL, but higher than PEG. The PDI value of the product shows that one product was observed as desired. ^1H NMR analyses also proved the success of the synthesis due to peaks at 3.62 ppm (br, 6H, -OCH₂CH₂, repeating unit of PEG and (NCH₂CH₂OC=O) and 4.0, 2.4-0.9 ppm (repeating unit of PCL) also disappearance of the characteristic peaks of anthracene proved the DA reaction formation and junction of the two chains.

Table 4.2: Molecular weight analyses of the PCL₂-PEG

Polymer	Precursor	$M_{n,\text{theo}}$ (g/mol)	$M_{n,\text{NMR}}$ (g/mol)	$M_{n,\text{GPC}}$ (g/mol)	M_w/M_n
PEG-(PCL) ₂	Anth-(PCL) ₂ + MI-PEG	6400	6200	8400	1.07

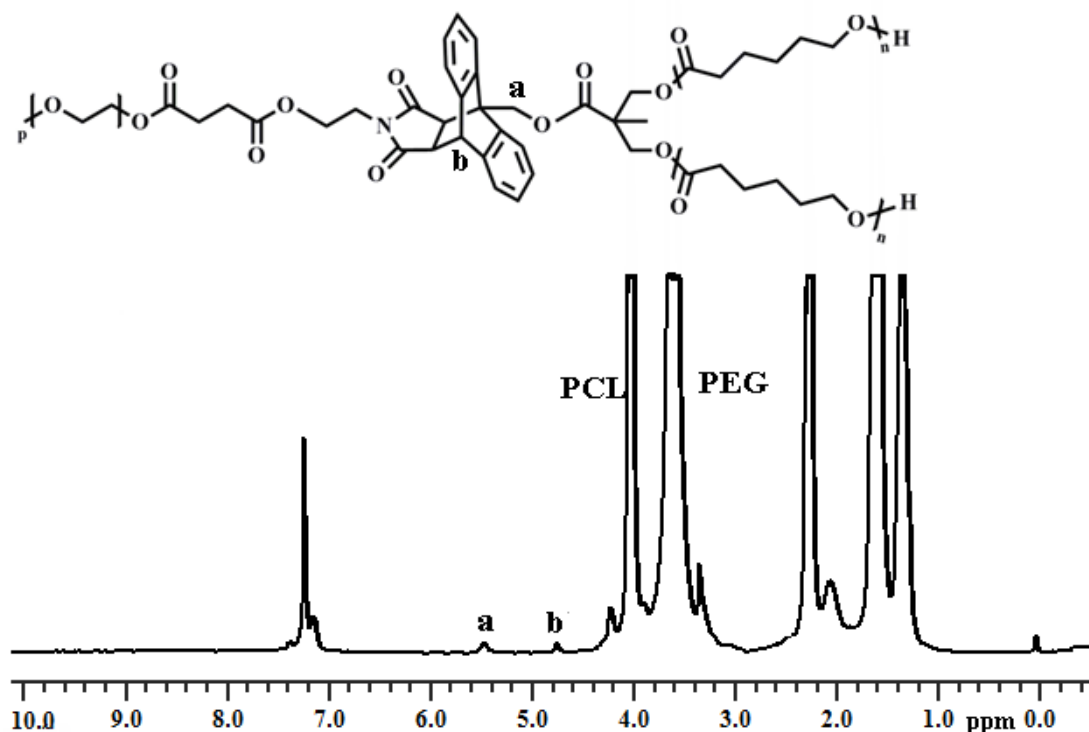


Figure 4.11: ^1H NMR spectra of the PCL₂-PEG

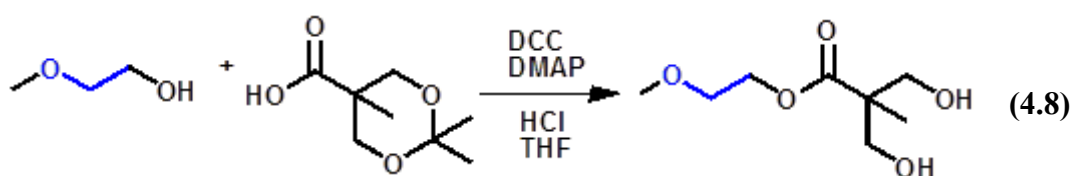
4.1.3 Synthesis of the PCL₂-PEG By Using Modified MePEG

The first production procedure of the PCL₂-PEG was given good result for micellar characterization and synthesis, but it was too long. The synthesis of the product was required too many steps that is not prefered for a product that will be used in pharmacy. Because it interacts with different solvents and also, due to nature of the polymers, shorter pathways are prefered for less use of the solvents and other chemicals. Also, economically shorter pathways are more favorable and one of the main goals of the DDS is to decrease the cost of the drugs.

Due to the reasons mentioned above the synthesis of the PCL₂-PEG was reformed to give shorter pathway. The use of the PEG chain as macroinitiator for ROP was accomplished by the previous works such pluronics of the Kabanov but in our synthesis we need two PCL chains so, two functional –OH groups. Me-PEG₂₀₀₀ is modified with 2,2,5-trimethyl-[1,3]dioxane-5-carboxylic acid. and then hydrolyzed to gain two functional –OH groups. After that simple modification on Me-PEG it becomes a proper initiator for production of PCL₂ moiety with ROP

4.1.3.1 Synthesis of the PEG-Diol

The modification of the Me-PEG to PEG-Diol was carried out in two steps. Firstly Me-PEG's –OH end was esterified in presence of the DCC/DMAP catalyst system (4.8) and purified by precipitating in cold diethylether. In the second step ketal protection of the diol was removed by hydrolysis in the acidic media. The steps were followed by both ¹H NMR and GPC analysis. The success of the esterification was proved with the formation of the peak at 4.30 ppm (CH₂OC=O) that proves the formation of the ester bond between –OH of the Me-PEG and –COOH of the 2,2,5-trimethyl-[1,3]dioxane-5-carboxylic acid. And the peaks that belongs to 2,2,5-trimethyl-[1,3]dioxane-5-carboxylic acid (1.38 ppm (CCH₃) 1.36 ppm (CCH₃) and 1.18 ppm (C=OC(CH₂O)₂CH₃). And the removal of the ketal protection is can be followed by the absence of the peaks at 1.38 ppm (CCH₃) 1.36 ppm (CCH₃) on ¹H NMR spectrum of the PEG-Diol.



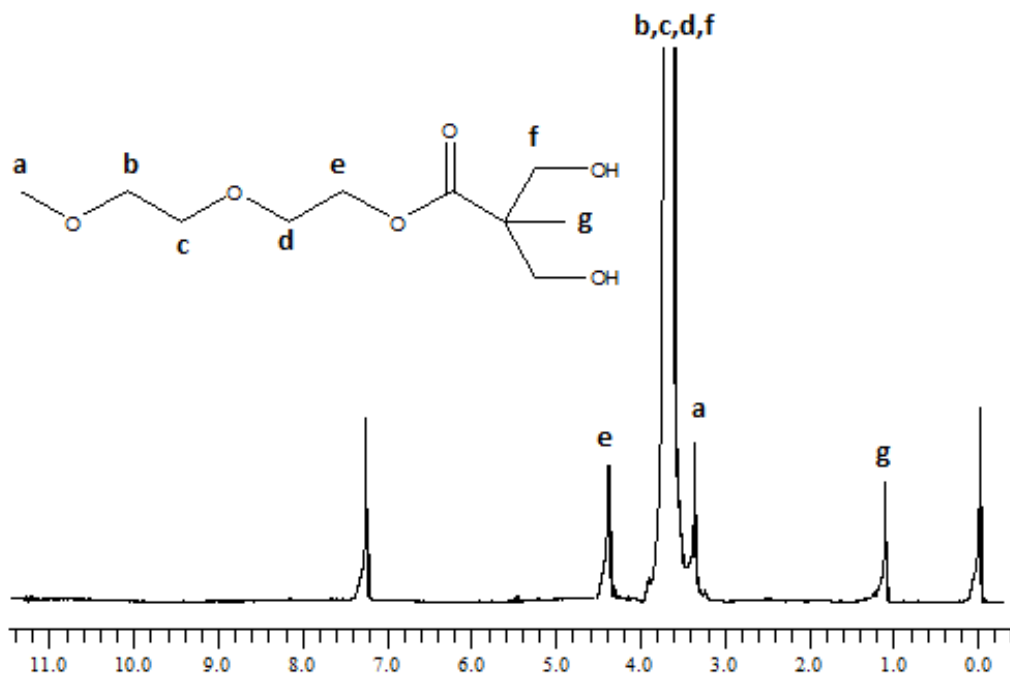
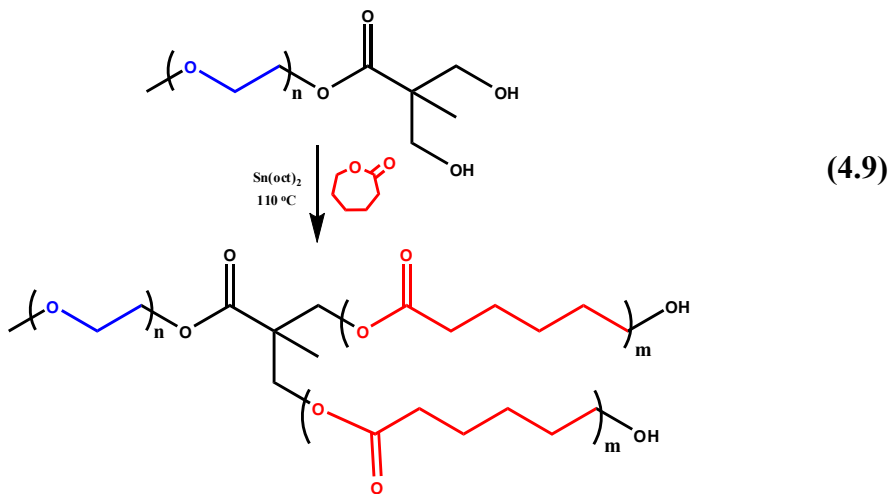


Figure 4.12: ¹H NMR Spectrum of the PEG-Diol

4.1.3.2 The Synthesis of the PCL₂-PEG via ROP

After preparation of the macroinitiator with only one step the miktoarm star block copolymer was synthesized by using modified PEG as macroinitiator. The synthesis was carried out in the standard conditions of the ROP of the \square -CL (**4.9**) and for purification cold diethylether is used for precipitation of the product which was used for the both purification of the PEG and PCL.



For the characterization of the product GPC, ¹³C NMR and ¹H NMR analysis were carried out. Both NMR spectrums are proves the addition of the \square -CL molecules to

macroinitiator via ROP with the peaks at 174, 64.1, 34.2, 28.3, 25.5 and 24.6 ppm (repeating CH_2 units of the PCL) on ^{13}C NMR (APT) and 4.04, 2.25, 1.6 and 1.30 ppm on ^1H NMR. Also, GPC chromatogram was proved the formation of the miktoarm star block copolymer by the increase to higher molecular weight with good PDI value.

Table 4.3: Molecular weight analyses of the PCL_2 -PEG synthesized with macroinitiator

Polymer	Precursor	$M_{n,\text{theo}}$ (g/mol)	$M_{n,\text{NMR}}$ (g/mol)	$M_{n,\text{GPC}}$ (g/mol)	M_w/M_n
PCL_2 -PEG	PEG-Diol	6000	5750	7000	1.10

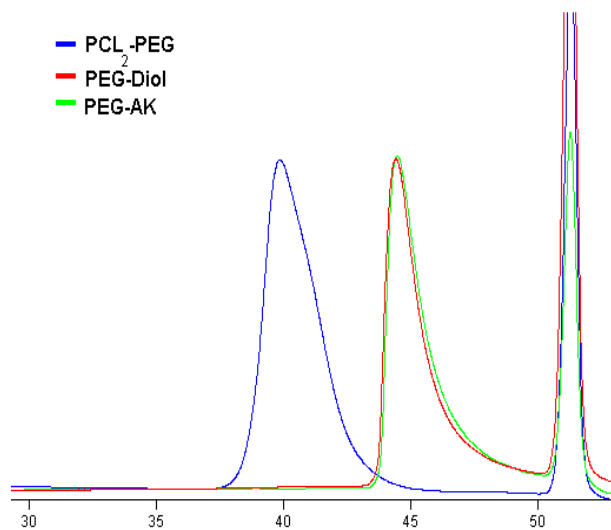


Figure 4.13: GPC analyses of PEG_2 , Ant-PCL and PEG_2 -PCL miktoarm star block copolymer.

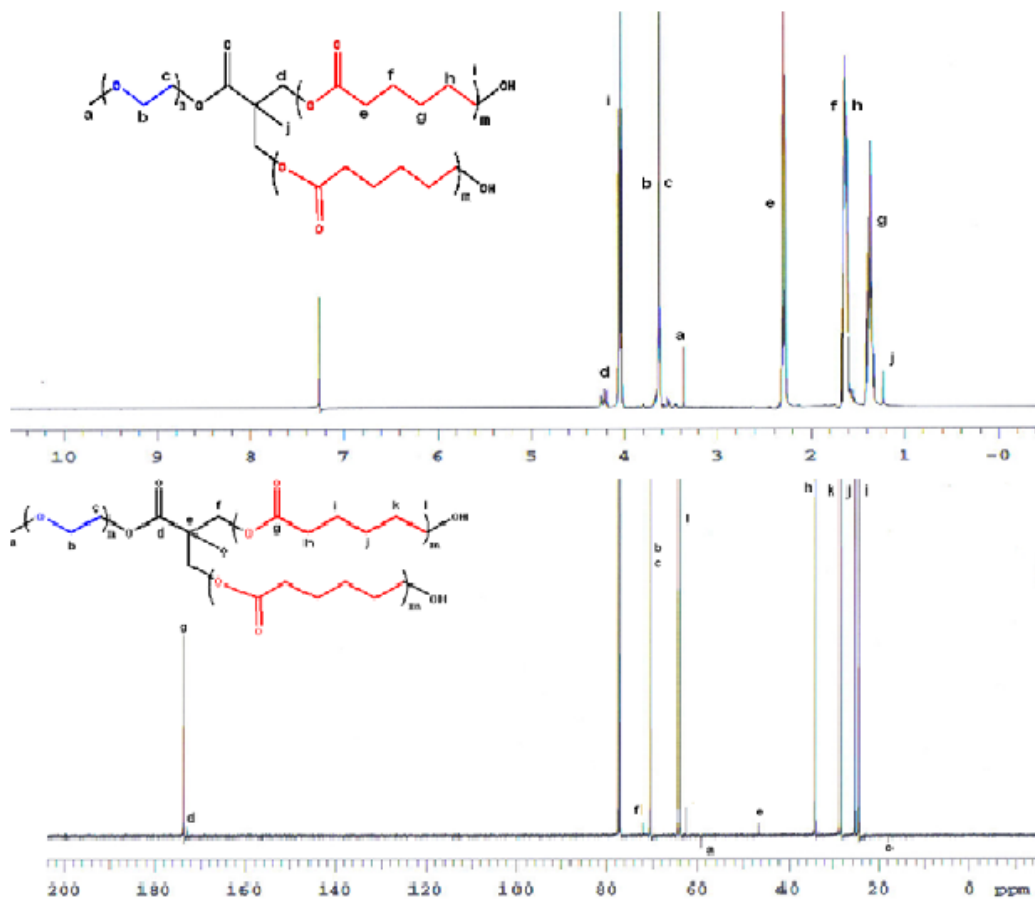


Figure 4.14: The ¹H NMR and ¹³C NMR spectra of the PCL₂-PEG miktoarm star block copolymer

4.2 Preparation and Characterization of the Micelles

The micellar characterization of the polymeric micelles were made by three ways size distribution, CMC analysis, and max. curcumin loading capacity of the micelles. But the micellar characterization of the PCL₂- PEG was done by the Fatemeh Bahadori so it won't be discussed in here

4.2.1 Preparation of the Micelles

In this study, we explored the potential of the PCL-PEG micelles as a drug delivery vehicle for lipophilic drugs. The PCL-PEG micelles can not be prepared in water due to the hydrophobicity of the polycaprolactone core. For this reason, the block copolymer was first dissolved in DMF, and micellization is induced by the dropwise addition of water, followed by dialysis.

Dialysis method is used for preparation of the micelle form the amphiphilic miktoarm star block copolymers. Copolymer is first dissolved in the DMF, but, as

mentioned in the theoretical part, this could cause an increase in the diameter of the micelles. Direct dialysis with water can reduce the size of the micelles. And, after dialysis the samples were freeze-dried at -50 °C, but, generally preferred degree was indicated to be -80 °C in the literature. This disadvantage is compensated by a longer lyophilisation time.

The morphology of the micelles are effected from the ratio of the DMF to observe this effect was observed by addition of the different amount of the water after dissolving in DMF. The molecular weight cut off value of the dialysis membrane was chosen as 3500 to get rid off impurities and DMF.

4.2.2 Particle Size Analyses

Size of the micelles were measured with Malvern Zeta-sizer. Conventional DLS instruments use scattered lights with a detection angle of 90° and this optical configuration may not be sensitive enough for the successful measurement of surfactant micelles. Therefore the scattered light was detected at an angle of 173° and this novel optics arrangement maximizes the detection of scattered light by maintaining signal quality. This provides exceptional sensitivity that is required for measuring the size of nanoparticles at low concentrations.

Firstly, PEG₂-PCL's micellar size was measured as 175 nm and 143 nm for PCL₂-PEG micelles. The measured sizes are reasonable which followed behaviour of the block copolymer after a series of dilution, the peak of the micelle was lost in the diagram because the concentration of the amphiphilic miktoarm star block copolymer was fallen under the CMC value, so the remaining peaks are belongs to aggregates that can be seen in the figure 4.16

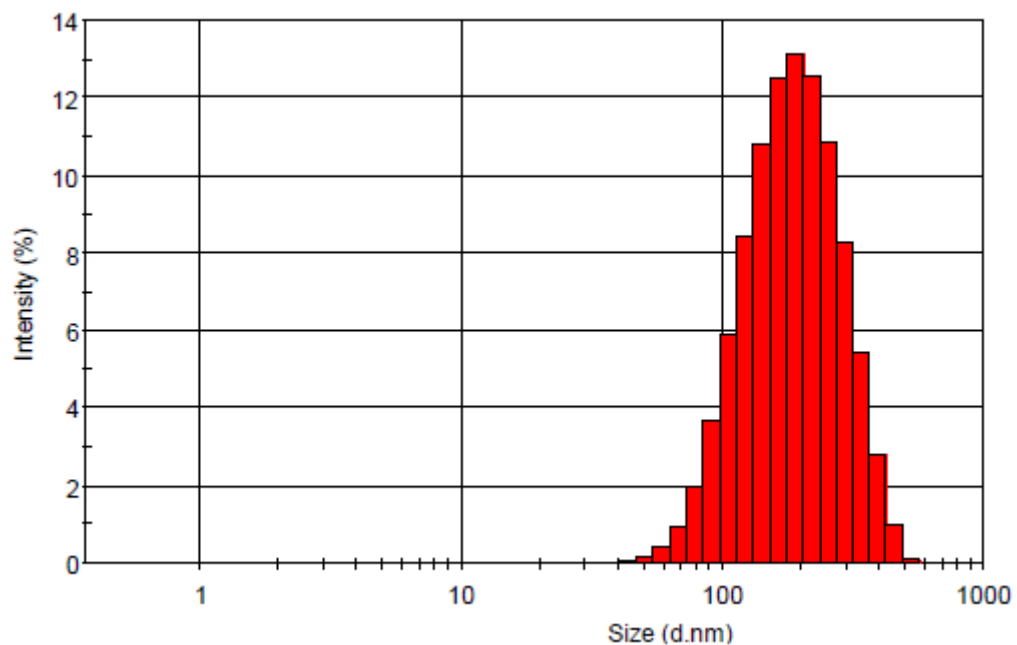


Figure 4.15: Particle size distribution of the PEG₂-PCL micelles

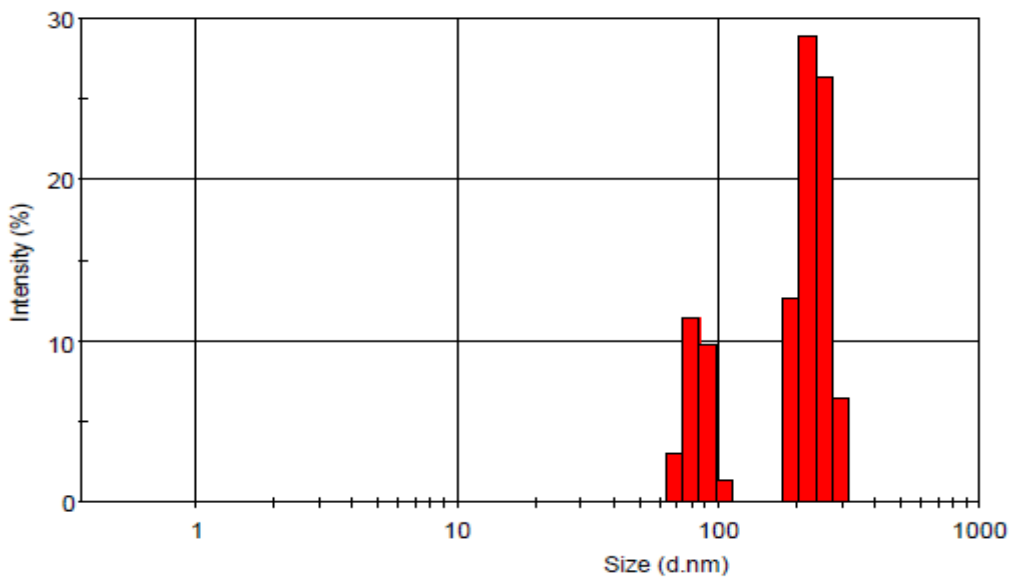


Figure 4.16: The particle size distribution of the PEG₂-PCL micelles after dilution

Secondly, micellar size of the PEG-PCL₂ micelles were studied with same procedure but this time to observe the effect of the water/DMF ratio on the size of the micelles, three different samples were prepared for Zeta-sizer analysis vary from 1/1 to 3/1 (v/v, water/DMF)

Table 4.4: DMF/H₂O (V/V) and the size of the micelles prepared with PCL₂-PEG

DMF/H ₂ O (V/V)	Micellar Size (nm)
1/1	154.0
1/2	179.2
1/3	143.1

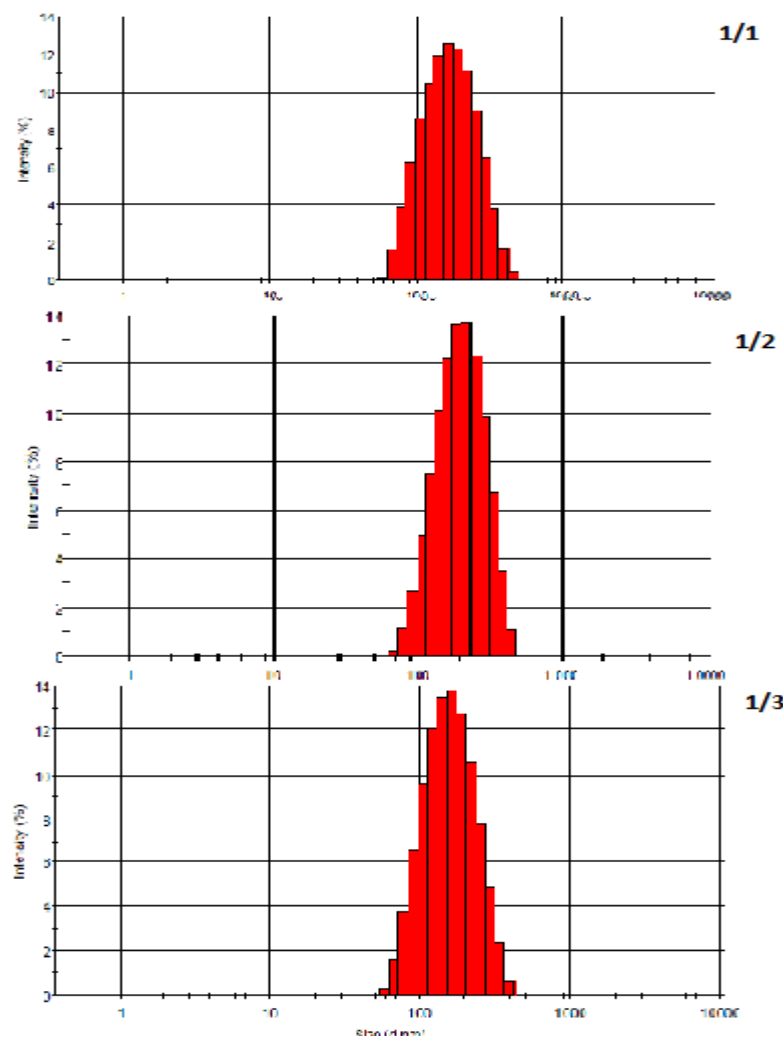


Figure 4.17: The size distributions of the polymeric micelles that prepared with different DMF/H₂O ratios

The effect of the ratio of the DMF did not show a linearity with the increase in the amount of the water, and the smallest micellar size was observed for the 1/3 ratio. Even with this unusual micellar sizes the prepared micelles can be used for DDS because it is still under the critical value of the polymeric carriers size range (200 nm) used for the passive targeting.

4.2.3 CMC Measurements

The CMC measurement of the polymeric micelles were done by using pyrene as fluorescent probe. Fluorescence behaviour of pyrene is changing due to the polarity of the chemical environment of the molecule. So this makes it a good fluorescent probe for determination of the CMC value of the amphiphilic block copolymers, the concentration of the polymer was diluted to half till to under the CMC value. The self-assembly of the micelles will break and the loaded pyrene will be released to water environment and red shift was observed in the emission spectrum of the pyrene. So, by plotting the polymer concentration with the ratio of the intensities of the emission wavelengths of pyrene CMC value can be observed with the sharp decrease in the ratio of the intensities at around 1.

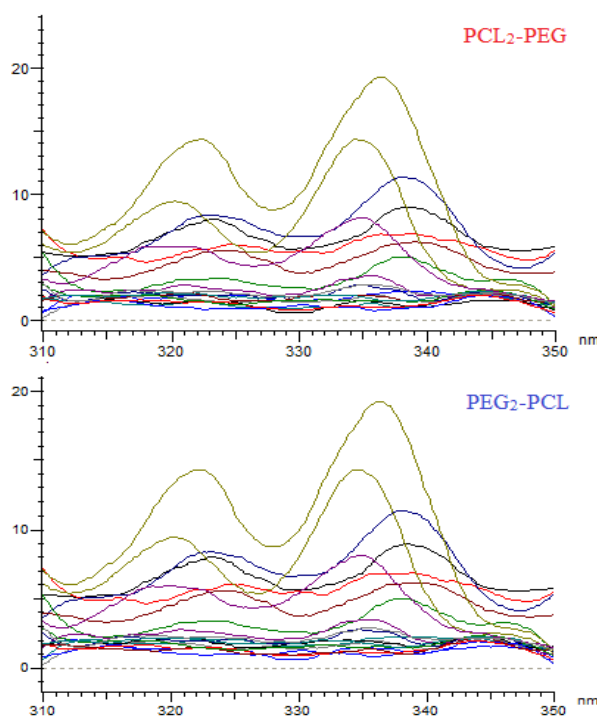


Figure 4.18: The fluorescence spectrum of the $\text{PCL}_2\text{-PEG}$ and $\text{PEG}_2\text{-PCL}$

The red-shift of the emission of pyrene can be both followed on the fluorescence spectrum of the polymeric micelles caused by the dilution of polymer concentration via change on the environment of the pyrene after degradation of polymeric micelles. But the aggregates that were formed during the degradation of the polymeric micelles keep some amount of the pyrene in hydrophobic area which cause to unexpected emissions, but they were underestimated while plotting on the diagram. The shift of the emission wavelength is observed differently for the polymers. However, the corona of the both polymer is composed of the same polymer (PCL),

same morphologies with different arm structures cause unequal fluorescent responses. So, red shift observed for PEG₂-PCL was from 336 nm to 339 nm and from 335 nm to 338 nm for PCL₂-PEG.

For determination of the CMC values I_3/I_1 is calculated for samples, then plotted with Log C (mg/mL). The CMC values 12 mg/L for PEG₂-PCL and 9 mg/L for PCL₂-PEG are determined. These values are good enough for a drug carrying micelle. However, the success of the CMC values are changing due to the loaded drugs depending on their effective doses and stability of the micellar structure related to several factors. Therefore, a complete judgement can not be made without *in vivo* tests.

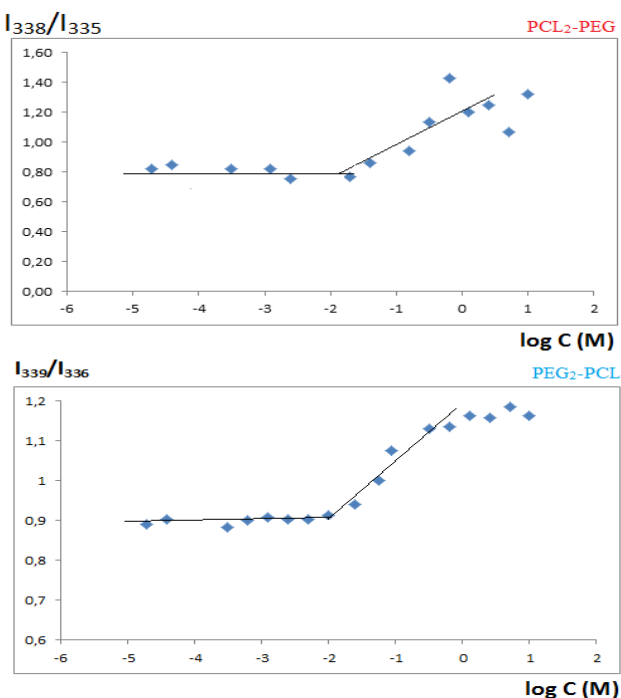


Figure 4.19: The CMC graphs of the polymeric micelles

4.2.4 Encapsulation of the Curcumin with Polymeric Micelles

The final step of the experiments was drug loading to polymeric micelles and measurement of the maximum loading capacity. Although, curcumin has high drug potential due to its antioxidant, cytotoxic (anticancer) and anti-Alzheimer properties unfortunately, its water solubility is very poor (0.6 $\mu\text{g}/\text{mL}$). In this experiment, the effect of the encapsulation of curcumin with prepared micellar formulation was observed via maximum loading capacity measurements.

The loaded curcumin amounts are found with the external standard method. Firstly, a calibration curve was drawn with the standard curcumin concentrations to observe the response of the column to curcumin, then the loaded curcumin amounts are calculated via plotting the area under curve values of the samples on the calibration curve (figure 4.20). This calibration curve was used for both the polymeric micelles.

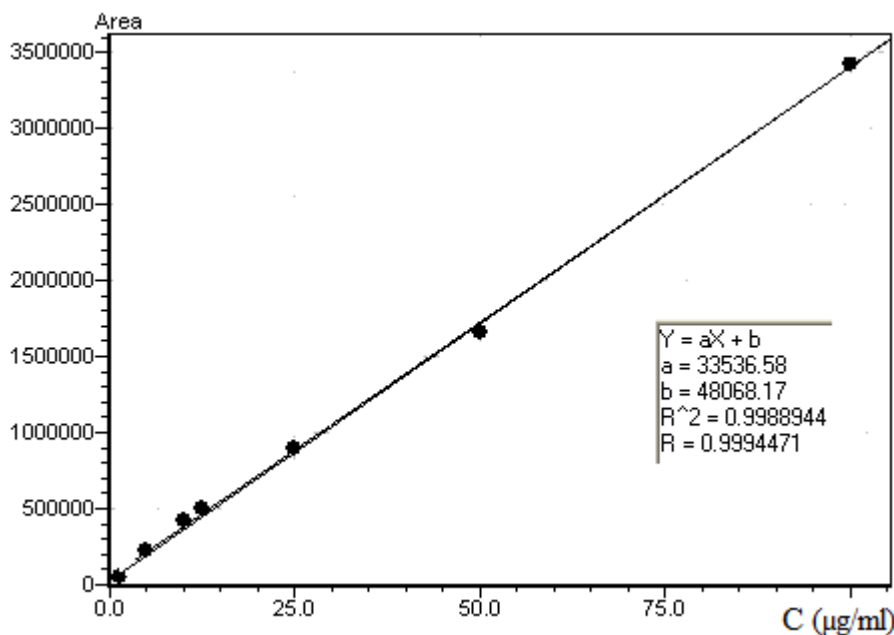


Figure 4.20 : The calibration curve of the curcumin standards used in calculations. The used standards were chosen at very low concentration to detect very low amount that loaded to polymeric micelles and also not to reach over the Beer-Lambert's law. The average of the three samples measurements was used to determine the loaded amount of the curcumin for each concentration to avoid the experimental errors.

The maximum curcumin loading capacity was calculated to be 126.7 μg in 20 mg of the $\text{PEG}_2\text{-PCL}$ polymeric micelle. The expected loaded amount must be higher than the observed loaded value 321.7 μg for the second 20 mg of the polymeric carrier $\text{PCL}_2\text{-PEG}$. Micelles higher concentrations will be experienced because it was seen to maximum loading capacity had not reached to the curcumin amounts can be accomplished from the Table 4.5. As seen the Table, the loaded amount of the curcumin is increasing depending on the initial curcumin amount, however, a better maximum point must be observed.

Table 4.5: The loaded curcumin amount to polymeric micelles.

Curcumin amount (μ g)	200.0	500.0	1000.0	2000.0	3000.0	4000.0
Cur. Conc. in PEG ₂ -PCL Micelles (mg/mL)	28.8	68.8	126.7	50.7	30.4	135.1
Curcumin Conc. in PCL ₂ -PEG Micelles (mg/mL)	27.8	31.0	59.3	91.5	146.7	321.7

The solubility of the curcumin increased from 0.6 μ g/mL to 135.1 μ g/mL with PEG₂-PCL micelles which means the solubility in water increased 211 fold. Although it has not reached to the maximum loading capacity for PCL₂-PEG micelles, however it increased 536 fold.

5. CONCLUSION

In conclusion, well-defined amphiphilic miktoarm star-block copolymers were successfully synthesized to prepare drug carrier polymeric micelles by benefit from their amphiphilic structure via a combination of ROP, highly efficient Diels–Alder and click reactions. In first study, PEG₂-PCL and PCL₂-PEG star block copolymers were synthesized based on "core-first" and "arm-first" methodology. As a result, well-controlled macromolecular architectures with controlled molecular weights and rather narrow molecular weight distributions were achieved.

In the first step of synthetical studies, synthesis of the PEG₂-PCL star block copolymer and PCL₂-PEG star block copolymer was carried out with two different methods. For this purpose, we have prepared a proper core that needs two alkyne and one dieneophile end group, and subsequently azide functionalized PEG₅₅₀ chains are attached to the core with Huisgen type copper catalyzed cycloaddition reaction. In the next step, synthesis of PEG₂-PCL star block copolymer was carried out using the anthracene end-functionalized (diene) PCL which bonded to core via Diels-Alder reaction.

For the synthesis of PCL₂-PEG type of block copolymer, the two methods were used; one of them was carried out through Diels-Alder reaction without Click chemistry, the other was realized using PEG as macroinitiator. The first type of PCL₂-PEG synthesis is accomplished by using "arm-first method". The PCL moiety was synthesized by ROP with modified anthracene initiator that hydroxy end turned to diol. PEG chain was also modified with to MI-PEG by changing hydroxy end of the Me-PEG in two steps. At the last step of this procedure, two moieties are bonded via high yield DA reaction. It is obvious that DA click reaction is a versatile and efficient method for the preparation of well-defined polymeric structures. But the second synthesis pathway is better due to less reaction steps and easy purification method. These advantages also bring the economical priority to the second method in the synthesis of PCL₂-PEG. In this method, the Me-PEG was used as macroinitiator for the ROP with modification on its hydroxy end to diol in the two simple steps.

Moreover, both GPC and ^1H NMR analysis confirmed a successful block copolymer formation.

In the second part of the study, the micellar characterization of the amphiphilic star block copolymers is carried out via CMC determinations and Zeta-size analyses. For the observation of effectivity of the prepared micelles, one of the most searched potent anticancer compounds curcumin is loaded to the prepared polymeric micelles. Because, the biggest obstacle for the curcumin is its low water solubility as observed for several drugs.

The CMC analysis was given brief information about the stability of the micelles which may conserve their self-assembly even at low concentrations. This property is required for drug carrier vehicles in order to keep the active compound unreleased until reach to the targeted tissue or organ without destroying self assembly or degradation.

Zeta-sizer results exhibited that the size of prepared micelles were out of the desired range (10-100 nm) for polymeric micelles. But, they are still in the range of passive targeting zone with size lower than 200 nm .

On the other hand, curcumin loading results are fairly satisfying with its increased water solubility. These results indicated that water solubility of curcumin is increased up to 211 fold with $\text{PEG}_2\text{-PCL}$, and reached to 560 fold for $\text{PCL}_2\text{-PEG}$ copolymers. But, without knowledge of the exact effective dose value, these results are considered to be only promising good solubility results. The best way to understand effectiveness of the polymeric micelles is to test them *in vivo* conditions.

REFERENCES

- [1] **Qiao W., Wang B., Wang Y., Yang L., Zhang Y., and Shao P.**, 2010, Cancer Therapy Based on Nanomaterials and Nanocarrier Systems, *Journal of Nanomaterials*, 796303
- [2] **Noshay, A. and McGrath, J.E.**, 1977, Block copolymers: overview and critical survey, *Academic Press*, New York.
- [3] **Halperin, A., Tirrell, M. and Lodge, T.P.**, 1992, Tethered chains in polymer microstructures, *Advances in Polymer Science*, 100, 31-71.
- [4] **Ivin, K. J., and Saegusa, T.**, eds. 1984. *Ring-opening Polymerization*, Vols. 1-3, Elsevier, London.
- [5] **Saegusa, T.**, 1977. Ed. *Ring-opening Polymerization*, ACS Symposium Series Vol. **59**, American Chemical Society, Washington D.C.
- [5] **McGrath, J. E.**, 1985. Ed. *Ring-opening Polymerization: Kinetics, Mechanism, and Synthesis*, American Chemical Society, Washington D.C.
- [7] **Brunelle, D. J.**, Ed. 1993. *Ring-opening Polymerization: Mechanisms, Catalysis, Structure, Utility*, Carl Hanser Verlag, NY.
- [8] **Huang S.Y.**, 1989. In Comprehensive Polymer Science, G. Allen, J Bevington, Eds., Pergamon press: New York, v. **6**, 567-607.
- [9] **Bea, S.J., Suh, J.M., Sohn, Y.S., Bae, Y.H., Kim, S.W., Jeong, B.**, 2005. Thermogelling poly(caprolactone-b-ethylene glycol-b-caprolactone) aqueous solutions. *Macromolecules*, **38**, 5260-5265.
- [10] **Wang, Y. C., Tang, L. Y., Sun, T. M., Li, C. H., Xiong, M. H., Wang, J.**, 2008. *Biomacromolecules*, **9**, 388.
- [11] **Diels, O.; Alder**, “Synthesen in der hydroaromatischen Reihe”. *Justus Liebig's Annalender Chemie* 460: 98, 1928.
- [12] **Diels, O.; Alder, K.**, *Synthesis in the hydroaromatic series, IV. Announcement: The rearrangement of maleic acid anhydride on arylated diene, triene and fulvene*, Ber. 1929, 62, 2081&2087.
- [13] **Long, V.C., Berry, G.C., and Hobbs, L.M.**, 1964, Solution and bulk properties of branched polyvinyl acetates 4. Melt viscosity, *Polymer*, **5**, 517-524.
- [14] **Gitsov I, Frechet JMJ.** *J Am Chem Soc* 1996, 118: 3785-6.
- [15] **Gitsov I, Frechet JMJ.** *Macromolecules* 1993, 26: 6536-46.

[16] **(Singh R., Lillard J. W.,** 2009, Nanoparticle-based targeted drug delivery, *Experimental and Molecular Pathology*, **86**, 215-223

[17] **Kedar U. et al**, 2010, Advances in polymeric micelles for drug delivery and tumor targeting, *Elsevier, Nanomedicine*

[18] **Aggarwal B. B., Kumar A. and Bharti A. C.,** 2003. Anticancer Potential of Curcumin: Preclinical and Clinical Studies, *Anticancer Research* **23**, 363-398

[19] **Vareed S. K., Kakarala M., T. Ruffin M., Crowell J. A., Normolle D. P., Djuric Z., and Brenner D. E.,** 2011., Pharmacokinetics of Curcumin Conjugate Metabolites in Healthy Human Subjects., *American Association for Cancer Research* **10**, 1158-1055

[20] **Hoffman A. S.,** 2008, The origins and evolution of “controlled” drug delivery systems., *Journal of Controlled Release*, **132**, 153–163

[21] **Lei, L.C., Gohy, J. F., Willet, N., Zhang, J. X., Varshney, S., Jerome, R.,** 2006. *Polymer*, **47**, 2723.

[22] **Lo, C. L., Huang, C. K., Lin, K. M., Hsiue, G. H.,** 2007. *Biomaterials*, **28**, 1225.

[23] **Wang, J. L., Wang, R., Li, L. B.,** 2009. *J. Colloid Interfaces Science*, **336**, 808.

[24] **Hans, M., Shimoni, K., Danino, D., Siegel, S. J., Lowman, A.,** 2005. *Biomacromolecules*, **6**, 2708.

[25] **Zhu, Z. S., Li, Y., Li, X. L., Ri, R. T., Jia, Z. J., Liu, B. R., Guo, W. H.,** 2010. *Journal Control Release*, **142**, 438.

[26] **Wang F., Bronich T. K., Kabanov A. V., Rauh R. D., and Roovers J.,** Synthesis and Evaluation of a Star Amphiphilic Block Copolymer from Poly(\square -caprolactone) and Poly(ethylene glycol) as a Potential Drug Delivery Carrier., 2005., *Bioconjugate Chem.*, **16**, 397-405

[27] **Zhang, W. L., Li, Y. L., Liu, X. L., Sun, Q. Q., Shuai, X. T., Zhu, W., Chen, Y. M.,** 2010. *Biomacromolecules*, **11**, 1331.

[28] **Duan, K. R., Chen, H. L., Huang, J., Yu, J. H., Liu, S. Y., Wang, D. X., Li, Y. P.,** 2010. *Carbohydrate Polymers*, **80**, 498.

[29] **Campbell, R. B., Balasubramanian, S. V., Straubinger, R. M.,** 2001. *Journal of Pharmaceutical Sciences.*, **90**, 1091.

[30] **Lee, S. C., Kim, C., Kwon, I. C., Chung, H., Jeong, S. Y.,** 2003. *Journal. Control Release*, **89**, 437.

[31] **Wang F., Tatiana K. B., Kabanov A. V., Rauh R. D., and Roovers J.** 2005. Synthesis and Evaluation of a Star Amphiphilic Block Copolymer from Poly(E-caprolactone) and Poly(ethylene glycol) as a Potential Drug Delivery Carrier., *Bioconjugate Chem.***16**, 397-405

[32] **Park J. H., Lee S., Kim J., Park K., Kim K., Kwon I. C.**, 2008 Polymeric nanomedicine for cancer therapy, *Progress in Polymer Science*, **33** 113–137

[33] **Sutton D., Nasongkla N., Blanco E., and Gao J.**, 2007. Functionalized Micellar Systems for Cancer Targeted Drug Delivery, *Pharmaceutical Research*, **24**

[34] **Francis M. F., Cristea M. and Winnik F. M.** 2004. **Polymeric micelles for oral drug delivery: Why and how.**, *Pure and Applied Chemistry*, **76**, 1321–1335,

[35] **Jones M. C., Leroux J. C.**, 1999, Polymeric micelles ± a new generation of colloidal drug carriers, *European Journal of Pharmaceutics and Biopharmaceutics*, **48**. 101-111

[36] **Allen C., Maysinger D., Eisenberg A.**, 1999 Nano-engineering block copolymer aggregates for drug Delivery, *Colloids and Surfaces B: Biointerfaces* **16**, 3–27

[37] **Jones M. C., Leroux J. C.**, 1999, Polymeric micelles ± a new generation of colloidal drug carriers, *European Journal of Pharmaceutics and Biopharmaceutics*, **48**. 101-111

[38] **Allen C., Maysinger D., Eisenberg A.**, 1999 Nano-engineering block copolymer aggregates for drug Delivery, *Colloids and Surfaces B: Biointerfaces* **16**, 3–27

[39] **Kataoka, K., Kwon, G. S., Yokoyama, M., Okano, T., Sakurai, Y.**, 1993. *Journal of Controlled Release*, **24**, 119.

[40] **Long, V. C., Berry, G. C. and Hobbs, L. M.**, 1964. Solution and Bulk Properties of Branched Polyvinyl acetates IV—Melt viscosity, *Polymer*, **5**, 517-524.

[41] **Roovers, J. E. L.**, 1985. Branched Polymers, *Encyclopedia of Polymer Science and Engineering*; Wiley, New York.

[42] **Hsieh, H. L. and Quirk, R. P.** 1996. Star Polymers, in, *Anionic Polymerization, Principles and Practical Applications*, Marcel Dekker, New York, 333-368.

[43] **Hadjichristidis, N., Iatrou, H., Pitsikalis, M., and Mays, J.**, 2006, Macromolecular architectures by living and controlled/living polymerizations, *Progress in Polymer Science*, **31**, 1068-1132.

[44] **Blencowe, A., Tan, J.F., Goh, T.K., and Qiao, G.G.**, 2009, Core cross-linked star polymers via controlled radical polymerisation, *Polymer*, **50**, 5-32.

[45] **Iatrou, H., and Hadjichristidis N.**, 1992. Synthesis of a Model 3-Miktoarm Star Terpolymer, *Macromolecules*, **25**(18), 4649–4651.

[46] **Cameron, N. S., Corbierre, M. K., Eisenberg, A.**, 1999. *Canadian Journal Chemistry.*, **77**, 1311. **Gref, R., Minamitake, Y., Peracchia, M. T., Trubetskoy, V., Torchilin, V., Langer, R.**, 1994. *Science*, **263**, 1600.

[47] **Tsukruk V.V.**, 1997. Assembly of supramolecular polymers in ultra-thin films, *Progress in Polymer Science*, **22**, 247-311. **Zhao B., Brittain W. J.**, 2000. Polymer brushes: surface-immobilized macromolecules, *Progress in Polymer Science*, **25**, 677-710.

[48] **Riess, G.**, 2003. *Prog. Polym. Sci.* **28**, 1107-1170. **b) Neiser, M. W., Muth, S., Kolb, U., Harris, J. R., Okuda, J., Schmidt, M.**, 2004. *Angewandte Chemmie, International Edition*, **43**, 3192-3195. **Tang, C., Qi, K., Wooley, K. L., Matyjaszewski, K., Kowalewski, T.**, 2004. *Angewandte Chemmie, International Edition*, **43**, 2783-2787.

[49] **Tuzar, Z., Kratochvil, P.**, 1993. Micelles of block and graft copolymers in solutions, *Colloids and surfaces Science*, **15**, 1-83. **Allen, C., Maysinger, D., Eisenberg, A.**, 1999. Nano-engineering block copolymer aggregates for drug delivery, *Colloids and Surfaces Science*, **16**, 3-27.

[50] **Kataoka, K., Kwon, G. S., Yokoyama, M., Okano, T., Sakurai, Y.**, 1993. *Journal of Controlled Release*, **24**, 119.

[51] **Shuai, X. T., Ai, H., Nasongkla, N., Kima, S., Gao, J. M.**, 2004. *Journal of Controlled Release*, **98**, 415.

[52] **Kwon, G. S., Yokoyama, M., Okano, T., Sakurai, Y., Kataoka, K. J.**, 1994. *Controlled Release*, **29**, 17. **Yu, K., Eisenberg, A.**, 1996. *Macromolecules*, **29**, 6359.

[53] **Gitsov, I., Frechet, J. M. J.**, 1996. *Journal of American Chemistry Society*, **118**, 3785-6. **Gitsov, I., Frechet, J. M. J.**, 1993. *Macromolecules*, **26**, 6536-46.

[54] **Angot, S., Taton, D., Gnanou, Y.**, 2000. *Macromolecules*, **33**, 5418-26.

[55] **Bae, Y. C., Faust, R.**, 1998. *Macromolecules*, **31**, 2480-7.

[56] **Pan, C. Y., Tao, L., Wu, D. C.**, 2001. *Journal of Polymer Science*, **39**, 3062-72.

[57] **Kurian, P., Zschoche, S., Kennedy, J. P.**, 2001. *Journal of Polymer Science*, **38**, 3200-9.

[58] **Feldthusen, J., Ivan, B., Muller, A.H.E.**, 1998. *Macromolecules*, **31**, 578-85.

[59] **Choi, Y. K., Bae, Y. H., Kim, S. W.**, 1998. *Macromolecules*, **31**, 8766-74.

[60] **Hedrick, J. L., Trollsas, M., Hawker, C. J., Atthoff, B., Claesson, H., Heise, A., Miller, R. D., Mecerreyes, D., Jerome, R., Dubois, P.,** 1998. *Macromolecules*, **31**, 8691-705.

[61] **O'Reilly, R. K., Hawker, C. J. and Wooley, K. L.,** 2006. *Chemical Society Reviews*, **35**, 1068–1083.

[62] **Ivin, K. J., and Saegusa, T,** eds. 1984. *Ring-opening Polymerization*, Vols. **1-3**, Elsevier, London.

[63] **Saegusa, T.,** 1977. Ed. *Ring-opening Polymerization*, ACS Symposium Series Vol. **59**, American Chemical Society, Washington D.C.

[64] **McGrath, J. E.,** 1985. Ed. *Ring-opening Polymerization: Kinetics, Mechanism, and Synthesis*, American Chemical Society, Washington D.C.

[65] **Brunelle, D. J.,** Ed. 1993. *Ring-opening Polymerization: Mechanisms, Catalysis, Structure, Utility*, Carl Hanser Verlag, NY.

[66] **A. C. Albertsson and I. K. Varma,** 2003. *Biomacromolecules*, **4**, 1466-1486. **E. S. Place, J. H. George, C. K. Williams and M. M. Stevens,** 2009. *Chemical Society Reviews*, **38**, 1139–1151.

[67] **A. C. Albertsson and I. K. Varma,** 2002. *Advances in Polymer Science*, **157**, 1-40.

[68] **O. Dechy-Cabaret, B. Martin-Vaca and D. Bourissou,** 2004. *Chemical Reviews*, **104**, 6147-6176.

[69] **Kleine, J., and Kleine, H.-H.,** 1959. Über Hochmolekulare, Insbesondere Optisch Aktive Polyester der Milchsäure, ein Beitrag zur Stereochemie Makromolekularer Verbindungen, *Makromolecular Chemistry*, **30**(1), 23-38.

[70] **Löfgren, A., Albertsson, A.C., Dubois, P. and Jerome, R.,** 1995. Recent Advances in Ring-Opening Polymerization of Lactones and Related-Compounds, *J. Macromol. Sci. Rev. Macromolecular Chemistry Physics*, **35**(3), 379-418.

[71] **Kuran, W.,** 1998. Coordination Polymerization of Heterocyclic And Heterounsaturated Monomers, *Progress in Polymer Science.*, **23**(6), 919-992.

[72] **Duda, A., and Penczek, S.,** 2000. In *Polymers from Renewable Resources: Biopolymers and Biocatalysis*, ACS Symposium Series 764, American Chemical Society, Washington, D.C., p 160.

[73] **O'Keefe, B., Hillmyer, M. A., and Tolman, W. B.,** 2001. Polymerization of Lactide and Related, Cyclic Esters by Discrete Metal Complexes, *Journal of Chemical Society, Dalton Trans*, 2215-2220.

[74] **Penczek, S.**, 2000. Cationic Ring-Opening Polymerization (Crop) Major Mechanistic Phenomena, *Journnal of Polymer Science Polymer Chemistry*, **38**(11), 1919-1933.

[75] **Penczek, S. and Slomkowski, S.**, 1987. Progress In Anionic Ring-Opening Polymerization, in “*Recent Advances in Anionic Polymerization*, Chap **19**, 275, Eds. Hogen, E.T. and Smid, J., Elsevier, New York.

[76] **Löfgren, A., Albertsson, A.C., Dubois, P. and Jerome, R.**, 1995. Recent Advances in Ring-Opening Polymerization of Lactones and Related-Compounds, *Journal of Macromolecular Science Reviews* **C35**(3), 379-418.

[77] **Mecerreyes, D., Jerome, R. and Dubois, P.**, 1999. Novel Macromolecular Architectures Based on Aliphatic Polyesters: Relevance of the "Coordination-Insertion" Ring-Opening Polymerization, *Advances in Polymer Science*, **147**, 1-59.

[78] **Lundberg, R.D. and Cox, E.F.**, 1969. Lactones, in *Ring-Opening Polymerization*, Frish, K., Reegen, S., Eds, 2:247 Marcel Dekker, New York.

[79] **Kricheldorf, H. R., Berl, M., and Scharnagl, N.**, 1988. Poly(Lactones). 9. Polymerization Mechanism of Metal Alkoxide Initiated Polymerizations of Lactide and Various Lactones, *Macromolecules*, **21**(2), 286-293.

[80] **Kowalski, A., Duda, A., and Penczek, S.**, 1998. Polymerization of L,L-Lactide Initiated by Aluminum Isopropoxide Trimer or Tetramer, *Macromolecules*, **31**(7), 2114-2122.

[81] **Schwach, G., Coudane, J., Engel, R., and Vert, M.**, 1998. Ring Opening Polymerization of D,L-Lactide in the Presence of Zinc Metal and Zinc Lactate, *Polym.* Initiated by Aluminum Isopropoxide Trimer or Tetramer, *Macromolecules, Int.* **46**(3), 177-182.

[82] **Kreiser-Saunders, I., and Kricheldorf, H. R.** 1998. Polylactones, 39. Zn Lactate- Catalyzed Copolymerization of L-Lactide with Glycolide or ϵ -Caprolactone, *Macromolecular Chemistry and Physics*, **199**(6), 1081-1087.

[83] **Schwach, G., Coudane, J., Engle, R., and Vert, M.**, 1997. More About the Polymerization of Lactides in the Presence of Stannous Octoate, *Journal of Polymer Chemistry, Part A: Polymer Chemistry*, **35**(16), 3431-3440.

[84] **Kricheldorf, H. R., Kreiser-Saunders, I., and Boettcher, C.**, 1995. Polylactones: 31. Sn(II)Octoate-Initiated Polymerization of L-Lactide: A Mechanistic Study, *Polymer*, **36**(6), 1253-1259.

[85] **Kowalski, A., Duda, A., and Penczek, S.**, 2000. Mechanism of Cyclic Ester Polymerization Initiated with Tin(II) Octoate. 2. *Macromolecules*

Fitted with Tin(II) Alkoxide Species Observed Directly in MALDI-TOF Spectra *Macromolecules*, **33**(3), 689-695.

[86] **Kricheldorf, H. R., Kreiser-Saunders, I., and Stricker, A.**, 2000. Polylactones 48. SnOct₂-Initiated Polymerizations of Lactide: A Mechanistic Study, *Macromolecules*, **33**(3), 702-709.

[87] **Kowalski, A., Duda, A., and Penczek, S.**, 1998. Kinetics and Mechanism of Cyclic Esters Polymerization Initiated with Tin(II) Octoate, 1. Polymerization of Epsilon-Caprolactone, *Macromolecular Rapid Communications* **19** (11), 567-572.

[88] **Löfgren, A., Albertsson, A.C., Dubois, P. and Jerome, R.**, 1995. Recent Advances in Ring-Opening Polymerization of Lactones and Related-Compounds, *Journal of Macromolecular Science Reviews*, **C35**(3), 379-418.

[89] **Kricheldorf, H. R., Kreiser, S. I.**, 1996. Polylactides - Synthesis, Characterization and Medical Application, *Macromolecular Symposia*, 103, 85-102.

[90] **Dubois, P., Ropson, N., Jérôme, R. and Teyssie, P.**, 1996. Macromolecular Engineering of Polylactones and Polylactides. 19. Kinetics of Ring-Opening Polymerization of Epsilon-Caprolactone Initiated With Functional Aluminum Alkoxides, *Macromolecules*, **29**(7), 1965-1975.

[91] **Schindler, A., Jeffcoat, A. R., Kimmel, G. L., Pitt, C. G., Wall, M. E., and Zweidinger R. A.**, 1977. Biodegradable Polymers for Sustained Drug Delivery, in *Contemporary Topics in Polymer Science*, Vol. **2**, E. M. Pearce and R. J. Schaefgen, Eds., Plenum, New York.

[92] **Pitt, C.G., Chasalow, Y.M., Hibionada, Y.M., Klimas, D.M. and Schlinder, A.**, 1981. Aliphatic Polyesters I. The Degredation of Poly(ϵ -caprolactone) *in vivo*, *Journal Applied Polymer Science*, **68**, 1534-1538.

[93] **Zhang Q., Remsen E.E., Wooley K.L.**, 2000. *Journal of American Chemistry Society*, **122**:3642.

[94] **Arnal M.L., Balsamo V., Lopez C.F., Contreras J., Carillo M., Schmalz H., et. 2001.** *Macromolecules*, **34**:7973.

[95] **a) Labet, M., Thielemans, W.**, 2009. *W. Chem Soc Rev*, **38**, 3484-3504. **b) Albertsson, A. C.; Varma, I. K.**, 2003. *Biomacromolecules*, **4**, 1466-1486.

[96] **a) Wang, L.; Dong, C. M.**, 2006. *J Polym Sci Polym Chem*, **47**, 3218-3228. **b) Dong C. M.; Guo, Y. Z.; Qiu, K. Y.; Gu, Z. W.; Feng, X. D.**, 2005. *Journal of Control Release*, **107**, 53-64.

[97] **Kolb, H.C., Finn, M.G., and Sharpless, K.B.**, 2001, Click chemistry: Diverse chemical function from a few good reactions, *Angewandte Chemie-International Edition*, **40**, 2004-2021.

[98] **Kolb, H. C.; Sharpless, K. B.**, 2003. The growing impact of click chemistry on drug discovery, *Drug Discovery Today*, **8**, 1128-1137.

[99] **Gacal, B.; Durmaz, H.; Tasdelen, M. A.; Hizal, G.; Tunca, U.; Yagci, Y.; Demirel, A. L.**, 2006. Anthracene-Maleimide-Based Diels Alder “Click Chemistry” as a Novel Route to Graft Copolymers, *Macromolecules*, **39**, 5330-5336.

[100] **Bock, V. D.; Hiemstra, H.; Van Maarseveen, J. H.**, 2006. Cu(I)-Catalyzed Alkyne-Azide “Click” Cycloadditions from a Mechanistic and Synthetic Perspective, *European Journal of Organic Chemistry*, 51-68.

[101] **Liu, Q.; Chen, Y.**, 2006. Synthesis of Well-Defined Macromonomers by the Combination of Atom Transfer Radical Polymerization and a Click Reaction, *Journal of Polymer Science: Part A: Polymer Chemistry*, **44**, 6103-6113.

[102] **Lutz, J. F.; Börner, H. G.; Weichencan, K.**, 2005. Combining Atom Transfer Radical Polymerization and Click Chemistry: A Versatile Method for the Preparation of End-Functional Polymers, *Macromolecular Rapid Communications*, **26**, 514-518.

[103] **Diels, O. and Alder, K.**, 1928, Synthesen in der hydroaromatischen Reihe, *Justus Liebig's Annalen der Chemie*, **460**, 98-122.

[104] **Corey, E.J.**, 2002, Catalytic enantioselective Diels-Alder reactions: Methods, mechanistic fundamentals, pathways, and applications, *Angewandte Chemie-International Edition*, **41**, 1650-1667.

[105] **Diels, O. and Alder, K.**, 1926, Über die Ursachen der Azoesterreaktion, *Justus Liebig's Annalen der Chemie*, **450**, 237-254.

[106] **Fringuelli, F. and Taticchi, A.**, 2002. *The Diels Alder reaction : selected practical methods*. Chichester, New York, Wiley.

[107] **Woodward, R.B. and Hoffmann, R.**, 1970. *The conservation of orbital symmetry*. Weinheim/Bergstr, Verlag Chemie.

[108] **Woodward, R.B. and Hoffmann, R.**, 1965, Stereochemistry of electrocyclic reactions, *Journal of the American Chemical Society*, **87**, 395-397.

[109] **Mantovani, G., Lecolley, F., Tao, L., Haddleton, D.M., Clerx, J., Cornelissen, J.J.L.M., and Velonia, K.**, 2005, Design and synthesis of N-maleimido-functionalized hydrophilic polymers via copper-mediated living radical polymerization: A suitable alternative to

PEGylation chemistry, *Journal of the American Chemical Society*, **127**, 2966-2973.

[110] **Malvern instruments ltd** , 2006, Surfactant micelle characterization using dynamic light scattering, *Malvern zetasizer application note 1*

CURRICULUM VITAE



Candidate's full name: Kerem KARAKUŞ

Place and date of birth: Baykan, 21/07/1985

Permanent Address: Ferahevler Mah. Şahin Sokak No:22 59860, Sarıyer/İstanbul, Turkey

Universities and Colleges attended: Hacettepe University-Faculty of Science, Chemistry, Ankara, Turkey